Curso 2011/12
CIENCIAS Y TECNOLOGÍAS/9
I.S.B.N.: 978-84-15910-02-2

JENS HERRMANN

Análisis y modelización de las propiedades reológicas de alimentos de viscosidades medias y altas

Directores
UWE GRUPA
ANDREA BRITO ALAYÓN

SERVICIO DE PUBLICACIONES
UNIVERSIDAD DE LA LAGUNA

SOPORTES AUDIOVISUALES E INFORMÁTICOS
Serie Tesis Doctorales

Logic will get you from A to B.
Imagination will take you everywhere.

Albert Einstein

Acknowledgements

I would like to express my deepest appreciation to Professor Andrea Brito Alayón and Professor Uwe Grupa for their effective guidance. Without their continuing support and encouragement this thesis would not have been possible.

My candidature was at all possible owing to a funding of Air Products PLC. In this regard I am grateful to Mr. Jon Trembley and his team for the trust, support and the invaluable discussions. In addition I would like to thank Mr. Uwe Rosenbaum for his support.

I am grateful to the Department of Ingeniería Química y Tecnología Farmacéutica at the University of La Laguna for their heartily acceptance.

In addition, I would like to thank Mr. Alejandro Hernandez Gonzales for helping to surmount difficult organizational obstacles, Mr. Frank Euring, Mr. Christoph Luckhardt and Ms. Nicole Müller for their invaluable support, communication and helpful discussions and to the numerous friends and people, whom I have not mentioned by name for their support during the course of my study, both directly and indirectly.

Finally, I am indebted to my family and Carola for much support in so many areas over the years.

Introducción

En la vida cotidiana de muchos consumidores, los alimentos de viscosidad media a alta como salsas, aliños y mayonesas, son usados comúnmente para mejorar el sabor de muchos platos y se pueden clasificar dentro de los llamados “alimentos de conveniencia” o “alimentos procesados terciarios”. Todos los productos comerciales tienen que cumplir requerimientos básicos similares tales como poseer calidad, estabilidad y seguridad estable durante su vida útil. Tomando en cuenta esos aspectos, las materias primas utilizadas admiten combinaciones casi ilimitadas dando como resultado productos con diferentes propiedades sensoriales y por tanto mecánicas.

Para satisfacer la demanda de los consumidores en cuanto a la consistencia, estabilidad y textura de las salsas, el desarrollo y la producción de los productos se requiere un conocimiento exhaustivo de su composición, asi como de las propiedades físicas de sus principales ingredientes y estructuras subyacentes, como resultado de la presencia de proteínas, carbohidratos, grasas y agua. En general, esos sistemas se pueden denominar dispersiones, que pueden distinguirse como emulsiones o suspensiones dependiendo del estado de agregación de la fase discontinua. Con el propósito de alcanzar las propiedades requeridas para el producto, se realizan numerosas combinaciones de operaciones unitarias durante la producción industrial. La información sobre las propiedades mecánicas de los productos es necesaria para dimensionar adecuadamente equipos y procesos y optimizar su funcionamiento.

Las medidas reológicas proporcionan una forma de caracterización del comportamiento del flujo y de la deformación de los productos, ya que la viscosidad es un importante parámetro físico en este contexto. Variables como la temperatura, gradiente de velocidad de cizalladura, tiempo, concentración, etc, pueden afectar el comportamiento reológico y por tanto la viscosidad de una muestra. Matemáticamente esas influencias pueden ser descritas con funciones de aproximación. Sin embargo no existen recomendaciones de uso de uno u otro modelo atendiendo a los diferentes tipos de productos.

La investigación de esos comportamientos y características producto por producto es laboriosa y costosa. Por tanto, los modelos predictivos de las propiedades de los productos basados en su composición pueden facilitar y agilizar el diseño de productos, procesos,

equipos e instalaciones. No obstante, los modelos predictivos basados en la composición en proteínas, grasas, carbohidratos y agua están disponibles para el caso de propiedades térmicas pero no para propiedades reologicas.

Objetivos

El presente trabajo se dirige al desarrollo de un modelo, basado en la observación, de predicción de propiedades reológicas de productos alimentarios de viscosidad media a alta en función de su composición comercial. Esto se materializa en dos objetivos específicos:

1. Caracterización reológica de productos comerciales de viscosidad media a alta.
2. Desarrallo de un modelo predictivo para las propiedades reológicas de un producto desconocido en función de su composición en proteínas, carbohidratos, grasas y agua.

Procedimiento Experimental

Para la investigación propuesta se seleccionaron 55 emulsiones y suspensiones alimentarias diferentes, adquiridas en establecimientos en España, Alemania, Reino Unido y Suiza. La información sobre la composición nutricional de dichos productos se obtuvo directamente de sus etiquetas, basadas en la Directiva 90/496/EEC. En una primera aproximación los alimentos se clasificaron en cuatro grandes grupos: kétchup (K), condimentos (C), mayonesas y aliños de bajas calorías (L) y mayonesa clásica (M). Para el cálculo de los procesos de flujo la función viscosidad es del mayor interés.

La viscosidad puede venir influenciada por diferentes parámetros y durante el procesado los alimentos están expuestos a tensiones mecánicas y térmicas, lo que lleva a investigar la dependencia de la velocidad de cizalladura y la temperatura durante el tiempo que se aplica la tensión.

Por tanto, los productos seleccionados fueron caracterizados reológicamente, a través de la medida de su viscosidad a diferentes condiciones de velocidad de cizalladura, temperatura y tiempo. Los resultados obtenidos se utilizaron en el desarrollo del modelo.

Reometría

Las medidas reológicas fueron tomadas con un reómetro Thermo Haake RS 300 combinado con un controlador de temperatura universal también de la marca Haake. Para evitar deslizamientos se seleccionó un dispositivo de medida de superficie rugosa plato/plato (diámetro 35 mm). El tamaño de abertura entre platos seleccionado se fijó en 1 mm. Cada una de las medidas se repitió un mínimo de tres veces.

La influencia del tiempo en las características del flujo fue estudiada mediante experimentos en condiciones constantes de gradiente de velocidad de cizalladura $\dot{\gamma} = 300\ s^{-1}$ y temperatura T = 5 °C para una duración total del experiment de t = 480 s.

Antes de realizar los ensayos de rampa de gradiente de velocidad de cizalladura y temperatura se realizó una etapa previa de aplicación de gradiente de velocidad de cizalladura constante de $\dot{\gamma} = 300\ s^{-1}$ durante t = 120 s para conseguir destruir la estructura de la muestra de tal forma que el comportamiento reológico no dependa del tiempo. Las medidas de rampa de gradiente de velocidad de cizalladura se realizaron aplicando una rampa ascendente de $\dot{\gamma} = 1 - 500\ s^{-1}$ a temperaturas de T = 5, 25, 55 °C durante t = 480 s. La influencia de la temperatura en las características del flujo fue evaluada aplicando una rampa de temperatura de T = 5 -55 °C para valores constantes de gradiente de velocidad de cizalladura de $\dot{\gamma} = 1, 10, 100, 500\ s^{-1}$ durante t = 480 s.

Tratamiento de datos

Los datos obtenidos fueron tratados mediante la aplicación de distintos modelos reológicos. La dependecia de las características del flujo con el tiempo fue identificada mediante el calculo del relación viscosidad inicial/viscosidad de equilibrio. Sólo los productos con una dependencia significativa se ajustaron los modelos de Weltman, disminución del esfuerzo de primer orden con esfuerzo cero en el equilibrio, y disminución del esfuerzo de primer orden con valor del esfuerzo en el equilibrio distinto de cero.

La dependecia de las características del flujo con el gradiente de velocidad de cizalladura fue tratada mediante la aplicación de los modelos de Bingham, Ostwald-de-Waele, Herschel-Bulkley, Casson, Casson modificado y Carreau. La influencia de la temperatura sobre las propiedades reológicas se ajustó a los modelos tipo Arrhenius y Williams-Landel-Ferry.

La bondad del ajuste del modelo se describió mediante el coeficiente de determinación y el error cuadrático medio. Para la validación de los residuos de los modelos, estos fueron analizados mediante la aplicación del test Shapiro Wilk, obteniendo un P valor $p > 0,05$, lo que indica una distibución normal de los residuos.

Predicción de propiedades reológicas

Para el desarrollo del modelo predictivo de las propiedades reológicas, los parámetros evaluados de medidas reológicas y los datos de composición de los productos fueron sujetos a análisis de regresión lineal y lineal múltiple. El rango de productos se clasificó de acuerdo con tres aproximaciones diferentes según su composición, propiedades funcionales y propiedades reológicas, para determinar las características reológicas específicas de los diferentes subgrupos de productos.

Selección de los modelos reológicos

Los resultados experimentales obtenidos se han analizado para seleccionar el modelo matemático mas fiable para describir la dependencia de las distintas muestras del tiempo, velocidad de cizalladura y temperatura. Una vez seleccionados los modelos apropiados para cada variable, se desarrolla un modelo general que incorpora la dependencia con la velocidad de cizalladura y la temperatura conjuntamente.

Influencia del tiempo en el comportamiento del flujo

Durante los primeros 100 s a velocidad de cizalladura constante las muestras reflejaron un rápido decrecimiento o crecimiento en el esfuerzo cortante y la viscosidad, a partir de este momento se observó un valor constante del esfuerzo cortante que se puede asignar al estado de equilibrio. La mayoría de los productos no mostraron una dependecia significativa con el tiempo, mientras que siete de ellos mostraron un comportamiento de flujo tixotrópico. En tres de ellos se observa un comportamiento significativo de flujo reopéctico.

Los productos con una dependencia significativa se ajustaron a los modelos Weltman, modelo de disminución del esfuerzo de primer orden con esfuerzo cero en el equilibrio, y modelo de disminución del esfuerzo de primer orden con valor del esfuerzo en el equilibrio distinto de cero. Sólo el último modelo podría ser validado para todos los

casos de dependencia significativa con el tiempo mostrando, en general, elevados coeficientes de determinación ($R^2 > 0,976$) y valores bajos de error cuadrático medio lo que indica un buen ajuste.

Influencia de la velocidad de cizalladura en el comportamiento del flujo

Para todos los productos se observó un comportamiento de flujo pseudoplástico, lo que se demuestra por la reducción no lineal de la viscosidad cuando aumentaba la velocidad de cizalladura. La dependecia de las características del flujo con la velocidad de cizalladura fue tratada mediante la aplicación de los modelos de Bingham, Ostwald-de-Waele, Herschel-Bulkley, Casson, Casson modificado y Carreau.

El modelo Herschel-Bulkley resultó ser el más apropiado para describir esta dependencia, y podría ser validado para casi todos los productos mostrando, de forma general, elevados coeficientes de determinación ($R^2 > 0,942$) y valores bajos de error cuadrático medio, comparado con el resto de modelos.

El punto de fluencia para todos los productos varió entre $\tau_0 = 0$ - 276 Pa, mientras que el coeficiente de consistencia estaba en el rango de K = 1,9 - 97,1 Pas^n. El índice de comportamiento de flujo varió en el rango de n = 0,169 - 0,68. Siete de los productos con un elevado contenido en sólidos totales comparado con el resto, podrían ser validados sólo con el modelo Carreau.

Influencia de la temperatura en el comportamiento del flujo

En general todos los productos mostraron una disminución en la viscosidad con el aumento de temperatura y viceversa. Los datos obtenidos en los experimentos de dependencia con la temperatura se ajustaron a modelos tipo Arrhenius y Williams-Landel-Ferry (WLF).

Ambos modelos dieron buenos resultados, siendo el modelo tipo Arrhenius válido para todos los productos excepto uno, mientras que el modelo WLF sólo podría ser validado para 49 productos de los 55 ensayados. El modelo tipo Arrhenius mostró un elevado coeficiente de determinación ($R^2 > 0,9$) y valores bajos de error cuadrático medio lo que permitió un buen ajuste al modelo. En general la viscosidad de referencia a velocidades de cizalladura de $\dot{\gamma} = 1, 10, 100, 500\ s^{-1}$ estaba en el rango de η_{ref} = 0,19 - 129,9 Pas una temperatura de referencia de T_{ref} = 25 °C = 289,15 K.

Los valores de energía de activación estaban en el rango de E_a = 0,18 - 19,9 kJ/mol y mostró una dependencia significativa con la velocidad de cizalladura, pudiendo ser descrita mediante una función logarítmica.

Influencia combinada de la velocidad de cizalladura y la temperatura en el comportamiento del flujo

Considerando los resultados obtenidos, se realizó una combinación del modelo de Herschel-Bulkley para la dependencia con la velocidad de cizalladura y el modelo tipo Arrhenius para la dependencia con la temperatura, que permitiera el cálculo de la viscosidad aparente $\eta_{\dot{\gamma},T}$ para cualquier combinación velocidad de cizalladura ($\dot{\gamma}$) - temperatura (T) dentro de las condiciones límites basadas en cinco parámetros característicos de acuerdo con la siguientes ecuación:

$$\eta_{T,\dot{\gamma}} = \left[\frac{\tau_{0ref}}{\dot{\gamma}} + K_{ref} \cdot (\dot{\gamma})^{[n_{ref} - 1]}\right] \cdot e^{\left[\left(\frac{(E_{a1} \cdot \ln\dot{\gamma} + E_{a2})}{R}\right) \cdot \left(\frac{1}{T} - \frac{1}{T_{ref}}\right)\right]}$$

Siendo los parámetros de referencia: punto de fluencia τ_{0ref} en (Pa) , coeficiente de consistencia K_{ref} en (Pas^n), índice de comportamiento de flujo n_{ref} en (-), pre-factor de energía de activación E_{a1} en ($J \cdot s \cdot mol^{-1}$), energía de activación E_{a2} en ($J \cdot mol^{-1}$), constante universal de los gases R en ($J \cdot mol^{-1} \cdot K^{-1}$) y temperatura T_{ref} en (K). La ecuación desarrollada mostró una buena correlación ($R^2 > 0,83$) entre los datos de viscosidad medidos y los calculados.

Desarrollo del modelo predictivo

Los datos de composición y sus correspondientes parámetros reológicos característicos, punto de fluencia τ_{0ref}, coeficiente de consistencia K_{ref}, índice de comportamiento de flujo n_{ref}, pre-factor de energía de activación E_{a1} y energía de activación E_{a2} fueron sometidos a análisis de regresión lineal y regresión lineal múltiple para identificar correlaciones entre los datos de composición y sus propiedades reológicas, no encontrándose correlación dentro de todo el rango de productos. Este hecho condujo a la implementación de la clasificación sistemática de los productos.

Clasificación basada en las propiedades funcionales

Esta clasificación se basa en el uso previsto del producto por parte del consumidor y su estructura macroscópica. El rango de productos estudiados se dividió en emulsiones clásicas, no clásicas y suspensiones. Las emulsiones clásicas se caracterizaron por un contenido en grasas de un 75 % - 84 % en peso. A su vez el grupo de emulsiones no clásicas se subdividió en "emulsiones no clásicas que se pueden coger en cuchara" y "emulsiones no clásicas que se pueden verter". Dentro del grupo de las no clásicas no se pudo distinguir entre subgrupos debido a que sus valores de composición estaban superpuestos. Se identificó el puré de tomate como ingrediente principal en las suspensiones con un máximo contenido en aceite de 0,5 % en peso.

Las características reológicas de los grupos y subgrupos resultantes y su composición correspondiente fueron sometidas a análisis de regresión lineal y regresión lineal múltiple, no mostrando correlación alguna.

Clasificaión basada en la composición

La clasificación basada en la composición tiene en cuenta el contenido en agua, aceite y sólidos totales de la muestra y el rango de productos se dividió en cuatro grupos. El primero está caracterizado el primero por un contenido máximo en grasas del 10 % en peso, un contenido mínimo de agua de un 75 % en peso y un contenido máximo en sólidos totales de un 30 %. Los productos típicos dentro de este grupo son los kétchups y salsas condimentadas.

Los kétchups con un aumento en la porción de concentrado de tomate podrían asignarse al segundo grupo, caracterizado por un máximo en grasas de un 10 % en peso, mientras que el contenido en agua está entre un 50 - 75 % en peso y un contenido en sólidos totales sobre un 30 %.

El tercer grupo, con un contenido en grasas en el rango de 10 - 50 % en peso, agua en un 50 - 75 % en peso y un contenido en sólidos totales máximo del 45 % en peso está representado por los productos reducidos en grasas. El último grupo, que comprende las mayonesas, se caracterizó por un contenido en grasas entre un 50 - 82 % en peso, un contenido en agua entre un 10 - 50 % en peso y un contenido en sólidos totales de un 30 % en peso.

Las características reológicas de los grupos resultaron superpuestas lo que no permitió la definición de estándares específicos de los grupos. Las composiciones de los grupos y sus características reológicas correspondientes fueron sometidas a análisis de regresión lineal y regresión lineal múltiple, no mostrando correlación alguna.

Clasificación en las propiedades reológicas

El criterio para la diferenciación de acuerdo con las propiedades reológicas es la estabilidad de la muestra, que se calculó en base a la relación entre el punto de fluencia y la densidad multiplicada por la aceleración de la gravedad.

Los resultados obtenidos permitieron clasificar los productos en fluidos, poco fluidos y estables. Sólo dos productos de todos los estudiados se clasificaron en el grupo de los fluidos, mientras que el resto se clasificaron como estables.

Por tanto, este modelo de clasificación no mostró mejoras comparado con los productos sin clasificar, debido a que los parámetros reológicos de los productos eran demasiado similares como para establecer una diferenciación de acuerdo con el criterio de la clasificación. Este hecho condujo a la conclusión de que todos los productos comerciales estudiados muestran propiedades reológicas similares.

Modelo independiente de la composición

Con los modelos de clasificación aplicados se concluye que los productos comerciales independientemente de su composición y estructura macroscópica, muestran valores en los parámetros reológicos dentro del mismo orden de magnitud. Por estas razones, se seleccionó una ecuación general con parámetros constantes que combina la dependencia de las características del flujo con la velocidad de cizalladura y la temperatura para todo el rango de productos, según:

$$\eta_{T,\dot{\gamma}} = \left[\frac{25.36}{\dot{\gamma}} + 26.27 \cdot (\dot{\gamma})^{[0.389 - 1]} \right] \cdot e^{\left[\left(\frac{7.95}{0.00831} \right) \cdot \left(\frac{1}{T} - \frac{1}{298.15} \right) \right]}$$

La ecuación desarrollada permite la estimación general de la dependencia con la velocidad de cizalladura y la temperatura de las dispersiones alimentarias estudiadas.

Conclusiones

El trabajo realizado ha dado lugar a las siguientes conclusiones:

1. Todas las emulsiones y suspensiones comerciales de alimentos analizadas presentan comportamiento no-newtoniano.

2. El comportamiento reológico de las emulsiones y suspensiones de los alimentos investigados depende del tiempo de esfuerzo, velocidad de cizallamiento y la temperatura.

3. La influencia en el comportamiento reológico de los parámetros antes mencionados están dentro de las condiciones limites de fiabilidad de:

   (a) modelo de disminución del esfuerzo de primer orden, con un esfuerzo en el equilibro distinto de cero para la dependencia con el tiempo.
   (b) modelo de Herschel-Bulkley para el comportamiento de flujo dependiente de la velocidad de cizalladura.
   (c) modelo tipo Arrhenius para la dependencia con la temperatura.

4. El desarrollo de una ecuación dependiente de la velocidad de cizalladura $\dot{\gamma}$ en (s^{-1}) y la temperatura T en (K) permite la estimación de la viscosidad aparente $\eta_{\dot{\gamma},t}$, de productos específicos a cualquier combinación de velocidad de cizalladura-temperatura, con los parámetros de referencia: límite de deformación τ_{0ref} en (Pa), el coeficiente de consistencia K_{ref} en (Pas^n), índice de comportamiento de flujo n_{ref} , pre-factor de la energía de activación, E_{a1} en ($J \cdot s \cdot mol^{-1}$), la energía de activación E_{a2} en ($J \cdot mol^{-1}$), la constante universal de los gases R en ($J \cdot mol^{-1} \cdot K^{-1}$) y una temperatura de referencia T_{ref} en (K).

$$\eta_{T,\dot{\gamma}} = \left[\frac{\tau_{0ref}}{\dot{\gamma}} + K_{ref} \cdot (\dot{\gamma})^{[n_{ref}-1]}\right] \cdot e^{\left[\left(\frac{(E_{a1} \cdot \ln\dot{\gamma} + E_{a2})}{R}\right)\cdot\left(\frac{1}{T} - \frac{1}{T_{ref}}\right)\right]}$$

5. Mediante regresión lineal y múltiple no se han podido predecir las propiedades reológicas basándose en la composición en proteínas, carbohidratos, grasas y agua de los alimentos. La clasificación de los productos siguiendo diferencias sistemáticas no condujeron a ninguna mejora en las capacidades de predicción.

6. Todos los productos comerciales investigados presentan similares propiedades reológicas con independencia de su composición.

7. Se ha establecido una ecuación de referencia, que representa toda la gama de productos comerciales estudiados, para la estimación de las propiedades reológicas con dependencia de la velocidad de cizalladura y la temperatura. Los parámetros encontrados para la ecuación son:

   (a) Límite de deformación $\tau_{0ref} = 25,36$

   (b) Coeficiente de consistencia $K_{ref} = 26,27$

   (c) Índice de comportamiento $n = 0,389$

   (d) Pre-factor de la energía de activación $E_{a1} = 0$

   (e) Energía de activación $E_{a2} = 7,95$

8. La precisión de la ecuación aumenta cuando lo hace la velocidad de cizalladura.

De los resultados de esta Tesis se pueden sugerir las siguientes futuras líneas de trabajo:

1. Para facilitar un modelo de predicción basado en la composición se necesitaría más información acerca de las condiciones del proceso de producción del alimento, así como datos de su composición con mayor precisión.

2. Como consecuencia de la información adicional que se necesita de la fase discontinua, que determina de una forma decisiva las propiedades reológicas del fluido, se debe examinar la forma y distribución de tamaño de las partículas presentes en el medio para mejorar la comprensión del comportamiento reológico resultante.

3. Desarrollar un test simple, que ofrezca la opción de observar las características reológicas básicas, por ejemplo, viscosímetro de vaso. Esto permitiría una mejor categorización de los producto y por lo tanto la predicción de otros parámetros reológicos.

4. Implementación de técnicas avanzadas de evaluación de datos, por ejemplo Red Neuronal Artificial, debido a su capacidad de tomar en cuenta las no linealidades e interacciones entre cada variable. En este sentido, se avanzará en el objetivo principal de la determinación de patrones específicos de productos e ingredientes que permitan su relación con las características reológicas del producto.

Contents

Nomenclature

α	[-]	Level of significance
β	[Pa^{-1}]	Pressure coefficient
ε	[K^{-1}]	Temperature pre-factor
$\dot{\gamma}$	[s^{-1}]	Shear rate
γ	[-]	Deformation
$\eta_{a,\gamma,\dot{T}}$	[Pas]	Temperature - shear rate dependent apparent viscosity
η_a	[Pas]	Apparent viscosity
η_f	[Pas]	Viscosity coefficient
$\eta_{t\infty}$	[Pas]	Apparent viscosity at equilibrium state
η_∞	[Pas]	Limit viscosity at high shear rate
η_{t0}	[Pas]	Apparent viscosity at initial state
η_{ref}	[Pas]	Apparent reference viscosity
η_0	[Pas]	Limit viscosity at low shear rate
η	[Pas]	Dynamic viscosity
λ	[s]	Time constant
ρ	[g/cm^3]	Density
τ_a	[Pa]	Modified shear stress
τ_e	[Pa]	Equilibrium shear stress
τ_i	[Pa]	Intial shear stress
τ_s	[$Pa \cdot K^{-1}$]	Shear stress prefactor
τ_0	[Pa]	Yield stress
τ_{0ref}	[Pa]	Yield stress at reference temperature
τ	[Pa]	Shear stress
g	[m/s^2]	Gravitational acceleration
h	[m]	Height

k	[-]	Breakdown rate constant
n_1	[-]	Modified Casson flow behavior index
n_a	[-]	Modified flow behavior index
n_b	[-]	Exponent of breakdown reaction
n_{ref}	[-]	Flow behavior at reference temperature
n_s	[-]	Flow behavior index pre-factor
$\overline{n}$	[-]	Temperature independent flow behavior index
n	[-]	Flow behavior index
p	[-]	Probability value
s	[m]	Deflection path
t	[s]	Time
v	[m/s]	Velocity
A	[m²]	Area
A_1	[Pa]	Initial shear stress
B_1	[Pa]	Time coefficient of thixotropic breakdown
C_1	[-]	Williams-Landel-Ferry constant 1
C_2	[K]	Williams-Landel-Ferry constant 2
Ea	[kJ·mol^{-1}]	Energy of activation
E_{a1}	[kJ·s·mol^{-1}]	Pre-factor activation energy
E_{a2}	[kJ·mol^{-1}]	Modified activation energy
$F_{cal,i}$	[-]	Calculated value
$F_{exp,i}$	[-]	Observed value
$\overline{F}_{exp,i}$	[-]	Mean of observed data
F	[N]	Force
G	[Pa]	Shear modulus
K	[Pas^n]	Consistency coefficient
K_a	[Pas^n]	Modified consistency coefficient
K_s	[Pas^n]	Pre-factor consistency coefficient
K_T	[Pas^n]	Temperature dependent consistency coefficient
K'	[Pas^n]	Temperature dependent consistency coefficient
K_{ref}	[Pas^n]	Consistency coefficient at reference temperature
K_s	[Pas^n]	Pre-factor consistency coefficient
L	[m]	Length

N	[-]	Number of observations
N_1	[Pa]	First normal stress difference
N_2	[Pa]	Second normal stress difference
P	[Pa]	Pressure
R^2	[-]	Coefficient of determination
R	[$J \cdot mol^{-1} \cdot K^{-1}$]	Universal gas constant
$RMSE$	[-]	Root mean square error
T	[K]	Absolute temperature
T_{ref}	[K]	Reference temperature
V_H	[$kg \cdot m^{-3}$]	Hole volume

List of Figures

List of Tables

0 Summary

Middle to high viscosity foodstuffs, namely sauces like condiment sauces, dressings, mayonnaise's can be assigned to the group of convenience food or tertiary processed foods respectively. These products consist of a mixture of lipids, proteins, carbohydrates, water and salts and are produced mostly in industrial scale.

The production processes consist of several combinations of unit operations to produce products with defined properties. Reliable dimensioning and optimization of production processes requires comprehensive knowledge of physical properties of the products. The investigations of the characteristics mentioned above are time consuming and involve laboratory resources. For this reason prediction models of product properties on the basis of product composition can ease and quicken product, process and equipment design. Prediction models on the basis of composition of proteins, carbohydrates, fats, and water are available for thermal but not for rheological characteristics.

The objectives of this research work are the comprehensive rheological characterization and modeling of commercial middle to high viscosity foodstuffs and the development of a prediction model for rheological properties based on the composition of proteins, carbohydrates, fats and water of an unknown product.

Middle to high viscosity foodstuff are complex systems, due to their variability of ingredients. The variety of raw materials complicates the assessment of technological properties and interactions of different ingredients. The resulting macroscopic structures of these mixtures can be ranging from suspension to emulsion, which can be distinguished according to their dispersed phase.

Different classification approaches based on the function, composition or rheological properties allow the systematic subdivision of dispersions into groups with specific characteristics. Rheometry allows the characterization of the flow and deformation

behavior of dispersions. From the processing point of view the rheological behavior of a sample can be affected by the parameters time, shear rate, temperature and pressure. These influencing parameters can be modeled by different mathematical approaches.

The time, shear rate and temperature dependent flow behavior of 55 commercial food emulsions and suspensions are measured and evaluated by application of various mathematical models. The goodness of fit of the different modeling approaches is compared and the most reliable model for each influencing parameter is selected.

All products, which exhibit time-dependent flow behavior can be successfully described by the first-order stress decay model, with a non-zero stress. The Herschel-Bulkley model is found to be most appropriate for the description of the shear rate dependent flow behavior. The temperature dependent flow behavior is best described by an Arrhenius type Equation. The models for shear rate and temperature dependent flow behavior are combined to allow an estimation of the apparent viscosity at any given shear rate- temperature combination based on five characteristic parameters.

The resulting rheological characteristics and the composition data of the corresponding products are subjected to linear and multiple linear regression. However no correlations are found for which reason the function, composition and rheological based classification approaches are applied for the formation of subgroups. No improvements regarding the predictive capabilities based on composition data are observed.

The performed evaluation methods do not allow the predictive estimation of the rheological properties based on the composition data. However the applied rheological classification model points out, that the selected commercial emulsions and suspensions of investigation originate from a main unit of commercial products with similar rheological properties, since all values of the characteristic parameters are almost within the same dimension, whereas the composition various.

For this reason a general Equation, which combines the shear rate and temperature dependent flow behavior with constant parameters is derived for the complete product range. The developed Equation allows the general estimation of the shear rate and temperature dependent flow behavior of commercial available food dispersion.

1 Introduction

In the everyday life of many consumers middle to high viscosity foodstuffs, namely sauces like condiment sauces, dressings, mayonnaises are commonly used to improve the taste of various dishes and can be assigned as convenience food or tertiary processed foods respectively [1]. Besides the classic products e.g. ketchup; mayonnaise; the development tends to compositions with new flavors and to products with reduced fat contents. The fat content has to be reduced or eliminated by non-lipid ingredients, while achieving properties of texture, appearance and taste comparable to classical products.

All these products consist of a mixture of lipids, proteins, carbohydrates and water are produced mostly in industrial scale. The production processes comprise several combinations of unit operations to produce products with defined properties. Reliable dimensioning and optimization of production processes requires comprehensive knowledge of physical properties of products. For flow process calculations mechanical properties, like flow and deformation behavior, and thermal properties like thermal conductivity, diffusivity, enthalpy, and specific heat capacity are from major importance. The investigation of these characteristics is time consuming and involves laboratory resources.

For this reason prediction models of product properties on the basis of product composition can ease and quicken product, process and equipment design [2]. However prediction models on the basis of composition of proteins, carbohydrates, fats, and water are only available for thermal but not for rheological characteristics [3,4,5]. The prediction of rheological properties is challenging since composition and underlying structures of these products are complex.

The prediction of physical properties of foodstuff based on the composition of proteins, carbohydrates, fats and water can be useful for food engineering and processing applications, since different scenarios during the design of food processing equipment can be considered without additional effort. Physical properties like density, specific heat

capacity, thermal conductivity, etc. can be calculated by empirical formulas based on the composition and have an accuracy of ± 10 percent [4]. On their own they are not sufficient for calculations of flow processes since mechanical properties like the viscosity are the pivot. Up to now a prediction model for this parameter has not been reported in the literature.

In general it can be distinguished between physics and observation-based modeling. Physics-based modeling is less common in food product, process and equipment design. The variability and complexities of transformations during production complicate the attempt to take physical universal laws as basis for a prediction [6]. In contrast observation-based modeling is more common in food industries, since the understanding of underlying physics is not necessarily required [7]. Models are usually generated by available data and fitted to the purpose of modeling [8].

1.1 Theoretical Fundamentals

In section 1.1.1 middle to high viscosity foodstuffs are defined. The main constituents are identified and their technological characteristics are evaluated in section 1.1.1.1, whereas in section 1.1.1.2 resulting structures of middle to high viscosity foodstuffs are identified.

For analysis of the mechanical properties, which subject flow properties, rheology is introduced as method for material characterization in section 1.1.2. Relevant fundamental terms of rheology are outlined and parameters shear rate, time, temperature, and pressure which can affect fluids are identified in section 1.1.2.1. Constitutive different approaches for modeling the different influencing parameters are presented and their application on different products is discussed in the sections 1.1.2.2 - 1.1.2.5.

1.1.1 Middle to high viscosity foodstuffs

Middle to high viscosity foodstuffs are commonly called sauces and can be assigned to be semi-solid food. The wide range of available products is usually used as seasoning or flavoring composition for meat and vegetables dishes or desserts. Depending on the type of utilization sauces are applied hot or cold, whereas hot-served sauces are usually divided into white and brown sauces and are industrially seen basic material for precooked frozen dishes [9]. The category of cold-served sauces comprises mayonnaises, condiment sauces,

salad dressings and others and is mostly industrially produced for direct consumption. In this work the term “sauces” is applied to the category of cold products.

In general all sauces have to fulfill similar basic demands concerning consistent product quality, stability, and security throughout the defined shelf life [10]. Considering these aspects manifold raw materials can be varied nearly in unlimited combinations resulting in products with different sensory and thus mechanical properties [11]. In order to meet consumers' demands on consistency, stability and texture of sauces the development and production require comprehensive knowledge of composition, technological properties of the main constituents and underlying structures. An useful overview of the main constituents of soups, sauces and dressings according to their textural properties is given by Sheldrake [12].

1.1.1.1 Composition

Sauces are complex systems due to their variability of raw materials, which complicates the assessment of technological properties and interactions of different ingredients. For simplification each product can be assigned to be a mixture of the basic constituents water, carbohydrates, proteins, fats and salts [11,13].

In general all sauces are characterized by a continuous water phase to which a mixture of carbohydrates, proteins, fats and salts is added to generate the desired properties. This mixture can be distinguished into a hydrophilic part which is represented by carbohydrates, proteins, salts and hydrophobic fats. Some of the hydrophilic substances exhibit amphiphilic behavior, which mark a key parameter for sauces with an increased fat content. Some ingredients are either oil- or water-soluble, which represent the third group [12]. Different technological purposes of the basic constituents are described subsequently.

Fats

Fats represent a very important constituent of sauces and can be equalized with the term “oil” in most cases, since most of these hydrophobic materials are utilized in liquid state of aggregation. The oils of rapeseed, sunflower and soya represent the group of commonly used oils for this purpose. The texture of a product is significantly affected by the amount, the distribution and the stabilization of the oil within the continuous water phase of a sauce [14].

Due to the immiscibility of oil and water the application of an emulsifier is required depending on the amount of oil. Low oil concentrations do not necessarily require an emulsifier to produce stable products, because small oil droplets can be scattered throughout the continuous phase reducing the probability for coalescence. However an increasing oil content results in an increasing viscosity and implicates an appropriate processing step for the dispersion of the oil in water as well as the application of an emulsifier to create a stable emulsion [12,15].

The need for fat reduced and low-fat products leads to the substitution of fat by non-fat ingredients. The substitutes have to mimetic the textural and mechanical behavior of fat, which is achieved usually by addition of a combination of carbohydrate or protein based hydrocolloids [16,17,18,19].

Carbohydrates

The group of carbohydrates can be distinguished into non-thickening and thickening. Mono- and disaccharides represent the non-thickening group of carbohydrates. Their technological function is to bind water leading to a decreased availability of water for other constituents. Furthermore the addition of saccharides leads to modification of the freezing, boiling point and the density. If added to greater extent a modification of the viscosity occurs [12].

The group of thickening carbohydrates, consisting of oligo- and polysaccharides, influences the viscosity to a great extent even by addition of small amounts. Starches from various plant sources, maltodextrines, and hydrocolloid gums like xanthan gum, guar gum, locust bean gum, carrageenan, and alginates are utilized commonly in sauces. These substances modify the structural and textural properties by bulking and formation of networks, which lead to partial immobilization of water and thus an increase of viscosity [12]. Besides their ability to increase the viscosity of the continuous water phase some polysaccharides in addition show emulsifying capacity e.g. gum arabic, modified starches, modified celluloses, glactomannans, and some pectins [20].

Proteins

Most proteins in sauces function as emulsifiers, which allow the stabilization of oil droplets. In addition proteins derived from milk and eggs like whey protein, caseinates, and vegetable proteins have the ability to bind and form networks and thus modify the viscosity

of a product, once present in sufficient quantities [21]. The emulsifying capabilities of proteins are caused by hydrophilic and hydrophobic groups of the macromolecules, leading to surface activity as well as further steric stabilization [22].

During homogenization emulsifiers will reduce the interfacial tension between the water and oil phase and therefore improve the disruption of emulsion droplets [19]. An adsorption of emulsifiers at the interfacial surface will result in the buildup of a protective layer, which will prevent coalescence of oil droplets [23].

Salts and ions

The texture and mechanical properties of sauces can be strongly influenced by charged molecules and ions, which is caused by strong interactions with proteins and carbohydrates. Depending on the concentration of the ions, the solubility of proteins can lead to increasing or decreasing interaction of different molecules, which may result in the formation of strong networks or to instabilities. Furthermore the freezing and boiling point is modified by the addition of salts [12].

The pH, which is a function of the hydrogen ion, also affects the solubility of proteins and carbohydrates, since it can have significant effect on the solubility and availability of the hydrogen ion and other salts which is critical for certain texturizing effects [12].

1.1.1.2 Macroscopic structure

The macroscopic structure of a sauce is the result of a mixture of carbohydrates, proteins, and fats in a continuous aqueous solution. In general these systems can be described as dispersions, which can be differentiated into emulsion and suspension character depending on the state of aggregation of the discontinuous phase (see Table 1.1) [11,23,24].

Table 1.1: Classification of two-phase systems

Continuous phase	Discontinuous phase	System	Example
Liquid	Liquid	Emulsion	Mayonnaise
Liquid	Solid	Suspension	Ketchup

Emulsions are defined as a fine dispersion of one liquid throughout a second, largely immiscible liquid [25,26]. Emulsions are in general unstable systems and tend to break down by time due to the unfavorable contact of water and oil molecules and their

differences in density [23]. Emulsions can either be characterized as oil-in-water (O/W) type, where the oil phase is dispersed in small droplets throughout the water phase or as water-in-oil (W/O) system, in which water is dispersed in small droplets throughout the oil phase, e.g. butter, margarine. The general mechanical properties of an emulsion are primarily determined by the external continuous phase [23,27]. Suspensions are defined as fluids which consist of a solid discontinuous phase and a continuous liquid phase [24].

Transferring these idealized definitions to real products allows further insight into the macroscopic structure and resulting textural and mechanical properties. Subsequently three different sauces with different compositions are exemplary presented and functional properties of the different ingredients are discussed.

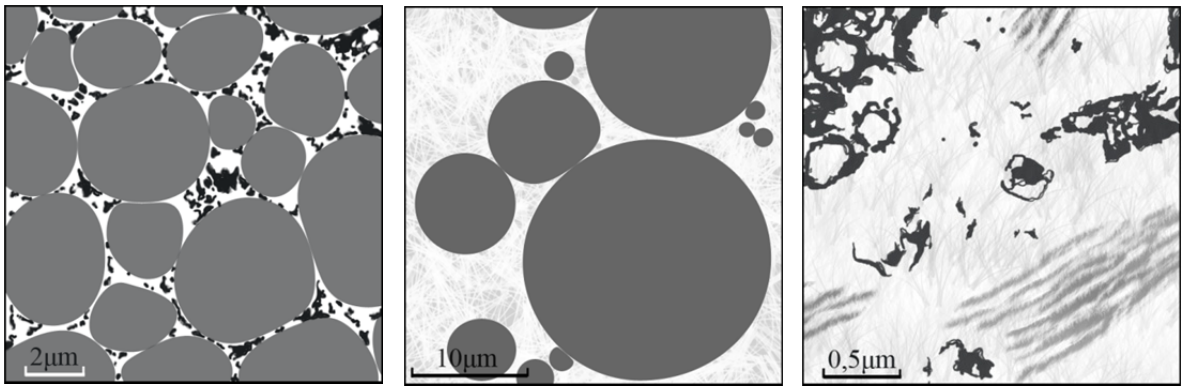

(a) Mayonnaise 80 % fat (b) Dressing 50 % fat (c) Ketchup

Figure 1.1: Macrostructure of emulsions and suspensions

Mayonnaise

Classic mayonnaise consists of a mixture of egg yolk, vinegar, oil and spices. Figure 1.1a shows for illustration a schematic drawing of a low-magnification transmission electron micrograph of mayonnaise with a fat content of 80 %. Mayonnaise is characterized as a high internal phase ratio oil-in-water emulsion due to its oil content ranging typically from 75 - 84 % [18,28]. As a result the volume fraction of the dispersed phase is larger than the maximum packing volume fraction, which is for hexagonal close packing at 74.5 %. Upon this maximum the droplets are deformed and possess a polyhedron shape, which is depicted in Figure 1.1a by the grey deformed areas [28].

The continuous phase is located between the oil droplets. The high fraction of oil tends to be destabilized due to coalescence, which can be prevented by a resistant interfacial film. Coalesced low density lipoprotein and micro particles of the egg yolk are

embedded in the continuous aqueous phase and act as emulsifier forming an interfacial film between continuous and discontinuous phase [28]. Egg yolk particles, which are represented by black particles in Figure 1.1a, form a network in the continuous phase and stabilize the emulsion to avoid coalescence [29,30,31].

Dressing

Most dressings can consider to be like mayonnaises oil-in-water emulsions and can be differentiated by their typical fat content, which ranges usually from 10 - 50 % [32]. Figure 1.1b depicts a schematic drawing of a low-magnification transmission electron micrograph of a dressing with a fat content of 50 %. Oil droplets (grey) are incorporated into a reticulum of fibrillar-like and amorphous matrix (light grey). The decrease of the discontinuous phase leads to an increase of the continuous aqueous phase implying a more diluted emulsion, since the volume fraction of the dispersed phase is lower than the maximum packing volume fraction. The non-deformed spherical oil droplets are surrounded by the continuous aqueous phase, which may contain spices and plant material e.g. tomato cell structure. The reticulum in Figure 1.1b can considered to be cooked starch paste [29].

The density difference of dispersed and continuous phase leads to an undesirable effect called creaming, which leads to phase separation of the emulsion [33]. In order to prevent this effect emulsifiers and thickeners have to be applied [34]. The emulsifiers form a protective layer at the surface of the dispersed oil droplets and thus prevent coalescence or respectively aggregation of single droplets. The formation of smaller oil droplets also retards the creaming effect by reduced buoyant forces of single droplets. Thickeners like hydrocolloids or starches are applied to increase the viscosity and form weak-gel-like polymer network to limit the movement of the droplets due to Brownian motion or gravity [19,22,23,35].

Ketchup

Tomato ketchup is a suspension of pectin, insoluble and soluble constituents in an continuous aqueous phase. Basically these components are tomato cell fragments and are embedded in a network of fibrillar-like material, which also originates from tomato cells. Figure 1.1c illustrates a schematic drawing of a low-magnification transmission electron micrograph where aggregates of plant cell fragments (dark grey) are embedded within a

matrix of fine fibrillar-like material (light grey). The fibrillar-like fibers function as water-binding agents and are comparable to hydrocolloids [29,36,37].

Ketchup can be produced from hot or cold extracted tomatoes, concentrates, purees and tomato paste. The variety of the cultivar leads to fluctuating pectic substances in the fruits and thus variability in consistency. Enzymatic degradations, pectin/protein interaction, pulp content, concentration as well as the production process can influence the consistency of tomato products. For this reason hydrocolloids are added to the composition to ensure stable product quality [36,37]. The textural and mechanical properties of ketchup depend on the content of solid particles in the suspension [36,38,39].

1.1.1.3 Classification

In the last preceding sections the main constituents as well as the resulting macroscopic structures of representative products were outlined. However not all products can be assigned directly to emulsion or suspension type. Most products can considered to be a mixture of both systems, which requires a differentiation in subgroups to identify their specific properties. For classification of these systems different systematic approaches based on rheological properties, function and composition are utilized and subsequently presented.

Function based classification

This type of classification is based on the intended application of the product by the consumer. The product range is divided into groups: classic emulsions like mayonnaise with a fat content of 75 - 84 %, non-classic emulsions and suspensions. The group of non-classic emulsions is subdivided into spoon-able and pourable. This differentiation is caused by the fact that some samples are portioned by a spoon, whereas others can be poured. These two categories comprise low-fat products, which cannot be emulsions by definition due to their composition. However they are formulated and processed to provide comparable “full fat” sensory properties like their corresponding classic emulsion based counterparts [29]. Condiment sauces represent an own group, their basic component is tomato puree with a maximum oil content of 0.5 % [12]. The different groups can be seen in Table 1.2.

Table 1.2: Function based classification scheme with exemplary products

Group	Sub-group	Examples
Classic emulsions		Mayonnaise
Non-classic emulsion	spoonable	Salad Mayonnaise; Salad crème
	Pourable	Fat reduced dressings
Suspension	condiment sauces	Ketchup, Barbecue sauce, etc.

Composition based classification

The composition based approach assumes the content of oil; water and the total solids can be used as categorizing criteria, since water represents the continuous phase and every addition of oil or solids influences the rheological and textural properties considerably [12]. Within an ingredient combination map, which is depicted in Figure 1.2 several product groups can be located, which are represented by circles. It can be assumed that products with similar properties are located in the same area of the classification map and possess similar characteristics.

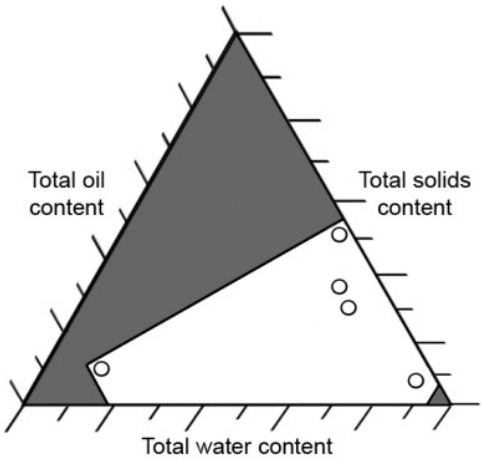

Figure 1.2: Ingredient combination map

Rheological classifications

Products can also be classified by previously investigated rheological parameters. The rheological properties generally depend on their molecular structure of different ingredients, their state of aggregation as well as on their structure in case of dispersed materials. The first approach classifies fluid foods into three subgroups, namely liquid, pasty-like and solid materials. The criteria for differentiation is the stability of a sample, which depends on the ratio of yield stress τ_0, which represents a finite stress to achieve

flow of the fluid, and density ρ multiplied by the gravitational acceleration g. This characteristic number x can be calculated using Equation 1.1 and allows the differentiation between easily flowing (x = 0.005 - 0.02); poorly flowing (x = 0.02 - 0.15). Values above x > 0.15 can be seen as inherently stable [24].

$$x = \frac{\tau_0}{\rho \cdot g} \qquad \textbf{1.1}$$

The second rheological classification differentiates products into five clusters, namely nectar, honey, pudding, puree, and pâté class by obtaining centroids by the fuzzy c-means clustering method. These modeled based on eleven rheological parameters, which represent shear rate and time dependency as well as viscoelastic properties of the samples. The knowledge of these parameters allows the establishment of viscous and viscoelastic characteristics of any objectively or subjectively similar product [40].

1.1.2 Rheology

Rheology is dealing with the behavior of materials which are exposed to physical forces. The most important form of strain is the shear flow. The objective of rheology is the detection of deformations and changes of material while being exposed to defined forces.

Food rheology serves different purposes and can be divided into three categories. The first category is characterized by the application of rheology for the development of food products. This implies the correlation of perception characteristics, stability, convenience aspects, and nutritive characteristics with the rheological characteristics of a product [41].

The second category focuses on relationships of structural and rheological properties and is related to material science and physics. Main objectives of this area are model food systems, analytical to semi-empirical modeling as well as rheometric model flows and simulations [41].

The third category is represented by the utilization of rheology for process or product optimization and correlates rheological and process parameters. Rheological data is typically used in numerical flow process simulations and in analytical to semi-empirical modeling [41]. Referring to this category fundamental terms of rheology are presented and

key process parameters are identified in section 1.1.2.1. The most important parameters and typical modeling approaches are subsequently discussed in the sections 1.1.2.2-1.1.2.5. The combination of shear rate and temperature dependent modeling approaches is presented in section 1.1.2.6.

1.1.2.1 Fundamental terms of rheology

Rheology is the dealing with deformation and flow behavior of matter. During rheological testing, substances are exposed to stress, which is defined as a force per unit area and can be shear, compressive, or tensile. Simple shear flow or respectively viscometric flow is of mayor interest for industrial applications since it covers axial flow of material in a tube, rotational flow between concentric cylinders, and rotational flow between a cone and a plate.

The description of the state of stress in a fluid during viscometric flow requires three shear rate dependent material functions, namely the viscosity function η, the first and second normal stress difference N_1 and N_2. In general it is satisfactory to assume that the second normal stress difference is equal to zero [42,43].

For Newtonian fluids the first normal stress difference is like the second stress difference equal to zero. The contrary to Newtonian fluids are Hookean solids, which store applied energy. Materials with high elastic component e.g. wheat dough or plastics exhibit different behavior of first and second normal stress differences and may lead to problems during processing since the effect of die swelling may occur. Most fluid foods possess to a small or negligible extent elastic behavior leaving the viscosity function as point of focus. In general all materials move between two extremes namely idealelastic behavior and idealviscous flow. For this reason the term viscoelastic is used for the description of these systems [43].

Elastic behavior

Matter can be called idealelastic or Hookean solid, if it stores all applied strain and recoils to its initial shape after removal of the strain. For illustration the Two-Plates-Model can be consulted, which is depicted in Figure 1.3 [44].

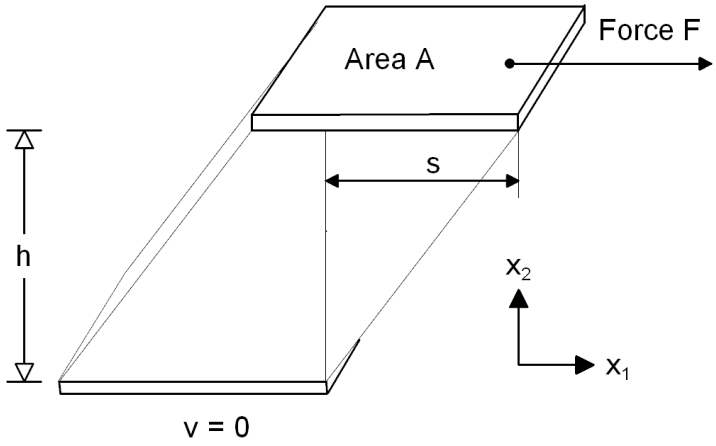

Figure 1.3: Deformation of a substance in the shear-gap of the Two-Plates-Model

The sample is located between two parallel arranged plates, whereas the lower plate is fixed. A force F is applied tangentially to the upper plate with the area A, the quotient is called shear stress τ or shear strain (see Equation 1.2).

$$\tau = \frac{F}{A} \qquad \textbf{1.2}$$

The application of the shear stress leads to the deflection path s as long as the force is acting. The resulting shear deformation γ is the quotient of deflection path and the gap size h and can be calculated using Equation 1.3 [44].

$$\gamma = \frac{s}{h} \qquad \textbf{1.3}$$

Direct proportionality of shear rate and deformation characterizes idealelastic materials. The constant of proportionality is defined as shear modulus G and corresponds to the rigidity of a sample. The mathematical relation is called Hooke's law (Equation 1.4) [43,44].

$$\tau = G \cdot \gamma \qquad \textbf{1.4}$$

Viscous behavior

Fluids like water and oil can be assigned as idealviscous and are characterized by a viscosity which is independent from the way and velocity of deformation. Complex fluids

like emulsions exhibit a differentiated flow behavior, which is caused by the existence and the dynamic formation of structure within the matter. If a material forms back into its original shape after stress, it is idealelastic [44].

Static shear measurements, which analyze the power transmission of matter with special measurement equipment, are the most common strain method for the characterization of fluids. In order to explain the fundamentals of static shear measurements the Two-Plates-Model, which can be seen in Figure 1.4 can be consulted.

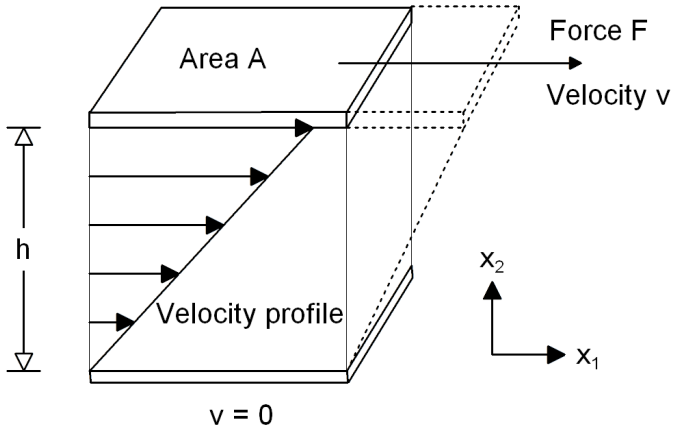

Figure 1.4: Velocity profile between parallel plates

The upper plate with a defined area A moves at a constant velocity v, whereas the lower plate is fixed. This can be seen as an incremental change in position L divided by a small time period t, $\delta L/\delta t$ [43]. The force F required for constant movement of the upper plate with the area A is defined as shear stress τ (Equation 1.2). Assuming laminar flow in the gap h between the plates the shear rate $\dot{\gamma}$ is defined as the rate of change of strain and can be calculated by Equation 1.5 [43,44].

$$\dot{\gamma} = \frac{d\gamma}{dt} = \frac{d}{dt}\left(\frac{\delta L}{h}\right) = \frac{v}{h} \qquad \textbf{1.5}$$

At presence of laminar flow the shear rate is direct proportionate with the shear stress. The constant of proportionality η is defined as shear or dynamic viscosity and its mathematical relation is called Newton's law (Equation 1.6).

$$\tau = \eta \cdot \dot{\gamma} \qquad \textbf{1.6}$$

The dynamic viscosity is a temperature dependent matter constant for Newtonian fluids e.g. water and oil. For non-Newtonian fluids, like emulsions and suspensions, this linear relationship is only valid for a very small range of shear rates [45]. Above the critical shear rate the viscosity is dependent on shear stress and thus not an independent matter constant. Besides shear rate the dynamic viscosity during processing can be also a function of time, temperature, and pressure. These variables are described in more detail in the sections 1.1.2.2 - 1.1.2.5. Available modeling approaches for these variables are discussed in each section and typical applications are presented.

1.1.2.2 Time dependency

Fluids can exhibit time-independent and time-dependent flow behavior, whereas time-dependency can be differentiated in thixotropic and rheopectic. Representative curve progressions are depicted in Figure 1.5.

Thixotropic flow behavior is characterized by decreasing shear stress over time at constant shear rate and the subsequent recovery when shearing is removed. This behavior is caused by the microstructure and its previous shear history. In most cases a network with relatively weak attractive forces is formed throughout a sample at rest. The exposure to strain leads to a breakdown of the interparticle bonds and thus the network. The reduction of strain will result in a recovery of the network structure.

The contrary flow behavior is called rheopectic and implies rising shear stress with increasing time at constant shear rate. This kind of flow behavior implies a buildup of structure and can be irreversible, partially reversible or completely reversible. Time-independent flow behavior is observed, if applied constant strain results in constant shear stress over time [15,43,46,47].

A large variety of foods exhibit structured behavior and can be classified as thixotropic, which is in some applications designated to ease processing. Typically some ketchups, mayonnaises, ice cream, etc. show reversible thixotropic behavior [15,47]. In addition various time-dependent structured fluids exhibit a yield stress, especially in the small stress range [46].

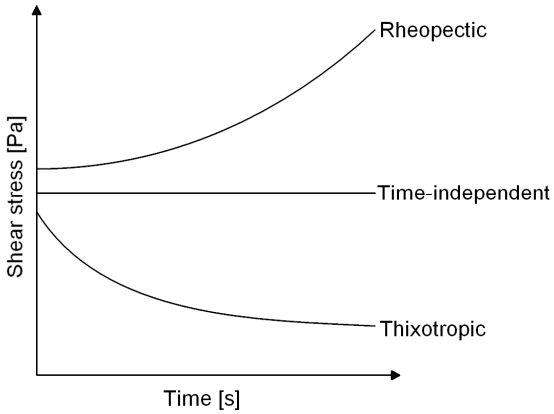

Figure 1.5: Time-dependent flow behavior of fluids

Structural models are most frequently used for the mathematical modeling of time dependent flow behavior. These models are characterized by the implementation of a structural parameter, which represents an indirect measure of the level of structure. In addition irreversible breakdown of the structure and no buildup in structure once the strain is removed has to be assumed.

The Weltman model (Equation 1.7) consists of the parameters t, representing the shearing time and two constants A_1 and B_1, which characterize the time-dependent behavior. The constant A_1 indicates the initial shear stress. The value B_1 represents the extent of the structural breakdown at constant shear conditions [48].

$$\tau = A_1 + B_1 \cdot \ln t \qquad \textbf{1.7}$$

The first-order stress decay model, with a zero equilibrium stress can be seen in Equation 1.8. It consists of the parameters shearing time t, the initial shear stress value τ_i and the constant k representing the breakdown rate.

$$\tau = \tau_i + e^{-kt} \qquad \textbf{1.8}$$

An extended version of the first-order stress decay model, with a zero equilibrium stress is the first-order stress decay model, with a non-zero equilibrium stress or Figone-Shoemaker model respectively, which is presented in Equation 1.9.

$$\tau = \tau_e + (\tau_i - \tau_e)\, e^{-kt} \qquad \textbf{1.9}$$

Where τ_i is the initial shear stress, τ_e is the equilibrium stress value, k is the breakdown rate constant and t the shearing time. The breakdown rate constant k is an indication of how fast a sample, under the action of shearing, reaches the equilibrium stress value beyond which the apparent viscosity remains constant [49].

The structural kinetics model, which can be seen in Equation 1.10, assumes that a shear-induced breakdown of the internal structure during shearing depends on the kinetics of the process from structured to non-structured state.

$$\left[\frac{(\eta - \eta_{t\infty})}{(\eta_{t0} - \eta_{t\infty})}\right]^{1 - n_b} = (n_b - 1)\, kt + 1 \qquad \textbf{1.10}$$

This model utilizes the apparent viscosity at structured state η_{t0} at $t = 0$ as well as at non-structured state $\eta_{t\infty}$ at $t \rightarrow \infty$. The order of the structure breakdown reaction is represented by n_b and the constant k is the breakdown rate [15]. Table 1.3 shows the application of these models to different products.

Table 1.3: Applied rheological models for different products

Products	Weltman	First-order stress decay model, with a non-zero stress	Structural kinetics model
Equation	1.7	1.9	1.10
Ketchup	[3]		
Dressing	[50]		
Mayonnaise			[15]
Fruit puree	[3,51]	[51]	
Hydrocolloid dispersion		[48,52]	[15]
Starch dispersion	[53,54]		

1.1.2.3 Shear rate

Processing of middle to high viscosity foodstuff can compromise different unit operations resulting in a wide range of shear rates. Depending on the process or situation these can vary from low values during sedimentation of particles up to high shear rates observed during spraying drying. In Table 1.4 typical shear rates from different areas are displayed.

Table 1.4: Typical shearrates of processes related to food and food processing

Situation	Shear rate $\dot{\gamma}$ (s^{-1})	Application	Source
Sedimentation of particles	10^{-6} - 10^{-3}	Spices in salad dressing, fruit juices	[43,55,56]
Chewing and swallowing	10^{1} - 10^{2}	Food, tooth paste	[43,55,56]
Mixing and stirring	10^{1} - 10^{3}	Food processing	[43,57,58]
Pipe flow	10^{0} - 10^{3}	Food processing	[43,55,56]
Spraying	10^{3} - 10^{5}	Spray drying, spray painting	[43]

The continuous phase of food suspensions and emulsions is typically water and thus in first proximity a Newtonian fluid. The rheological behavior however is dependent on the dispersed discontinuous phase either solid particle, liquid droplet or a mixture of both. In section 1.1.1.2 the basic structuring components of suspensions like fibers and cell fragments as well as oil droplets in emulsions are identified. Figure 1.6 shows the arrangement of these dispersed particles at rest and under shearing conditions. Suspensions show a randomly dispersed particles which change to an orientated status under shearing (Figures 1.6a and 1.6b). Emulsions tend to disaggregation of agglomerates and deformation of spheroidal droplets to elliptical shape (Figures 1.6c and 1.6d) [44].

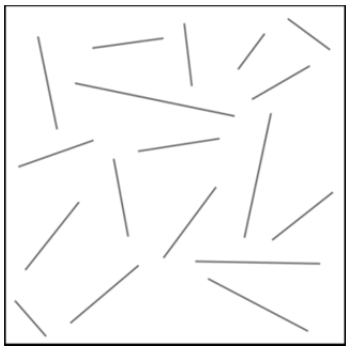

(a) Suspension at rest

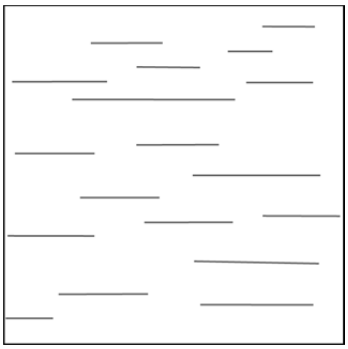

(b) Suspension during shearing

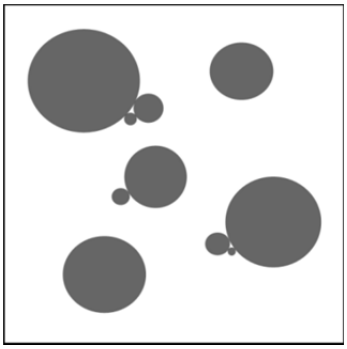

(c) Emulsion at rest

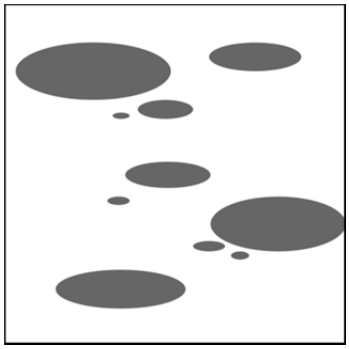

(d) Emulsion during shearing

Figure 1.6: Structural changes of dispersions showing non-Newtonian flow behavior

As a result of different compositions and thus different microscopic structures the rheological behavior of these fluids can be assigned as non-Newtonian. Typical flow and viscosity curves of time-independent non-Newtonian fluids are depicted in Figure 1.7. Depending on the characteristics of a fluid, shear-thinning flow behavior can occur, which is characterized by decreasing viscosity at increasing shear rate and can also be called pseudoplastic.

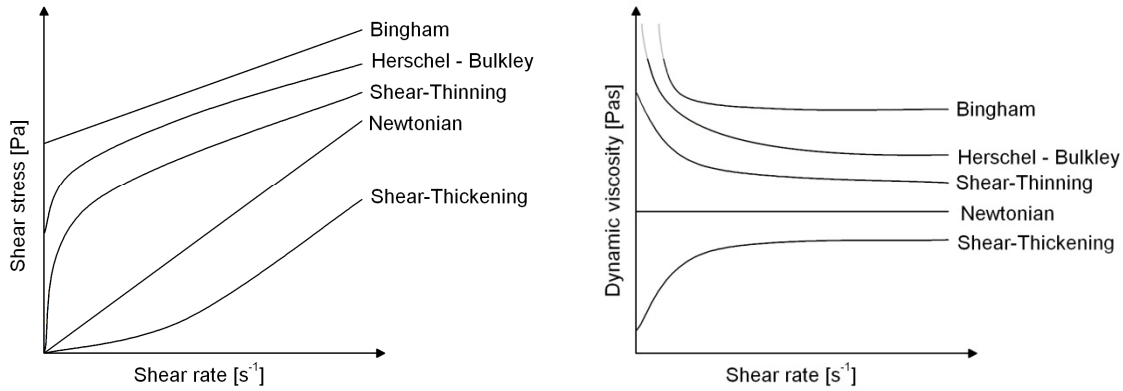

(a) Flow curves (b) Resulting viscosity curves

Figure 1.7: Flow and viscosity curves for typical time-independent fluids

As consequence of the capability to store mechanical energy some fluids possess a yield stress τ_0, which represents a finite stress to achieve flow of the fluid. Bingham plastic and Herschel-Bulkley materials are characterized by the presence of a yield stress and possess solid like characteristics below the yield stress. Beyond this characteristic stress the internal structure collapses resulting in a drop in viscosity and elasticity [46].

Fluids which exhibit an increase of viscosity with rising shear rate are called shear-thickening or dilatant respectively [43].

Various mathematical models are utilized to describe functional relationships of viscosity and shear rate or shear stress and shear rate respectively. However most of these relationships can be derived by variation of the elements of the general Equation 1.11, where the shear stress τ is the sum of yield stress τ_0 and the product of consistency coefficient K and shear rate $\dot{\gamma}$ to the power of the flow behavior index n. The flow behavior index gives further detail on the general flow behavior, namely $n < 1$ for shear thinning, $n = 1$ for Newtonian and $n > 1$ for shear thickening.

$$\tau = \tau_0 + K\,\dot{\gamma}^{\,n} \qquad \textbf{1.11}$$

Newtonian fluids are considered to be the simplest type of matter, since the shear rate is direct proportionate with the shear stress resulting in a shear rate independent material constant (see Equation 1.12) with a flow behavior index n = 1. In this case the consistency coefficient K is usually written as dynamic viscosity η.

$$\tau = K\,\dot{\gamma}^{\,1} = \eta\,\dot{\gamma}^{\,1} \qquad \textbf{1.12}$$

The flow function of most middle to high viscosity foodstuffs follows non-Newtonian flow behavior, which can be mathematically described by various attempts, which are described subsequently. The Bingham plastic basically consists of the Equation for Newtonian fluids but adds a yield stress τ_0 to Newtonian behavior resulting in Equation 1.13.

$$\tau = \tau_0 + K\,\dot{\gamma}^{\,1} \qquad \textbf{1.13}$$

The Ostwald-de-Waele differs from the before mentioned model by implementation of the parameter flow behavior index n as an exponent (see Equation 1.14).

$$\tau = K\,\dot{\gamma}^{\,n} \qquad \textbf{1.14}$$

Equation 1.15 shows the Herschel-Bulkley model, which extends the Ostwald-de-Waele Equation by the addition of a yield stress τ_0 to the basic Equation.

$$\tau = \tau_0 + K\,\dot{\gamma}^{\,n} \qquad \textbf{1.15}$$

The Casson model (Equation 1.16) is a structure based model, which was initially developed for printing ink and was adopted for interpretation of chocolate flow behavior by the International Office of Cacao and Chocolate. The Casson is similar to the Bingham plastic model since both have a yield stress; the difference is the power of 0.5 of each element [43].

$$\tau^{0,5} = \tau_0^{\,0,5} + K\,\dot{\gamma}^{\,0,5} \qquad \textbf{1.16}$$

The modified Casson model, which can be seen in Equation 1.17 substitutes the power of 0.5 with the exponent n_1, allowing the modeling of non-linear relationships.

$$\tau^{0,5} = \tau_0^{0,5} + K\,\dot{\gamma}^{n} \qquad \textbf{1.17}$$

The Carreau model represents an expanded version of the before mentioned non-Newtonian models, where consistent values flow behavior over the entire shear rate range are assumed. However this model takes very low and very high shear rates into consideration, which is for some samples characterized by Newtonian flow. The model (Equation 1.18) introduces the parameters limit viscosity at low shear rate η_0, η_∞ is the viscosity at high shear rates the time constant λ, which represents the inversion of the shear rate at which the fluid changes from Newtonian to power-law behavior, and n is the flow behavior index [44].

$$\eta = \eta_\infty + (\eta_0 - \eta_\infty)\,[1 + (\lambda\,\dot{\gamma})^2]^{\frac{n-1}{2}} \qquad \textbf{1.18}$$

Various other models besides the presented models exist, however these are mostly used for the mathematical characterization of flow curves of middle to high viscosity foodstuffs.

Table 1.5 shows the most common rheological models in literature and their application to different food products.

Table 1.5: Applied rheological models for different food products

Products	Ostwald-de-Waele	Herschel-Bulkley	Casson	Modified Casson	Carreau
Equation	1.14	1.15	1.16	1.17	1.18
Ketchup	[36,59,60,61]	[59,62,63,64]		[62]	[38]
Dressing	[50,65,66]		[50]		[22,50,67,68]
Mayonnaise	[69,70]	[18,30,65,71,72,73,74,75]			[18,76,77]
Low-fat mayonnaise		[18,62,73]		[62]	
Fruit puree	[78]	[79,80]		[62]	
Tomato concentrate	[60,63,81]				[38]
Hydrocolloid dispersion	[48,49,52,70,82,83,84]	[82,84,85]			[86]
Starch dispersion	[13,53,82,87,88,89]	[53,90]	[91]		

1.1.2.4 Temperature

Foods are exposed to variations in temperature during manufacturing processes e.g. pasteurization, sterilization, evaporation, cooking, freezing, chilling, etc.. These temperature changes can cause desired alterations in the chemical and physical properties of a sample. During the production of sauces different processing routes can occur, implying varying temperature profiles depending on the specific product. Full fat mayonnaises are usually produced at lowered or ambient temperatures without additional application of heat to prevent creaming and coalescence, whereas only applied mechanical energy during homogenization or pumping processes can lead to increased temperatures.

Fat reduced products with a continuous phase thickened by starch for example require a processing step during which gelatinization can occur to allow bulking and formation of networks of these substances. In addition the increased water content due to fat replacement may cause microbiological instabilities, which require a pasteurization step at temperatures of 85 - 95 °C for 15 - 120 minutes. Likewise most of ketchups are exposed to heat during a pasteurization step [12].

The rheological properties of matter considerably depend on temperature [42,43]. In many cases depending on the ingredients of a product, viscosity decreases with rising temperature and vice versa [54,66].

The influence of temperature on the viscosity of Newtonian fluids can be mathematically modeled by utilization of an Arrhenius type equation (Equation 1.19), where η_{ref} is the proportionality constant at a reference temperature, T is the absolute temperature, T_{ref} is the reference temperature, R the universal gas constant and E_a the energy of activation for the viscosity. A stronger dependency on temperature is indicated by a higher energy of activation value [92].

$$\eta = \eta_{ref} e^{\left[\frac{E_a}{R}\left(\frac{1}{T} - \frac{1}{T_{ref}}\right)\right]} \qquad \textbf{1.19}$$

Equation 1.19 can be modified for Ostwald-de-Waele fluids to Equation 1.20. The reference viscosity η_{ref} is changed to consistency coefficient K_{ref} at a reference temperature. In addition it is assumed that temperature has a negligible influence on the

flow behavior index n (see Equation 1.14), leaving the consistency coefficient K' as variable [43,49].

$$K' = K_{ref}\, e^{\left[\frac{E_a}{R}\left(\frac{1}{T} - \frac{1}{T_{ref}}\right)\right]} \qquad \textbf{1.20}$$

The effect of temperature can also be modeled using the Williams-Landel-Ferry Equation, which is specified by a viscosity η_{ref} at a reference temperature T_{ref} and the constants C_1, C_2 and the absolute temperature T (see Equation 1.21).

$$\eta = \eta_{ref}\, e^{\left(\frac{-C_1 (T - T_{ref})}{C_2 (T - T_{ref})}\right)} \qquad \textbf{1.21}$$

The Williams-Landel-Ferry Equation was initially developed in the field of polymer science, employing the averaged values of glass transition temperature as reference temperature and the constants $C_1 = 8{,}86$ and $C_2 = 101{,}6$ K of several polymers, allowing a good fit for most polymers [93]. In systems with an unknown or a not reliably measurable glass transition temperature, the adaptation of constants C_1 and C_2 to another reference temperature is convenient [94]. The Williams-Landel-Ferry Equation is very useful in modeling the viscosity of amorphous foods above the glass transition temperature. The mentioned models are commonly applied to different products and can be seen in Table 1.6.

Table 1.6: Applied temperature dependent models for different food fluids

Products	Arrhenius	Williams-Landel-Ferry
Ketchup	[59]	
Dressing	[50]	
Fruit puree	[78,79]	
Hydrocolloid dispersion	[52]	
Honey		[95,96]

1.1.2.5 Pressure

In continuous industrial production fluid products are usually pumped through pipe system from a processing step to following. Increasing pipe length or rising amount of installed equipment implies an increasing pressure drop, which is caused by frictional forces of the fluid during flow processes. For the compensation of the pressure drop the application of pumps is required.

For some substances the relationship between pressure P and dynamic viscosity η can expressed by Equation 1.22.

$$\eta = \eta_f e^{(\beta P)} \qquad \textbf{1.22}$$

Whereas η_f is a viscosity coefficient and β is the pressure coefficient, which is a function of the hole volume V_H and absolute temperature T and R is the universal gas constant (Equation 1.23) [97].

$$\beta = \frac{V_H}{RT} \qquad \textbf{1.23}$$

For non-Newtonian fluids the Ostwald-de-Waele model is incorporated and leads to Equation 1.24. The consistency coefficient K and ε are constants, T is the absolute temperature, $\dot{\gamma}$ the shear rate and n the flow behavior index and η_f in Equation 1.22 is substituted by the expression 1.24 [97].

$$\eta_f = K e^{(\varepsilon T)} \dot{\gamma}^{n-1} \qquad \textbf{1.24}$$

Investigations of the influence of pressure on the viscosity function of foodstuffs are few and mostly referring to high pressure processing with pressures in the range of 100 MPa to 1000 MPa [98]. For normal processes it is assumed, that the influence of pressure on the viscosity of most liquids is constant up to 10 MPa and thus negligible [99].

1.1.2.6 Combination of shear rate and temperature

The effect of shear rate and temperature dependency of non-Newtonian fluids can be combined into a single expression. Whereas the Ostwald-de-Waele and the Arrhenius type Equation are combined, which can be seen in Equation 1.25, with the assumption that the consistency coefficient K_T is temperature dependent and the flow behavior index $\bar{n}$ index is independent from temperature [43,100].

$$\tau = f(T, \dot{\gamma}) = K_T e^{\left(\frac{E_a}{RT}\right)} (\dot{\gamma})^{\bar{n}} \qquad \textbf{1.25}$$

The apparent viscosity in dependency of shear rate and temperature can be calculated using Equation 1.26.

$$\eta_a = f(T, \dot{\gamma}) = K_T \, e^{\left(\frac{E_a}{RT}\right)} (\dot{\gamma})^{\bar{n}-1} \qquad \textbf{1.26}$$

The final model is capable to predict the flow or viscosity curves at any temperature in the determined range and can be useful in solving food engineering problems such as those requiring a prediction of the fluid velocity profile or pressure drop during tube flow [43].

1.2 Objectives

The present research work "Examination and Modeling of Rheological Properties of Middle to High Viscosity Foodstuff" focuses on the development of an observation-based prediction model for rheological properties of foodstuff with middle to high viscosity on the basis of the underlying food composition. Resultant two objectives can be derived:

1. Comprehensive rheological characterization of commercial middle to high viscosity foodstuffs.

2. Development of a prediction model for rheological properties of an unknown product based on the composition of carbohydrates, proteins, fats and water.

2 Experimental Part

The present work “Examination and Modeling of Rheological Properties of Middle to High Viscosity Foodstuff” can be divided into two parts, whereas in the first part a representative range of commercial products with middle to high viscosity were investigated rheologically under application-orientated boundary conditions.

The variables for this examination were time, shear rate and temperature. Depending on the particular parameter the resulting data was fitted using different approximation models. The most appropriate models for the description of time, shear rate and temperature dependent flow behavior were determined.

In the second part the composition data was correlated with previous investigated rheological parameters aiming at a model for the prediction of the rheological properties of an unknown product based on the composition of proteins, carbohydrates, fats and water.

2.1 Products of investigation

For characterization 55 different sauces were purchased at retail markets in Spain, Germany, United Kingdom and Switzerland and stored in a cold store at 5 °C. The list of investigated products and their corresponding composition of proteins, carbohydrates, fats and water can be seen in Table 2.1.

In addition the products are roughly classified for the sake of conciseness in groups: ketchup (K), condiment (C), fat reduced mayonnaise and dressings (L) and classical mayonnaise (M). The composition information was taken from nutrition labeling of the manufacturer, which is based on the Directive 90/496/EEC on nutrition labeling for foodstuffs, Article 6 [101].

The declared values can be based on the manufacturer's analysis of the food, a calculation from the known or actual average values of the ingredients used or a calculation from generally established and accepted data [101].

Table 2.1: Investigated commercial products and corresponding composition of proteins, carbohydrates, fats and water

No.	Product name	Group	Proteins [%]	Carbo-hydrates [%]	Fats [%]	Water [%]	Thickener
1	MClassic Hot Ketchup	K	1.5	24	0	74.5	1
2	MClassic Ketchup	K	1.5	24	0	74.5	1
3	Tomato ketchup COOP	K	1.5	22	0	76.5	1
4	COOP Naturplan Bio Ketchup	K	2	23	0	75	1
5	MAHRAM Ketchup	K	0.2	22.3	0	77.5	
6	Prix Garantie Ketchup COOP	K	1	16	0	83	1
7	Jütro Ketchup	K	1.9	23	0.1	75	2, 3, 4
8	Livio Tomaten Ketchup	K	2.6	21.8	0.1	75.5	
9	Knorr Tomaten Ketchup	K	1	18	0.1	80.9	2, 5
10	Linessa Light Tomaten Ketchup	K	1.8	6.3	0.1	91.8	
11	Kania Tomaten Ketchup	K	1.6	24	0.1	74.3	
12	Halal Tomatenketchup	K	0.8	18.7	0.1	80.4	2
13	Heinz BIO Ketchup	K	1.5	28.9	0.2	69.4	
14	Knorr Curry Ketchup	K	0.7	22	0.2	77.1	2, 4, 5
15	Kim Tomaten Ketchup	K	1.6	23.7	0.2	74.5	1
16	BeLight Tomaten Ketchup	K	1.7	6.6	0.2	91.5	1, 5
17	Jütro Tomaten Ketchup Hot	K	1.5	18.1	0.3	80.1	2, 3
18	Knorr Tomato Joe	K	1	18	0.4	80.6	2, 3, 5
19	Heinz Ketchup	K	1.33	27.33	0.67	70.67	
20	Heinz LIGHT-Ketchup	K	1.07	18.67	0.67	79.59	
21	Daddies Favourite Brown Sauce	C	0.9	24.3	0.1	74.7	
22	HP Sauce The Original	C	1.1	27.1	0.2	71.6	1
23	Hela Schaschlik Gewürzketchup pikant	C	1.1	30.8	0.3	67.8	1
24	Hela Knoblauch Gewürzketchup würzig	C	1	29.9	0.3	68.8	1
25	Hela Barbecue Gewürz Ketchup	C	1.2	36.9	0.3	61.6	1
26	Vitakrone Gewürzketchup Curry	C	0.6	20.6	0.3	78.5	1, 3, 6
27	Heinz Curry Gewürz Ketchup Chili	C	0.9	28.5	0.5	70.1	2, 3, 5
28	Calvé Salsa Barbacoa	C	0.8	29	0.6	69.6	1
29	Kraft Barbecue Sauce	C	1	19	1.9	78.1	2, 7
30	LOUIT Mostaza – mustard	C	3.3	8.3	4	84.4	1
31	Mclassic Currysauce	C	1.5	4	35	59.5	1, 5
32	COOP Curry Sauce	C	3.5	11	39	46.5	3, 5

No.	Product name	Group	Proteins [%]	Carbo-hydrates [%]	Fats [%]	Water [%]	Thickener
33	THOMY légère	L	0.9	14.2	4.8	80.1	2,3,4
34	Miracel Whip Balance	L	0.4	10.5	10.5	78.6	2, 5
35	Thomynaise ohne Cholesterin	L	1.5	8	13	77.5	2, 5
36	Extraleichte Salatcreme 15%	L	1.4	12.9	15.4	70.3	2, 5
37	BeLight leichte Salatcreme	L	0.4	9.8	16.7	73.1	2, 3, 5
38	Miracel Whip	L	0.3	12	22.5	65.2	2, 3, 4
39	Heinz Salad Creme Original	L	1.4	20	26.8	51.8	1, 3, 5
40	Thomy Joghurt Salat-Creme	L	1.2	10.9	27.1	60.8	2, 3
41	Vita D´or Leichte Salatcreme	L	1	12	30.3	56.7	1, 2, 3, 4
42	MIGROS Léger Fit-onnaise Classic	L	1.5	4	32	62.5	1, 5
43	Mayonnaise Weightwatchers COOP	L	1.5	3	37	58.5	1, 5
44	Thomy Salatmayonnaise	L	0.4	8.3	54.1	37.2	2
45	Freeform mayonnaise	M	0.5	0.5	69	30	2, 3
46	Hellmann´s Gran Mayonesa	M	1.1	2.1	69	27.8	1
47	PRIX Garantie Mayonnaise	M	1	2	70	27	5
48	Prima Alioli Suave	M	0.9	1.5	71.8	25.8	3, 5
49	MIGROS Budget Mayonnaise	M	1	0.8	72	26.2	5
50	MClassic Mayonnaise mit Senf	M	1.5	1	76	21.5	1
51	MIGROS Mayonnaise	M	1.5	0.5	81	17	
52	COOP Naturaplan bio Mayonnaise	M	1.5	0	81	17.5	
53	MClassic Mayonnaise (free range eggs)	M	1.5	0.5	81	17	
54	MIGROS Bio Mayonnaise	M	1.5	0.5	82	16	
55	MClassic Mayonnaise	M	1	0.5	82	16.5	

1-maize starch 2-modified starch 3-guar gum 4-locust bean gum 5-xanthan gum 6-tara gum 7-alginate

2.2 Rheometer and software

All rheological measurements were performed with a Thermo Haake R-S 300 rheometer combined with a Haake universal temperature controller (UTC). A Lauda MGW RCS/RG6 water bath was connected to the UTC and was set at T = 6 °C. In order to avoid slippage a parallel serrated plate/plate measuring device was selected [22,71,76,102]. The detailed characteristics of the plate PP35 PR with a diameter of 35 mm can be seen in Table 2.2. The gap size for all tests was set at 1 mm according to literature [71,103,102,104,105]. Each time the measurement device was fitted to the rheometer the zero point was adjusted.

Table 2.2: Characteristics of measuring device; Plate PP35 PR

A-factor	118725 Pa
M-factor	8.752 s^{-1}
Diameter	35.006 mm
Torque of inertia	1.316 e^{-06} kg·m²
Absorption	30

The rheometer was controlled by the software HAAKE RheoWin Job Manager 4.20.0002. The export of the measurement data was performed with the HAAKE RheoWin Data Manager 4.20.0002. The exported text files were evaluated by a specifically developed program in National Instruments LabVIEW 2009 integrating the statistic software R 2.12.1 (The R Foundation for Statistical Computing), the general program routine for data evaluation can be seen in chapter [sub:Data-evaluation]. The prediction model for rheological properties of an unknown product based on the composition of carbohydrates, proteins, fats and water was evaluated with the statistic software R 2.12.1 (The R Foundation for Statistical Computing) and the add-on R Commander 1.6-3 [106].

2.3 Methodology of rheological measurements

For the calculation of flow processes the viscosity function of a fluid is of main interest. The viscosity can be influenced by various parameters as in sections 1.1.2.2- 1.1.2.5 discussed. During production processes products are exposed to mechanical and thermal stress, which results in the investigation of the dependency on shear rate, temperature, and duration of stress.

The dependency of concentration on the viscosity was not evaluated since commercial products were part of the investigation, which did not allow systematic variation of this parameter. The influence of pressure on the viscosity was neglected, because it was assumed that middle to high viscosity foodstuffs are not exposed to a high pressure process step ($p > 100$ MPa) once in final composition. For the acquisition of the needed data a number of different rheological tests with boundary conditions similar to production processes were performed.

2.3.1 Time dependency at constant shear rate and temperature

Many middle to high viscosity foodstuffs exhibit time dependent flow behavior, which have to be considered for proper design and process evaluation [15]. The time dependent flow behavior was examined by performance of measurements at constant shear rate and constant temperature for 480 s. The performance of a hystersis loop, which comprises an ascending and subsequently descending shear ramp, whereas the area between the resulting curves indicates the degree of thixotropy or rheopexy, was not conducted. In doing so, time and shear rate dependency are observed superimposed, complicating the assignment of the single influences [47]. The detailed measurement procedure can be seen in Table 2.3. Each setting was repeated five times.

Table 2.3: Procedure for time-dependent measurements

Program step	Temperature in (°C)	Duration in (s)	Shear rate in (s^{-1})	Measuring point duration
Temperature equalization	5	300	-	-
Constant shear	5	480	300	linear

2.3.2 Shear rate dependency at constant temperature

During pipe flow, mixing and stirring shear rates are typically in the range of $\dot{\gamma} = 10^0 - 10^3\ s^{-1}$ (see

Table 1.4). In order to cover this range the shear rate was increased from low value to a maximum. Before the measurement of the shear rate dependent flow behavior a pre-shear step was incorporated in the program sequence to ensure that the material reached destructed structure at which the rheological behavior is no longer dependent on shearing time [15].

In the following subsections the detailed measurement program sequences are described. The test was performed at different temperatures. The detailed measurement procedure can be seen in Table 2.4. Each test was repeated at least three times.

Table 2.4: Procedure for shear rate dependent measurements

Program step	Temperature in (°C)	Duration in (s)	Shear rate in (s^{-1})	Measuring point duration
Temperature equalization	5, 25, 55	300	-	-
Pre-shear	5, 25, 55	120	300	-
Shear ramp	5, 25, 55	180	1-500	linear

2.3.3 Temperature dependency at constant shear rate

Foodstuff with middle to high viscosities are exposed to thermal stress, either during heating and chilling processes or during intensive mechanical stress by heat dissipation e.g. during homogenization. For the avoidance of phase separation of emulsions and phase changes of ingredients e.g. gelatinization of starch; a temperature range of T = 5-55 °C for the investigation was chosen. The temperature was gradually increased, whereas the shear rate was kept constant. The test was performed at four different shear rates. Before the measurement of the temperature dependent flow behavior a pre-shear step was incorporated in the program sequence to ensure that the material reached destructed structure at which the rheological behavior is no longer dependent on shearing time [15].

The detailed measurement procedure can be seen in Table 2.5. Each test was repeated at least three times.

Table 2.5: Procedure for temperature dependent measurements

Program step	Temperature in (°C)	Duration in (s)	Shear rate in (s^{-1})	Measuring point duration
Temperature equalization	5	300	-	-
Pre-shear	5	120	300	-
Temperature steps	5-55	480	1, 10, 100, 500	linear

2.4 Evaluation of measurement data

The evaluation of the rheological measurement data followed a general program sequence, which is depicted in the flowchart in Figure 2.1. After data extraction from the

measurement files the subprogram “Fitting model to data” was performed, whereas different models depending on the underlying test are fitted to acquire measurement data using the least square method.

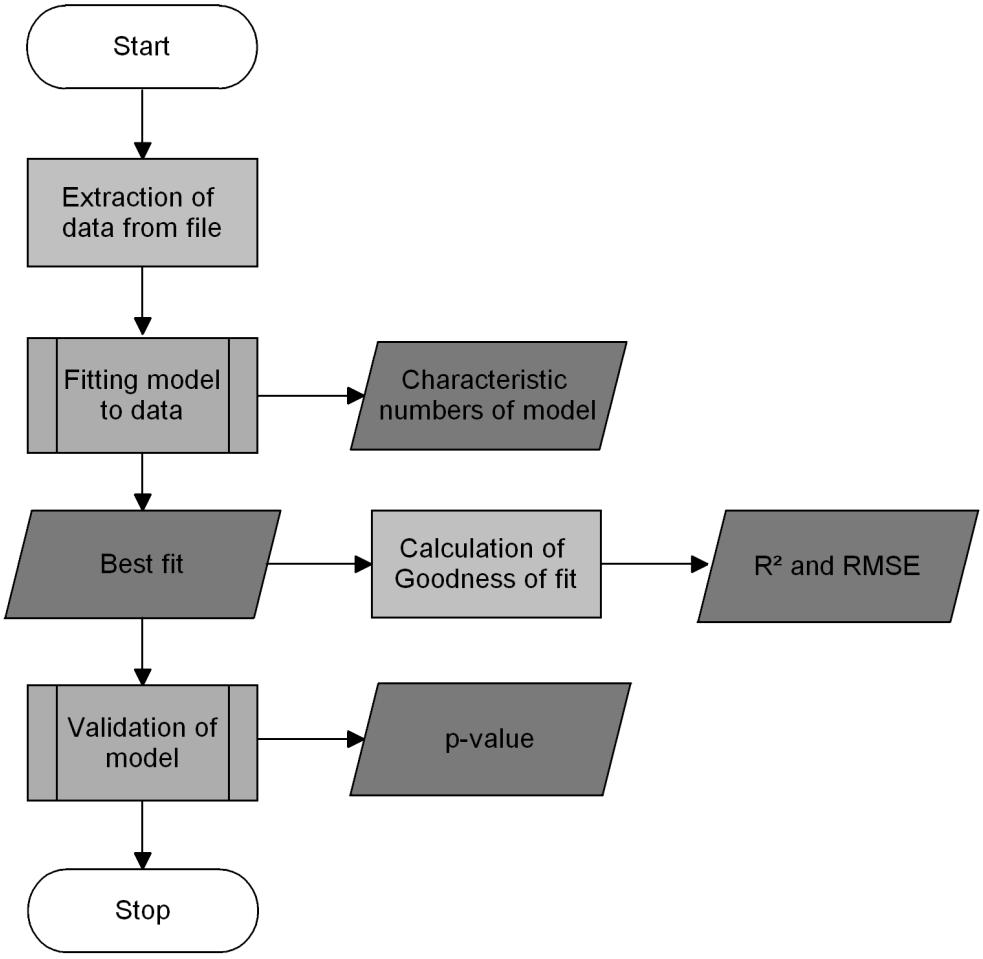

Figure 2.1: General program routine for data evaluation

The applied models for the dependency of viscosity on time were fitted to Weltman, First-order stress decay model, with a zero stress, First-order stress decay model, with a non-zero stress and the Structural kinetics model (Equations 1.7-1.10). The shear rate dependent flow behavior was modeled by application of Bingham, Ostwald-de-Waele, Herschel-Bulkley, Casson, Modified Casson, and Carreau according to Equations 1.13-1.18. The influence of temperature on the rheological properties was described by Arrhenius and Williams-Ferry-Landel (Equations 1.19 and 1.21).

In a next step the goodness of fit of each model was described by calculation of the statistical measures coefficient of determination R^2 (Equation 2.1) and the root mean square error RMSE (see Equation 2.2).

$$R^2 = \sqrt{\frac{\sum_{i=1}^{N} (F_{exp,i} - \bar{F}_{exp,i})^2 - \sum_{i=1}^{N} (F_{exp,i} - F_{cal,i})^2}{\sum_{i=1}^{N} (F_{exp,i} - \bar{F}_{exp,i})^2}} \quad \textbf{2.1}$$

$$RMSE = \sqrt{\frac{\sum_{i=1}^{N} (F_{exp,i} - F_{cal,i})^2}{N}} \quad \textbf{2.2}$$

The selection procedure of the models consisted of different steps. At first the coefficient of determination R^2, which is a normalized parameter to measure the goodness of fit, was evaluated. The closer the R^2 value to 1, the better was the fit. In a second step the root mean square error RMSE was analyzed, whereas smaller RMSE values imply a better the fit. In a third step the residua of a model were tested for normal distribution for validation by application of the Shapiro-Wilk-Test at a level of significance of $\alpha = 0.05$ [107]. The significance of the normal distribution was stated by the p-value, which is the probability of obtaining an experimental situation assuming that the null hypothesis is true. The null hypothesis was rejected when the p-value was less than $p < 0.05$ [107]. A model was selected if it was conform to the mentioned parameters.

If more than 65 % of the overall measurements of a product could be validated by a specific model, it was assumed that it was applicable to reproduce the characteristics of the underlying product. In the case of two or more applicable models according to this definition the model with the fewest parameters was selected.

The parameters of the validated model were tested for normal distribution applying the David Test, whereas the null hypothesis states that there is no difference between the observed and the normal distribution [108]. If the null hypothesis was not rejected, the arithmetic average value and the standard deviation were calculated. The adequate models for the description of shear rate, time and temperature dependency of the product range were defined and used for the prediction of the rheological properties.

2.5 Prediction of rheological properties

The prediction of the rheological properties represented by different characteristic parameters and the composition data were checked for linear and multiple linear

regression. In a first step a multiple two-variable scatter plot was created, to identify graphically general correlation.

If a correlation was observed a potential model was established. The coefficients of the determined model were checked for significance using the t-test. When no significance of a coefficient was observed, the model was modified and rechecked statistically. The goodness of fit was described by calculation of the coefficient of determination R^2 and the root mean square error RMSE. The coefficient of determination R^2 was tested for significance utilizing the Omnibus F-Test, which states the null hypothesis corresponds zero [109]. After rejection of the null hypothesis the residua of the model were tested for normal distribution using the Shapiro-Wilk-Test [107].

3 Selection of rheological models

In the following sections 3.1-3.3 the results of the experimental measurements are presented with the focus on the selection of reliable mathematical models for the description of the time, shear rate and temperature dependency of different samples. After the selection of appropriate models for each influencing factor a general model, which incorporates shear rate and temperature dependencies, is developed.

3.1 Time-dependent flow behavior

The time-dependent flow behavior was determined by the performance of shear stress measurements at a constant shear rate and constant temperature. Typical experiments obtained for the various products are exemplary shown in Figure 3.1.

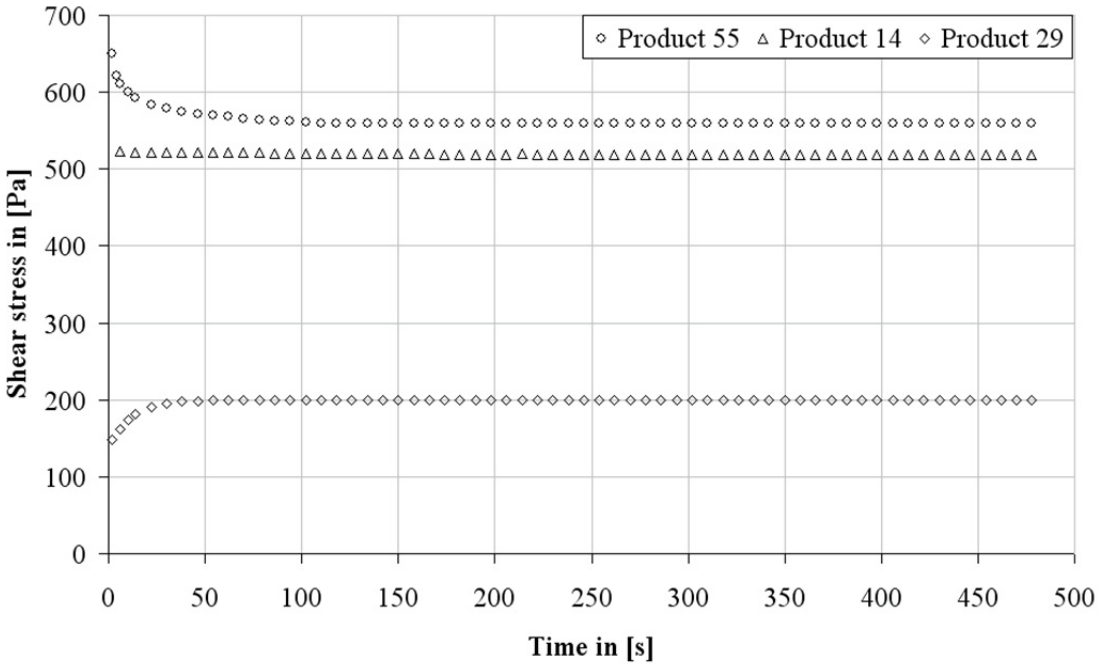

Figure 3.1: Shear stress data of products 55, 14, 29 as a result of constant shear rate $\dot{\gamma} = 300\ s^{-1}$ at T = 5 °C for 480 s.

Different flow behaviors ranging from time-independent e.g. curry ketchup no. 14 to time-dependent flow behavior e.g. MClassic mayonnaise no. 55 and Kraft barbecue sauce no. 29 was observed. During the first 100 s of constant shearing the time-dependent samples exhibited a rapid decrease in shear stress and thus viscosity. This observation was conform to the ones made for thixotropic seed gum solutions [49], salep and balangu [48], model mayonnaise [15] and ketchup [64]. After 120 s a constant value of shear stress, which can be assigned as equilibrium state, was observed for almost all products. Koocheki and Razavi [49] as well as Razavi and Karazhiyan [48] report of longer times to obtain steady state values at constant shear rate $\dot{\gamma}$ = 14, 25, 50 s^{-1}, but also admit that the breakdown of the internal structure is strongly dependent on the applied shear rate implying a more rapid breakdown with increasing shear rate.

The ratio of the initial and equilibrium viscosity $\frac{\eta_0}{\eta_\infty}$ was used to identify time-dependent flow behavior and describe the extent of hysteresis. In addition this value gives a relative measurement of the amount of structural breakdown or buildup [49,110].

Table 3.1 shows the ratios of initial and equilibrium viscosity for all products and allows the differentiation of the product range into time-independent $\left(\frac{\eta_0}{\eta_\infty} = 1\right)$, rheopectic $\left(\frac{\eta_0}{\eta_\infty} < 1\right)$, and thixotropic $\left(\frac{\eta_0}{\eta_\infty} > 1\right)$ samples. Samples 2, 9 and 44 show significant negative difference from time-independent flow behavior and thus can be considered to exhibit rheopectic flow behavior, which implies an increase of viscosity in dependence on time.

The products could not be accounted to a one specific group, however all products were thickened according to their list of ingredients (see Table 2.1) with maize starch. Sharoba et al. [64] report as well of rheopectic flow behavior for some commercial tomato ketchups, which can be referred to the high percentage of starch in the products. Dewar and Malcolm [111] also observed rheopectic behavior for maize starch thickened foods and assume that shearing results in structure formation due to additional starch granules to be sheared open and restricted Brownian motion in thicker samples due to less solvent between starch molecules.

A significant decrease of viscosity with ongoing shearing time and thus thixotropic flow behavior could be observed for the products 4, 21, 24, 30, 34, 36 and 40. The

remaining samples did not show significant time-dependent flow behavior under the applied boundary conditions.

Table 3.1: Arithmetic means and standard deviation of the ratio of initial and equilibrium viscosity for characterization of time-dependent flow behavior. Letters indicate significant difference (α = 0.05) from time-independent flow behavior

No.	Group	$\frac{\eta_0}{\eta_\infty}$		No.	Group	$\frac{\eta_0}{\eta_\infty}$		No.	Group	$\frac{\eta_0}{\eta_\infty}$	
1	**K**	0.87 ± 0.01		**20**	**K**	1.01 ± 0.04		**38**	**L**	1.07 ± 0.02	
2	**K**	0.84 ± 0.02	**a**	**21**	**C**	1.08 ± 0.02	**b**	**39**	**L**	0.98 ± 0.01	
3	**K**	1.11 ± 0.04		**22**	**C**	0.97 ± 0.03		**40**	**L**	1.10 ± 0.04	**b**
4	**K**	1.24 ± 0.21	**b**	**23**	**C**	1.00 ± 0.05		**41**	**L**	1.03 ± 0.02	
5	**K**	1.02 ± 0.06		**24**	**C**	1.15 ± 0.05	**b**	**42**	**L**	1.09 ± 0.07	
6	**K**	1.03 ± 0.04		**25**	**C**	0.99 ± 0.01		**43**	**L**	1.04 ± 0.03	
7	**K**	1.06 ± 0.02		**26**	**C**	1.02 ± 0.01		**44**	**L**	0.87 ± 0.03	**a**
8	**K**	0.97 ± 0.01		**27**	**C**	1.00 ± 0.00		**45**	**M**	1.07 ± 0.04	
9	**K**	1.00 ± 0.02		**28**	**C**	0.99 ± 0.02		**46**	**M**	1.08 ± 0.03	
10	**K**	1.03 ± 0.01		**29**	**C**	0.83 ± 0.01	**a**	**47**	**M**	1.06 ± 0.04	
11	**K**	1.00 ± 0.01		**30**	**C**	1.20 ± 0.01	**b**	**48**	**M**	0.99 ± 0.07	
12	**K**	1.00 ± 0.06		**31**	**C**	0.99 ± 0.02		**49**	**M**	1.07 ± 0.07	
13	**K**	1.07 ± 0.02		**32**	**C**	1.03 ± 0.06		**50**	**M**	0.91 ± 0.02	
14	**K**	1.00 ± 0.01		**33**	**L**	1.02 ± 0.01		**51**	**M**	1.10 ± 0.07	
15	**K**	1.08 ± 0.02		**34**	**L**	1.06 ± 0.03	**b**	**52**	**M**	1.02 ± 0.07	
16	**K**	1.00 ± 0.00		**35**	**L**	1.00 ± 0.05		**53**	**M**	1.05 ± 0.05	
17	**K**	1.00 ± 0.02		**36**	**L**	1.20 ± 0.04	**b**	**54**	**M**	1.04 ± 0.02	
18	**K**	1.01 ± 0.00		**37**	**L**	1.00 ± 0.02		**55**	**M**	1.13 ± 0.05	
19	**K**	1.02 ± 0.02									

The products with significant time-dependent flow behavior were fitted by means of the Weltman, first-order stress decay with a zero stress and first-order stress decay with a non-zero stress, second-order structural kinetic models. Figure 3.2 depicts exemplary the measured and predicted values calculated with previous mentioned mathematical models for product 36, whereas differences in the fit are obvious.

The resulting characteristic parameters of the models of product 36 are shown in Figure 3.2. For validation the residua of a model were tested for normal distribution, whereas a p-value exceeding 0.05 indicated normal distribution. Only the residua of the first-order stress decay with a non-zero equilibrium stress model followed normal distribution $p > 0.05$. The coefficient of determination $R^2 = 0.963$ and the small root mean

square error RMSE = 3.17 indicate a good fit. The other models could not be validated and showed in comparison a worse R^2 and higher values of RMSE. This procedure was repeated for each measurement.

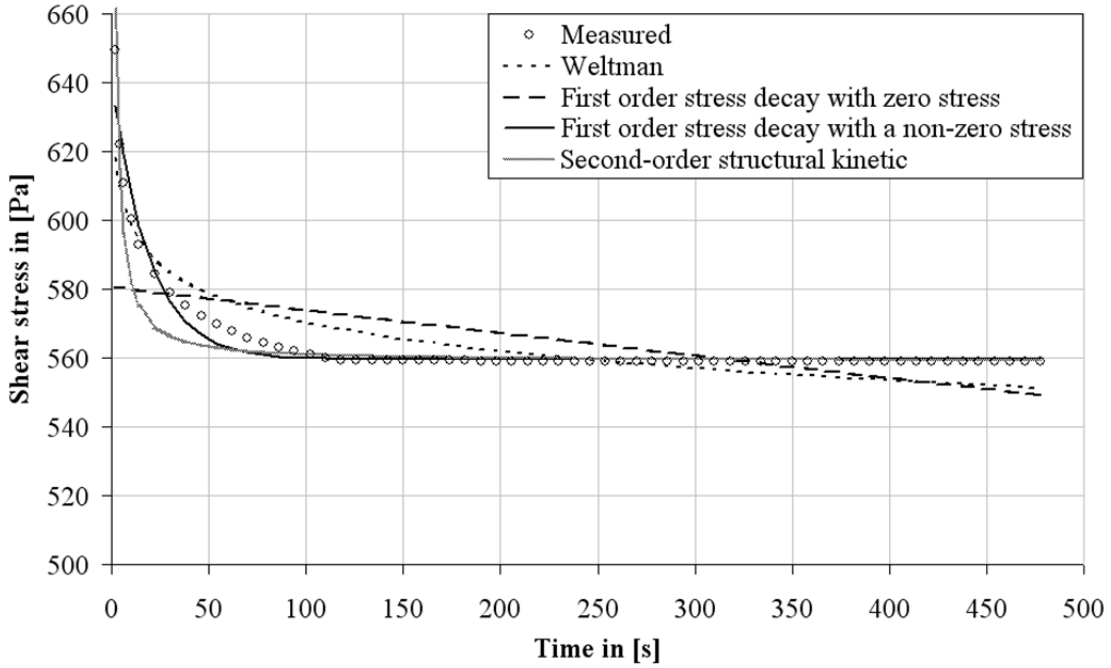

Figure 3.2: Time-dependent models at constant shear rate ($\dot{\gamma}$ = 300 s^{-1}) applied to measured shear stress data of product 36

Table 3.2: Resulting characteristic model parameters, goodness of fit and the probability value of the residua for product 36

Model	Equation	Parameters	R^2	RMSE	Residua p-value
Weltman	1.7	A = 634.37 Pa B = -14.35 Pa	0.819	7.09	$2.1 \cdot 10^{-5}$
First-order stress decay with a zero stress	1.8	τ_i = 604.99 Pa k = -0.0011	0.331	14.48	$4.6 \cdot 10^{-11}$
First-order stress decay with a non-zero stress	1.9	τ_i = 646.51 Pa τ_e = 562.53 Pa k = -0.0653	0.963	3.17	0.059
Structural kinetic model	1.10	η_{t0} = 2.156 Pas $\eta_{t\infty}$ = 1.683 Pas n_b = 2 k = 0.4023	0.875	5.71	0.0002

For evaluation of the most appropriate model for a product the selection procedure, as defined in section 2.4, was followed, at which at least 65 % of a model have to be validated to fulfill the demands of being accepted as general model for a product.

Table 3.3a shows the percentage of models, which can be validated for each model. The first-order stress decay with a non-zero stress model could be validated for all thixotropic products. However product 24, is an exception, because all models could be validated. Similar observations were made for rheopectic products (Table 3.3b) at which the first-order stress decay with a non-zero stress model could be validated for all products. In addition the Weltman model fulfilled the predefined requirements for no. 2 and 44 of the rheopectic samples.

Table 3.3: Comparison of time-dependent models and their corresponding percentage of acceptance depending on the applied model

(a) Thixotropic products

No.	Weltman	accepted (a) - rejected (x)	First-order stress decay with a zero stress	accepted (a) - rejected (x)	First-order stress decay with a non-zero stress	accepted (a) - rejected (x)	Second order structural model	accepted (a) - rejected (x)
4	0	x	0	x	***67***	***a***	33	x
21	40	x	0	x	***100***	***a***	0	x
24	***100***	***a***	***100***	***a***	***100***	***a***	***80***	***a***
30	33	x	0	x	***67***	***a***	0	x
34	0	x	0	x	***80***	***a***	40	x
36	0	x	0	x	***80***	***a***	60	x
40	40	x	20	x	***80***	***a***	0	x

(b) Rheopectic products

No.	Weltman	accepted (a) - rejected (x)	First-order stress decay with a zero stress	accepted (a) - rejected (x)	First-order stress decay with a non-zero stress	accepted (a) - rejected (x)	Second order structural model	accepted (a) - rejected (x)
2	***67***	***a***	0	x	***100***	***a***	0	x
9	60	x	40	x	***100***	***a***	40	x
44	***80***	***a***	0	x	***100***	***a***	0	x

The first-order stress decay model with a non-zero stress (Equation 1.9) was selected for further modeling purposes, since it represented the flow behavior of all thixotropic and rheopectic products. Table 3.4 shows the arithmetic means and their standard deviations of the parameters of the first-order stress decay model with a non-zero equilibrium stress, for a shearing period of 480 s. A good agreement $R^2 > 0.945$ was found between the model-fitted results and experimental shear stress data for all samples. Koocheki and Rizavi [49] also observed that the first-order stress decay model was the more suitable for hydrocolloid suspensions in comparison to the Weltman and second-order structural kinetic models.

Table 3.4: Results of thixotropic fluids modeled with first-order stress decay model with a non-zero stress

No.	Group	τ_i	τ_e	k	R^2	*RMSE*
4	**K**	156.0 ± 8.7	107.3 ± 6.9	-0.060 ± 0.002	0.987	1.03
21	**C**	152.3 ± 6.8	110.6 ± 7.7	-0.066 ± 0.007	0.996	0.43
24	**C**	283.4 ± 9.1	234.5 ± 8.0	-0.053 ± 0.021	0.677	6.39
30	**C**	336.2 ± 22.2	275.7 ± 15.1	-0.025 ± 0.000	0.988	1.57
34	**L**	570.6 ± 33.3	517.0 ± 23.9	-0.107 ± 0.047	0.976	1.18
36	**L**	659.2 ± 23.1	514.5 ± 27.2	-0.074 ± 0.012	0.976	3.70
40	**L**	414.9 ± 21.4	370.7 ± 35.1	-0.020 ± 0.007	0.993	0.72

Table 3.5: Results of rheopectic fluids modeled with first-order stress decay model with a non-zero stress

No.	Group	τ_i	τ_e	k	R^2	*RMSE*
2	**K**	128.1 ± 11.7	160.3 ± 15.4	0.028 ± 0.002	0.999	0.11
9	**K**	416.1 ± 16.4	421.8 ± 6.8	0.014 ± 0.025	0.963	0.36
44	**L**	371.9 ± 27.0	605.2 ± 43.0	0.110 ± 0.025	0.945	6.18

3.2 Shear rate dependent flow behavior

The influence of the shear rate on the flow behavior was evaluated by the performance of shear ramp tests $\dot{\gamma} = 1 - 500\ s^{-1}$ at constant temperatures (T = 5, 25, 55 °C). Typical flow curves of the investigated products e.g. no. 16 at different temperatures are exemplary shown in Figure 3.3 and indicate in general non-Newtonian flow behavior. In addition it can be observed that increasing temperature leads to decreasing shear stress values.

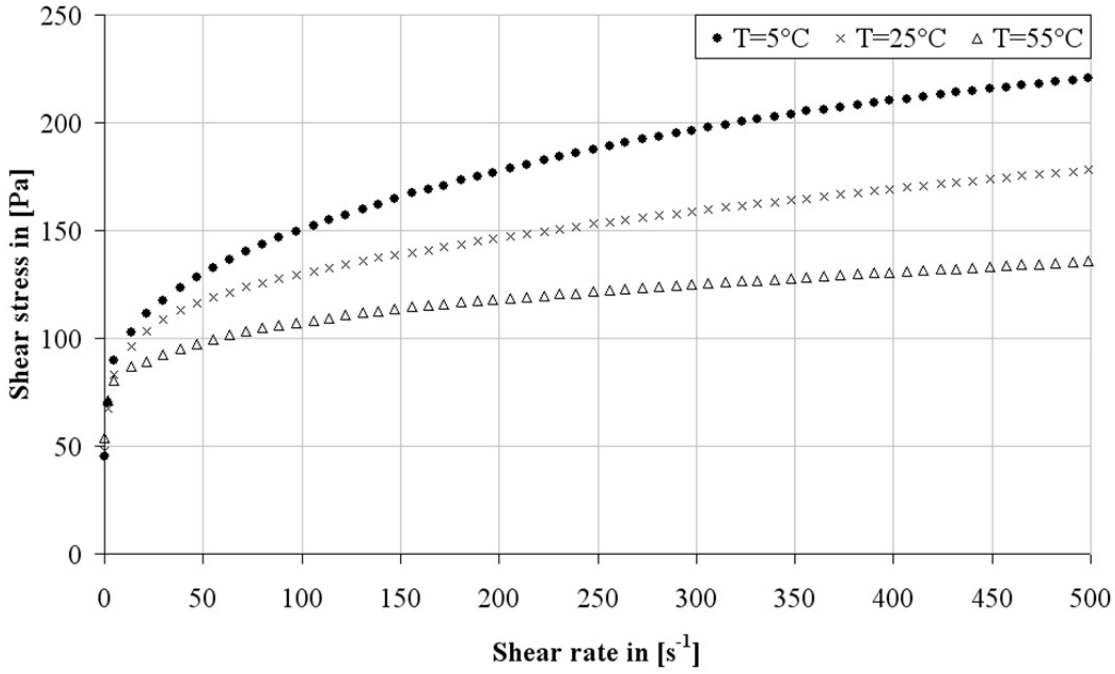

Figure 3.3: Flow curves of product 16 in dependency of shear rate ($\dot{\gamma} = 1 – 500\ s^{-1}$) at constant temperatures of (T = 5; 25; 55 °C).

The Bingham, Ostwald-de-Waele, Herschel-Bulkley, Casson, modified Casson and Carreau model were fitted to the measured shear rate dependent data and evaluated according to the procedure explained in section 2.4.

Figure 3.4 and Figure 3.5 show exemplary the flow curves predicted by application of the models described in section 1.1.2.3 and illustrate the differences between the different models. The Ostwald-de-Waele, the modified Casson, the Herschel-Bulkley as well as the Carreau model represent the curve progression of the measured data points quite well. The Bingham and the Casson model showed apparently the worst fit.

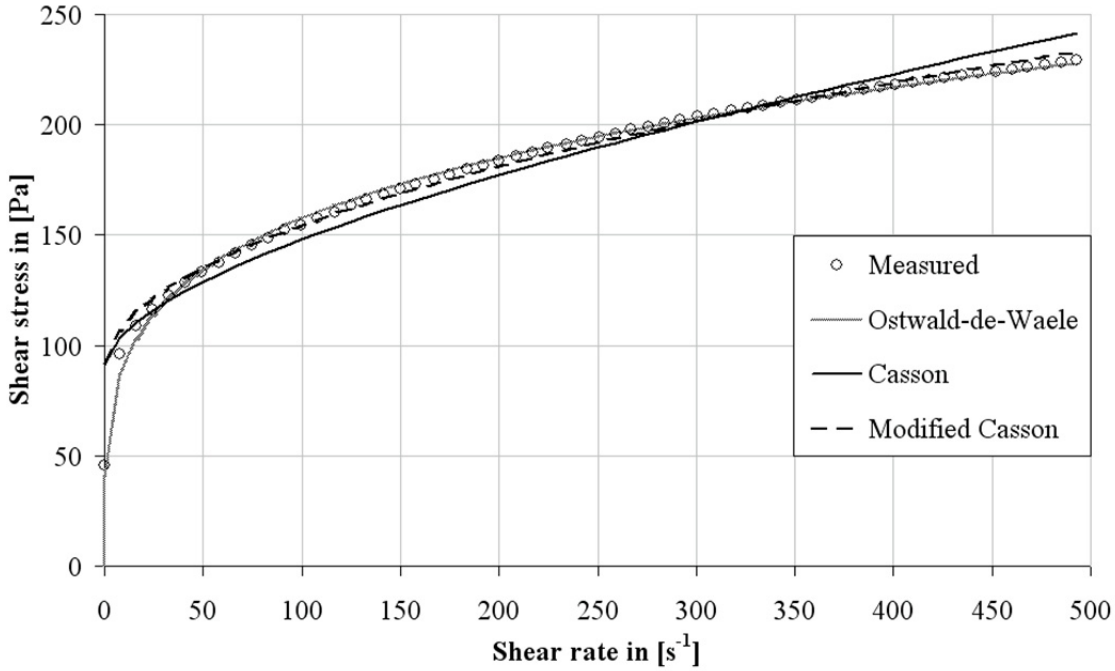

Figure 3.4: Ostwald-de-Waele, Casson and modified Casson model fitted to measurement data of product 16 at a constant temperature (T = 5 °C)

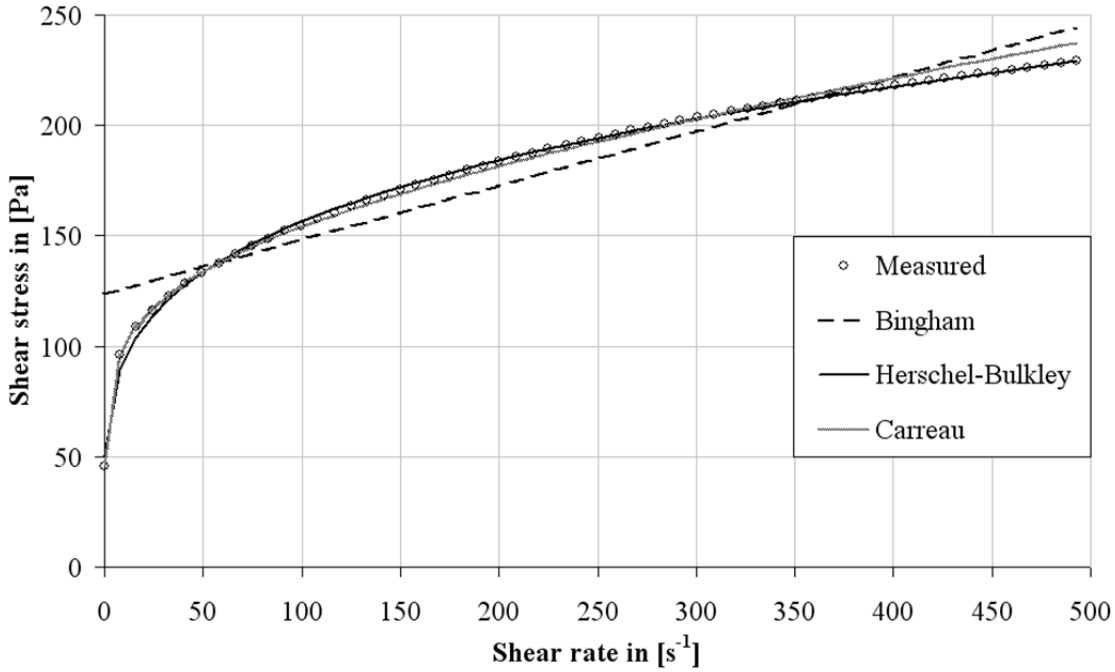

Figure 3.5: Bingham, Herschel-Bulkley and Carreau model fitted to measurement data of product 16 at a constant temperature (T = 5 °C)

The characteristic parameters of the different fitting models are tabulated in Table 3.6. For validation, the residua of a model were tested for normal distribution, whereas a p-value exceeding 0.05 indicated normal distribution. Only the residua of the Herschel-Bulkley model followed normal distribution ($p > 0.05$). The coefficient of determination $R^2 = 0.999$ and the smallest root mean square error RMSE = 1.345 indicate a very good fit.

The other models could not be validated and showed in comparison a slightly lower coefficient of determination (R^2 = 0.931 - 0.998) and higher values of RMSE.

Table 3.6: Exemplary model parameters and goodness of fit of Bingham, Ostwald-de-Waele, Herschel-Bulkley, Casson, modified Casson and Carreau models for product 16

Model	Equation	Parameters	R^2	RMSE	Residua p-value
Bingham	1.13	τ_0 = 119.51 Pa K = 0.258 Pas^n n = 1	0.837	17.104	$6.7 \cdot 10^{-7}$
Ostwald-de-Waele	1.141.8	K = 54.14 Pa n = 0.232	0.998	1.961	0.0034
Herschel-Bulkley	1.15	τ_0 = 18.17 Pa K = 41.25 Pas^n n = 0.263	0.999	1.345	0.0526
Casson	1.16	τ_0 = 82.19 Pa K = 0.088 Pas^n n = 0.5	0.931	11.163	0.0001
Modified Casson	1.17	τ_0 = 82.19 Pa K = 8.346 Pas^n n = 0.934	0.967	8.071	$4.6 \cdot 10^{-10}$
Carreau	1.18	η_0 = 245.81 Pas η_∞ = 0.09 Pas λ = 4.777 s n = 0.168	0.997	2.291	0.0013

This procedure was repeated for each measurement and the overall percentage of a model which could be validated is shown in Table 3.7. In general the Herschel-Bulkley model was accepted for 48 products, only the products no. 12, 14, 23, 24, 25, 26, 27 could not be validated. The Carreau model was accepted for 23 products, the Ostwald-de-Waele model seven products and the modified Casson was accepted for only one product. The Bingham and Casson model were not accepted for any product according to the definition made in section 2.4.

Table 3.7: Comparison of shear rate dependent models and their corresponding percentage of acceptance depending on the applied model

28	**27**	**26**	**25**	**24**	**23**	**22**	**21**	**20**	**19**	**18**	**17**	**16**	**15**	**14**	**13**	**12**	**11**	**10**	**9**	**8**	**7**	**6**	**5**	**4**	**3**	**2**	**1**	**No.**
C	C	C	C	C	C	C	C	K	K	K	K	K	K	K	K	K	K	K	K	K	K	K	K	K	K	K	K	**Group**
0	50	0	5	10	10	0	0	0	0	0	0	0	0	0	0	0	0	0	0	0	0	0	0	0	0	0	0	**Bingham**
x	x	x	x	x	x	x	x	x	x	x	x	x	x	x	x	x	x	x	x	x	x	x	x	x	x	x	x	accepted (a) - rejected (x)
0	55	35	50	45	50	0	5	35	0	85	75	70	75	40	5	17	0	45	70	35	30	17	17	0	58	0	25	**Ostwald-de-Waele**
x	x	x	x	x	x	x	x	x	x	a	a	a	a	x	x	x	x	x	a	x	x	x	x	x	x	x	x	accepted (a) - rejected (x)
83	85	60	60	40	55	85	95	100	70	95	95	100	95	40	95	50	75	80	90	80	100	100	75	92	100	92	92	**Herschel-Bulkley**
a	a	x	x	x	x	a	a	a	a	a	a	a	a	x	a	x	a	a	a	a	a	a	a	a	a	a	a	accepted (a) - rejected (x)
0	65	0	20	45	35	10	10	0	0	0	0	0	0	35	0	8	0	0	10	10	5	8	0	0	0	0	0	**Casson**
x	a	x	x	x	x	x	x	x	x	x	x	x	x	x	x	x	x	x	x	x	x	x	x	x	x	x	x	accepted (a) - rejected (x)
0	15	0	5	10	10	0	0	20	20	0	0	0	0	10	60	17	5	0	0	20	50	58	0	8	0	0	0	**modified Casson**
x	x	x	x	x	x	x	x	x	x	x	x	x	x	x	x	x	x	x	x	x	x	x	x	x	x	x	x	accepted (a) - rejected (x)
8	40	85	95	95	65	20	90	75	50	80	85	80	80	65	65	92	35	80	65	15	90	75	42	83	33	25	33	**Carreau**
x	a	a	a	a	a	x	a	a	x	a	a	a	a	a	a	a	x	a	a	x	a	a	x	a	x	x	x	accepted (a) - rejected (x)
55	**54**	**53**	**52**	**51**	**50**	**49**	**48**	**47**	**46**	**45**	**44**	**43**	**42**	**41**	**40**	**39**	**38**	**37**	**36**	**35**	**34**	**33**	**32**	**31**	**30**	**29**	**No.**
M	M	M	M	M	M	M	M	M	M	M	L	L	L	L	L	L	L	L	L	L	L	L	C	C	C	C	**Group**
17	17	0	8	25	0	25	0	17	0	0	0	0	8	5	0	0	0	0	0	17	0	0	0	0	0	0	20	**Bingham**
x	x	x	x	x	x	x	x	x	x	x	x	x	x	x	x	x	x	x	x	x	x	x	x	x	x	x	x	accepted (a) - rejected (x)
8	17	25	58	17	75	25	8	17	42	17	35	42	8	85	0	50	5	35	55	25	5	10	0	8	0	0	0	**Ostwald-de-Waele**
x	x	x	x	x	a	x	x	x	x	x	x	x	x	a	x	x	x	x	x	x	x	x	x	x	x	x	x	accepted (a) - rejected (x)
83	83	92	75	75	100	92	83	83	67	67	65	75	92	80	80	100	90	65	65	83	80	70	75	100	83	70	**Herschel-Bulkley**
a	a	a	a	a	a	a	a	a	a	a	a	a	a	a	a	a	a	a	a	a	a	a	a	a	a	a	accepted (a) - rejected (x)
17	17	0	25	25	0	25	8	25	33	0	50	0	8	20	5	25	10	25	10	8	15	0	0	33	8	0	**Casson**
x	x	x	x	x	x	x	x	x	x	x	x	x	x	x	x	x	x	x	x	x	x	x	x	x	x	x	accepted (a) - rejected (x)
17	8	0	33	17	75	25	8	17	25	0	15	8	8	5	5	0	5	0	15	17	15	0	8	17	0	25	**mod. Casson**
x	x	x	x	x	a	x	x	x	x	x	x	x	x	x	x	x	x	x	x	x	x	x	x	x	x	x	accepted (a) - rejected (x)
17	25	0	25	42	0	25	0	58	25	50	35	8	0	70	35	67	25	70	40	8	40	35	83	25	17	10	**Carreau**
x	x	x	x	x	x	x	x	x	x	x	x	x	x	a	x	a	x	a	x	x	x	x	a	x	x	x	accepted (a) - rejected (x)

3.2.1 Herschel-Bulkley

For further modeling purposes the Herschel-Bulkley model was selected, since it was the only model which described the vast amount of products in a sufficient way and allows a comparison of different products in dependence of the composition. The products, which could not be validated by means of the Herschel-Bulkley, namely no. 12, 14, 23, 24, 25, 26, 27 could be successfully approximated by application of the Carreau model and corresponding results are described in the consecutive section 3.2.2.

Table 3.8 shows the Herschel-Bulkley (Equation 1.15) parameters and their standard deviation at constant temperatures of T = 5, 25, 55 °C. In order to evaluate the influence of temperature on the Herschel-Bulkley parameters an analysis of variance of the means was performed, assuming normal distribution within each group.

In general the yield stress of all products varied from τ_0 = 0 - 276 Pa, whereas the consistency coefficient was in the range of K = 1.9 - 97.1 Pas^n. The flow behavior index ranged from n = 0.169 - 0.68 and thus clearly indicates shear thinning flow behavior with n < 1 for all products [43].

Table 3.8: Resulting averaged Herschel-Bulkley parameters at different temperatures and their corresponding goodness of fit (different letters imply significant differences (α = 0.05))

No.	Group	T [°C]	τ_0 [Pa]		K [Pas^n]		n [-]		R^2	RMSE
1	K	5	53.31 ± 7.54	a	9.7 ± 1.1	b	0.461 ± 0.022	a	0.996	2.368
		25	42.94 ± 3.74	ab	6.0 ± 0.6	a	0.461 ± 0.018	a	0.997	1.406
		55	30.02 ± 6.72	b	7.7 ± 0.2	a	0.397 ± 0.029	b	0.998	1.212
2	K	5	48.43 ± 5.69	a	8.1 ± 0.9	a	0.457 ± 0.007	b	0.995	2.166
		25	38.36 ± 6.06	ab	5.4 ± 1.2	a	0.464 ± 0.015	b	0.996	1.340
		55	19.72 ± 1.54	b	8.4 ± 3.2	a	0.368 ± 0.061	a	0.996	0.319
3	K	5	1.24 ± 0.00	a	76.6 ± 5.9	a	0.228 ± 0.015	a	0.999	1.809
		25	11.06 ± 7.74	a	56.0 ± 6.1	a	0.244 ± 0.015	a	0.999	1.058
		55	32.95 ± 5.46	b	26.8 ± 6.8	b	0.321 ± 0.032	b	0.999	0.263
4	K	5	0.00 ± 0.00	a	23.9 ± 4.9	a	0.279 ± 0.021	a	0.967	4.171
		25	0.00 ± 0.00	a	18.0 ± 0.8	ab	0.265 ± 0.033	a	0.980	2.140
		55	0.00 ± 0.00	a	14.8 ± 1.6	b	0.263 ± 0.015	a	0.984	0.396
5	K	5	0.00 ± 0.00	a	21.4 ± 2.1	b	0.339 ± 0.036	a	0.993	2.855
		25	1.52 ± 0.12	a	15.2 ± 2.1	a	0.357 ± 0.044	a	0.997	1.294
		55	3.07 ± 4.64	a	10.4 ± 1.3	a	0.376 ± 0.050	a	0.999	0.030
6	K	5	19.47 ± 1.19	a	12.8 ± 1.1	a	0.434 ± 0.027	a	0.999	1.163
		25	16.44 ± 2.11	ab	14.0 ± 1.1	a	0.389 ± 0.022	ab	1.000	0.671
		55	12.87 ± 1.55	b	14.1 ± 1.7	a	0.358 ± 0.020	b	1.000	0.113

No.	Group	T [°C]	τ_0 [Pa]		K [Pas^n]		n [-]		R^2	RMSE
		5	4.40 ± 0.69	a	45.9 ± 2.0	b	0.316 ± 0.042	a	0.999	2.229
7	**K**	25	5.22 ± 0.60	a	49.0 ± 2.3	b	0.278 ± 0.012	a	0.999	1.555
		55	5.79 ± 0.68	a	39.0 ± 1.3	a	0.280 ± 0.015	a	1.000	0.136
		5	72.67 ± 6.71	a	39.9 ± 3.4	a	0.332 ± 0.013	a	0.997	3.414
8	**K**	25	64.76 ± 6.32	a	29.0 ± 3.2	a	0.332 ± 0.022	a	0.995	3.105
		55	118.90 ± 11.46	a	60.4 ± 6.1	a	0.307 ± 0.073	a	0.968	2.512
		5	0.00 ± 0.00	a	46.1 ± 2.4	c	0.351 ± 0.009	c	0.999	2.921
9	**K**	25	7.96 ± 0.98	ab	35.1 ± 4.6	a	0.382 ± 0.016	a	0.999	2.015
		55	16.98 ± 1.08	b	24.9 ± 2.2	b	0.421 ± 0.015	b	0.999	0.336
		5	50.73 ± 3.51	a	39.6 ± 4.0	a	0.240 ± 0.042	a	0.990	2.730
10	**K**	25	49.38 ± 3.49	a	39.5 ± 6.9	a	0.214 ± 0.063	a	0.992	1.793
		55	54.32 ± 2.77	a	21.5 ± 3.4	a	0.247 ± 0.020	a	0.997	0.131
		5	43.56 ± 6.76	b	30.4 ± 2.9	b	0.332 ± 0.025	a	0.998	2.242
11	**K**	25	35.57 ± 2.41	a	10.9 ± 2.2	a	0.336 ± 0.022	a	0.994	1.290
		55	32.04 ± 2.41	a	8.5 ± 1.7	a	0.324 ± 0.027	a	0.996	0.029
		5	26.56 ± 1.69	b	22.8 ± 2.4	a	0.332 ± 0.009	a	0.998	1.610
13	**K**	25	49.95 ± 2.51	a	14.3 ± 1.9	a	0.347 ± 0.014	a	0.993	2.150
		55	42.76 ± 4.38	a	17.5 ± 1.1	a	0.319 ± 0.096	a	0.979	1.547
		5	1.84 ± 0.15	a	52.9 ± 4.0	c	0.319 ± 0.014	c	0.994	5.922
15	**K**	25	2.97 ± 1.95	a	37.7 ± 1.4	a	0.346 ± 0.005	a	1.000	0.944
		55	19.99 ± 6.19	b	24.7 ± 1.3	b	0.387 ± 0.012	b	1.000	0.086
		5	1.87 ± 0.32	a	42.2 ± 2.4	c	0.337 ± 0.005	a	0.998	3.272
16	**K**	25	2.71 ± 0.71	a	31.3 ± 1.5	a	0.350 ± 0.004	a	1.000	0.438
		55	15.67 ± 3.88	b	20.4 ± 0.8	b	0.381 ± 0.017	b	0.999	1.026
		5	2.86 ± 5.74	a	49.4 ± 4.5	a	0.251 ± 0.042	a	0.998	1.654
17	**K**	25	2.74 ± 0.00	a	48.2 ± 3.0	a	0.227 ± 0.020	a	0.999	0.893
		55	15.89 ± 1.87	b	30.2 ± 2.7	b	0.262 ± 0.033	a	0.999	0.344
		5	3.20 ± 0.33	a	56.0 ± 5.1	c	0.318 ± 0.034	b	0.993	6.486
18	**K**	25	2.15 ± 0.29	a	43.0 ± 3.3	a	0.297 ± 0.014	0	0.987	6.111
		55	1.02 ± 0.14	a	25.7 ± 2.0	b	0.352 ± 0.008	a	0.999	0.157
		5	17.53 ± 2.35	a	39.3 ± 2.5	a	0.268 ± 0.015	c	0.998	1.630
19	**K**	25	22.32 ± 1.43	a	40.0 ± 1.3	a	0.210 ± 0.012	a	0.990	2.887
		55	28.28 ± 3.06	a	42.1 ± 3.4	a	0.169 ± 0.308	b	0.994	1.298
		5	34.51 ± 0.00	a	27.9 ± 0.0	a	0.300 ± 0.005	c	0.999	1.256
20	**K**	25	38.79 ± 1.94	a	30.1 ± 2.0	a	0.253 ± 0.004	a	0.996	1.541
		55	46.76 ± 4.65	b	24.7 ± 2.5	b	0.231 ± 0.014	b	0.997	0.064
		5	8.90 ± 0.52	a	24.5 ± 1.1	c	0.446 ± 0.007	a	1.000	1.781
21	**C**	25	12.33 ± 1.19	ab	15.5 ± 0.0	a	0.472 ± 0.005	a	1.000	1.116
		55	14.43 ± 3.37	b	9.5 ± 1.6	b	0.516 ± 0.025	b	1.000	0.188
		5	21.45 ± 3.49	a	15.1 ± 1.6	a	0.450 ± 0.020	c	0.995	1.637
22	**C**	25	19.75 ± 0.49	a	14.1 ± 0.8	a	0.477 ± 0.004	a	0.999	1.637
		55	23.21 ± 1.54	a	6.8 ± 0.5	b	0.549 ± 0.010	b	0.999	0.143
		5	38.54 ± 1.93	a	18.8 ± 6.7	a	0.461 ± 0.059	a	0.999	2.646
28	**C**	25	38.99 ± 2.01	a	15.3 ± 5.2	a	0.446 ± 0.044	a	0.998	2.363
		55	30.21 ± 1.82	b	14.1 ± 1.3	a	0.427 ± 0.046	a	0.998	0.371
		5	38.98 ± 2.62	a	6.0 ± 1.1	b	0.503 ± 0.020	c	0.992	2.866
29	**C**	25	35.50 ± 3.00	a	2.7 ± 0.4	a	0.584 ± 0.028	a	0.994	1.944
		55	25.35 ± 2.90	b	2.8 ± 0.1	a	0.544 ± 0.023	b	0.992	0.029

No.	Group	T [°C]	τ_0 [Pa]		K [Pas^n]		n [-]		R^2	RMSE
		5	5.23 ± 1.14	c	38.7 ± 3.2	a	0.336 ± 0.008	a	0.999	2.094
30	**C**	25	22.41 ± 0.62	a	23.2 ± 0.8	a	0.358 ± 0.003	a	0.998	1.814
		55	48.37 ± 2.71	b	49.6 ± 2.1	a	0.223 ± 0.097	a	0.942	1.676
		5	18.99 ± 2.00	b	6.1 ± 0.2	c	0.557 ± 0.006	a	0.999	1.515
31	**C**	25	15.03 ± 0.42	a	3.6 ± 0.6	a	0.584 ± 0.018	a	0.999	1.041
		55	14.25 ± 1.14	a	1.9 ± 0.1	b	0.656 ± 0.017	b	0.998	0.140
		5	11.65 ± 0.17	a	11.5 ± 0.4	b	0.535 ± 0.004	a	1.000	1.643
32	**C**	25	15.35 ± 2.50	a	6.6 ± 0.4	a	0.554 ± 0.015	a	1.000	0.803
		55	13.17 ± 1.22	a	4.9 ± 1.9	a	0.561 ± 0.059	a	0.999	0.367
		5	77.50 ± 5.62	a	41.3 ± 1.2	c	0.363 ± 0.044	a	0.998	3.151
33	**L**	25	61.77 ± 2.86	a	31.2 ± 0.2	a	0.378 ± 0.003	a	0.999	1.732
		55	76.98 ± 5.45	a	12.1 ± 0.8	b	0.515 ± 0.006	b	0.999	0.214
		5	68.83 ± 4.25	a	37.9 ± 5.0	b	0.538 ± 0.044	a	0.997	7.964
34	**L**	25	60.83 ± 2.12	a	22.5 ± 1.8	a	0.496 ± 0.027	a	0.998	4.848
		55	33.87 ± 3.63	b	22.1 ± 2.1	a	0.377 ± 0.022	b	0.998	2.877
		5	15.85 ± 2.11	a	80.5 ± 6.6	b	0.358 ± 0.007	a	0.963	2.804
35	**L**	25	68.09 ± 7.98	a	46.1 ± 6.6	a	0.326 ± 0.023	a	0.999	4.345
		55	62.67 ± 5.55	a	51.4 ± 5.7	a	0.368 ± 0.020	a	0.992	2.394
		5	32.72 ± 2.95	b	38.43 ± 3.8	a	0.451 ± 0.055	a	0.998	6.091
36	**L**	25	18.34 ± 2.43	a	33.1 ± 5.9	a	0.441 ± 0.034	a	0.999	3.555
		55	10.92 ± 1.26	a	25.4 ± 3.6	a	0.430 ± 0.018	a	1.000	1.124
		5	4.54 ± 1.14	a	88.3 ± 7.0	c	0.311 ± 0.013	a	0.997	6.180
37	**L**	25	4.97 ± 1.11	a	50.6 ± 8.9	a	0.307 ± 0.026	a	0.998	3.117
		55	13.73 ± 4.46	a	27.1 ± 2.0	b	0.355 ± 0.010	b	0.999	0.334
		5	55.52 ± 3.49	a	20.2 ± 1.2	b	0.517 ± 0.004	a	0.999	3.775
38	**L**	25	47.11 ± 1.79	a	13.5 ± 0.6	a	0.520 ± 0.005	a	1.000	1.311
		55	48.32 ± 6.67	a	13.9 ± 3.2	a	0.496 ± 0.025	a	0.999	0.785
		5	19.26 ± 4.16	a	11.6 ± 1.3	c	0.612 ± 0.014	b	0.996	1.923
39	**L**	25	14.63 ± 4.11	a	8.4 ± 0.3	a	0.604 ± 0.016	0	0.996	1.202
		55	14.23 ± 5.21	a	5.1 ± 0.6	b	0.641 ± 0.025	a	1.000	0.511
		5	56.16 ± 3.69	a	18.8 ± 2.2	b	0.491 ± 0.024	a	0.999	3.135
40	**L**	25	52.70 ± 3.73	a	11.6 ± 0.4	a	0.517 ± 0.013	a	0.999	2.234
		55	54.85 ± 4.50	a	8.4 ± 3.3	a	0.600 ± 0.056	b	0.999	0.315
		5	94.99 ± 4.05	a	44.1 ± 16.9	a	0.438 ± 0.057	a	0.992	13.334
41	**L**	25	72.75 ± 4.93	a	37.1 ± 23.5	a	0.449 ± 0.082	a	0.994	9.620
		55	57.53 ± 3.81	a	29.1 ± 22.9	a	0.474 ± 0.094	a	0.994	2.197
		5	39.84 ± 4.59	a	52.5 ± 1.1	c	0.474 ± 0.004	a	1.000	1.937
42	**L**	25	45.38 ± 1.71	a	25.2 ± 0.2	a	0.477 ± 0.003	a	1.000	1.149
		55	96.88 ± 3.82	b	19.0 ± 1.6	b	0.469 ± 0.083	a	0.728	1.325
		5	18.98 ± 1.64	a	56.2 ± 5.0	c	0.351 ± 0.077	a	0.994	5.931
43	**L**	25	67.86 ± 4.42	b	25.7 ± 4.6	a	0.347 ± 0.033	a	0.999	2.710
		55	165.43 ± 22.19	c	6.1 ± 1.0	b	0.336 ± 0.162	a	0.806	22.148
		5	61.44 ± 6.55	a	88.0 ± 6.3	c	0.313 ± 0.039	c	0.990	11.437
44	**L**	25	70.50 ± 7.09	ab	27.3 ± 3.3	a	0.473 ± 0.051	a	0.991	10.542
		55	85.69 ± 9.99	b	6.6 ± 2.6	b	0.681 ± 0.079	b	0.993	2.274
		5	32.32 ± 5.99	a	79.7 ± 4.6	c	0.298 ± 0.012	c	1.000	2.022
45	**M**	25	43.61 ± 6.16	a	45.6 ± 1.7	a	0.338 ± 0.006	a	0.995	1.072
		55	58.92 ± 9.42	b	18.1 ± 3.1	b	0.465 ± 0.027	b	1.000	0.464

No.	Group	T [°C]	τ_0 [Pa]		K [Pas^n]		n [-]		R^2	RMSE
		5	25.24 ± 3.85	c	62.2 ± 4.7	c	0.339 ± 0.000	a	0.998	4.254
46	**M**	25	42.63 ± 4.20	a	37.7 ± 9.5	a	0.363 ± 0.025	a	0.999	1.772
		55	72.89 ± 4.32	b	13.4 ± 1.1	b	0.433 ± 0.000	b	0.968	2.315
		5	52.67 ± 1.59	c	24.0 ± 0.5	c	0.454 ± 0.003	c	1.000	2.023
47	**M**	25	49.99 ± 0.91	a	21.2 ± 1.0	a	0.439 ± 0.004	a	0.999	1.743
		55	59.28 ± 2.83	b	9.9 ± 0.6	b	0.505 ± 0.004	b	0.997	0.230
		5	24.60 ± 3.35	a	17.5 ± 0.2	c	0.476 ± 0.005	c	1.000	1.066
48	**M**	25	28.77 ± 2.84	a	10.1 ± 0.3	a	0.518 ± 0.011	a	1.000	0.707
		55	29.34 ± 1.95	a	4.8 ± 0.2	b	0.585 ± 0.006	b	0.987	1.023
		5	32.71 ± 3.12	a	10.5 ± 0.8	c	0.528 ± 0.023	a	0.994	1.689
49	**M**	25	28.76 ± 2.97	a	7.7 ± 0.3	a	0.514 ± 0.036	a	0.999	1.042
		55	33.02 ± 6.65	a	2.6 ± 1.5	b	0.671 ± 0.073	b	0.995	0.550
		5	10.66 ± 1.43	a	28.6 ± 1.1	a	0.483 ± 0.091	a	0.994	9.256
50	**M**	25	1.61 ± 0.13	b	6.5 ± 0.6	b	0.638 ± 0.008	b	0.998	4.418
		55	n.e.		n.e.		n.e.		n.e.	n.e.
		5	38.98 ± 1.35	a	42.9 ± 4.5	b	0.393 ± 0.015	a	0.999	2.622
51	**M**	25	47.79 ± 6.40	a	33.3 ± 2.5	a	0.389 ± 0.013	a	1.000	1.474
		55	56.50 ± 5.83	a	26.8 ± 3.4	a	0.367 ± 0.020	a	0.996	0.803
		5	276.81 ± 12.20	c	36.6 ± 3.1	a	0.292 ± 0.109	a	0.916	3.442
52	**M**	25	251.98 ± 14.68	a	31.5 ± 2.0	a	0.374 ± 0.022	a	0.990	7.422
		55	238.86 ± 11.23	b	22.9 ± 2.2	b	0.220 ± 0.000	a	0.111	15.762
		5	24.92 ± 1.28	a	71.3 ± 6.3	c	0.329 ± 0.023	a	0.995	7.595
53	**M**	25	27.71 ± 1.59	a	38.7 ± 5.0	a	0.365 ± 0.018	a	0.999	2.254
		55	55.23 ± 3.21	b	15.2 ± 1.2	b	0.367 ± 0.021	a	0.999	2.710
		5	14.80 ± 3.19	a	50.0 ± 2.3	c	0.369 ± 0.006	a	0.994	3.923
54	**M**	25	43.33 ± 2.21	a	41.0 ± 2.1	a	0.414 ± 0.013	a	1.000	1.719
		55	94.52 ± 5.89	b	30.0 ± 2.2	b	0.445 ± 0.088	a	0.777	10.007
		5	6.38 ± 4.76	c	97.1 ± 9.0	c	0.374 ± 0.020	a	0.999	3.271
55	**M**	25	30.62 ± 0.53	a	40.4 ± 1.4	a	0.412 ± 0.006	a	1.000	1.325
		55	140.30 ± 9.24	b	25.4 ± 5.1	b	0.348 ± 0.196	a	0.880	7.104

For comparison of the observed results and values reported in literature the previous classification from section 2.1 into the groups ketchup (K), condiment (C), fat reduced mayonnaise and dressings (L) and classical mayonnaise (M) was revisited.

Ketchups

All ketchups, namely products no. 1 - 20, exhibited non-Newtonian shear-thinning flow behavior, indicated by a flow behavior index n below 1, which is a result of a complex interaction of the components pulp, organic acids, soluble pectin, soluble solids and the high volume concentration of particles [64,59].

The values for the flow behavior index n ranged from 0.17 to 0.46. These results can be confirmed with the data obtained by Sharoba et al. [64], who indicated that the values

for the flow behavior index ranged between 0.25 and 0.42 for various commercial tomato ketchups in the temperature range from 0 – 50 °C. Barbosa-Canovas and Peleg [62] also observed n values in the range of 0.38 and 0.40 for commercial ketchups.

The dependency of the flow behavior index n on temperature followed no homogeneous pattern. A significant decrease of this value was observed for the products no. 1, 2, 3, 6, 19 and 20. This observation was consonant with the observations made by Sharoba et al. [64]. Koocheki et al. [59] also describe a declining trend for the flow behavior index n with increasing temperature for ketchups, indicating a higher pseudo-plasticity at higher temperatures. No significant influence of temperature was observed for the products no. 4, 5, 7, 8, 10, 11, 13 and 17. The products no. 9, 15, 16 and 18 showed contrary behavior and thus a significant increase of the flow behavior index.

The consistency coefficient K of the investigated ketchups was ranging from 5.42 to 76.60 Pas^n and showed a significant decrease with increasing temperature for the products no. 1, 3, 4, 5, 7, 9, 11, 15, 16, 17, 18 and 20. The values of the consistency index for the remaining products exhibited no significant dependence of temperature. Other researchers observed similar results for the consistency coefficient ($K = 10 - 30\ Pas^n$) of ketchup [64,59]. They also observed a decrease in consistency coefficients with the increasing temperature, which indicates a decrease in apparent viscosity at higher temperatures.

The yield stress τ_0 was ranging between 0 and 120 Pa. The influence of temperature was heterogeneous, whereas no significant temperature dependency for the products no. 4, 5, 7, 8, 10, 18 and 19 was observed; however the products no. 3, 9, 13, 15, 16, 17 and 20 exhibited a significant increase of the yield stress with rising temperature. Contrary behavior, implicating decreasing yield stress values with rising temperature, were observed for the products 1, 2, 6 and 11.

Condiment sauces

Condiment sauces, represented by no. 21 - 32, can be distinguished from ketchup by their higher amount of spices, which implies a higher amount of rigid particles suspended within the aqueous phase. The high concentration of particles, with a density close to that of water, is responsible for the overall homogeneous appearance [61].

The yield stress τ_0 was ranging from 5.23 to 48.37 Pa, whereas a consistency coefficient K in the range 1.89 - 49.65 Pas^n was observed. The flow behavior index was in the range of n = 0.22 - 0.66.

Martínez [61] investigated the rheological behavior of different commercial condiment sauces at 25 °C and observed shear thinning behavior, which was modeled by the Ostwald-de-Waele with a consistency coefficient K ranging from 3.1 - 17 Pas^n and flow behavior index of n = 0.25 - 0.33. A direct comparison of the values is not valid, since the models are differing. However the magnitude is similar, which confirms the observed results.

The influence of temperature on the yield stress was heterogeneous like for ketchup. The products 21 and 30 showed a significant increase of the yield stress with rising temperature. Contrary behavior, significant decrease with increasing temperature, was observed for the products 28, 29 and 30. The yield stress values of the products 22 and 32 showed no significant dependency on temperature.

The consistency coefficient exhibited in most instances, products no. 21, 22, 29, 31 and 32 a significant decrease with rising temperature, only products no. 28 and 30 showed no significant increase or decrease.

A significant increase of the flow behavior index with rising temperature was observed for the products 21, 22, 29 and 31. The flow behavior index of the products 28, 30 and 32 were independent from temperature. In general the observations for this group are similar to the ones made for the ketchup group, because tomato concentrate as primary ingredient is similar for both groups.

Fat reduced mayonnaises

The group of fat reduced mayonnaises and dressings (no. 33 - 44) can considered to be like mayonnaises oil-in-water emulsions and can be differentiated by their fat content below 50 % and the necessity of a thickened continuous phase to prevent phase separation. All samples were found to exhibit non-Newtonian pseudo-plastic flow behavior.

The values of the yield point varied from τ_0 = 4.54 - 165.43 Pa. The consistency coefficient K was in the range of 5.13 to 88.26 Pas^n and the flow behavior index ranged from n = 0.31 - 0.68. Liu et al. [18] observed similar results for fat reduced mayonnaise-

type dressings (40 % of fat) using different fat mimetics at 25 °C, whereas the Herschel-Bulkley parameters observed were τ_0 = 0.02 - 9.59 Pa, K = 0.57 - 7.24 Pas^n and n = 0.47 - 0.81. The values of fat reduced mayonnaises with a fat content of 34 % by Dolz et al. [71] are conform with the measured ones, since the reported yield stress values were in the range of τ_0 = 76 – 194 Pa. The consistency index ranged from 19 - 31 Pas^n and the flow behavior index was in the range of n = 0.36 - 0.47.

Juszczak et al. [72] also investigated commercial fat reduced mayonnaises with a fat content ranging from 33 to 51 % at 25 °C and reported of yield stress values in the range of τ_0 = 17.6 - 33.1 Pa, consistency coefficients ranging from K = 19.4 - 29.3 Pas^n and flow behavior indices of n = 0.28 - 0.38. However the results do not confirm the conclusion made by Izidoro et al. [74], which states that a decrease in yield stress, viscosity and shear stress is directly connected with a decrease in oil content.

The influence of temperature on the yield stress was diverse. The products 42, 43 and 44 showed a significant increase of the yield stress with rising temperature. Contrary behavior, significant decrease with increasing temperature, was observed for the products 34 and 36. The yield stress values of the products 33, 35, 37, 38, 39, 40 and 41 showed no significant dependency on temperature. The consistency coefficient exhibited for all products a significant decrease with rising temperature, only product no. 36 showed no significant decrease. A significant increase of the flow behavior index with rising temperature was observed for the products 33, 37, 39, 40 and 44. Significant decrease of the flow behavior was observed for product 34. The flow behavior index of the products 35, 36, 38, 41, 42 and 43 were independent from temperature.

Classical mayonnaise

Classical mayonnaises, which represent the last group no. 45 - 55, are an oil-in-water emulsion containing 65 - 82 % of fat [28]. The products of this group can be characterized as well as all other groups as non-Newtonian shear thinning fluids [18]. This behavior is caused by the high concentration of oil droplets and their interaction with each other, which may lead to the formation of a three-dimensional network of aggregated droplets. With increasing shear rate, these aggregates will be deformed and eventually disrupted resulting in a reduction of the viscosity [23].

The yield stress τ_0 was ranging for the mayonnaises from 1.61 to 276.81 Pa, whereas the consistency coefficient K in the range 2.56 - 97.09 Pas^n was observed. The flow behavior index was in the range of n = 0.22 - 0.67. These results can be approved by the observations made by Juszczak et al. [72], who investigated commercial mayonnaises with a fat content ranging from 68 to 78.5 % at 25 °C. The reported values for the yield stress were in the range of τ_0 = 7.9 - 34.8 Pa, consistency coefficients ranging from K = 11.86 - 67.19 Pas^n and flow behavior indices of n = 0.25 - 0.46. Liu et al. [18] report of the flow characteristics of mayonnaise with a fat content of 80 % at 25 °C, which had the same magnitude than the measured ones τ_0 = 12.71 Pa, K = 7.238 Pas^n, n = 0.4821 and thus confirmed the results.

The influence of temperature on the yield stress was heterogeneous. The products 45, 46, 47, 53, 54 and 55 showed a significant increase of the yield stress with rising temperature. Contrary behavior, significant decrease with increasing temperature, was observed for the products 50 and 52. The yield stress values of the products 48, 49, and 51 showed no significant dependency on temperature. The consistency coefficient exhibited for all products a significant decrease with rising temperature. A significant increase of the flow behavior index with rising temperature was observed for the products 45, 46, 47, 48, 49 and 50. A temperature independent flow behavior index was observed for the products no. 51, 52, 53, 54 and 55, which were in addition the products with a fat content above 80 % and without any thickener.

3.2.2 Carreau

Products no. 12, 14, 23, 24, 25, 26 and 27 could be validated successfully by the application of the Carreau model. Table 3.9 shows the different model parameters and their standard deviation at different temperatures of 5, 25 and 55 °C. The observed parameters of the viscosity at low shear rates η_0 were in the range of 7.3 to 130.2 Pas. The viscosity at very high shear rate η_∞ ranged from 0.048 - 0.622 Pas. In general it was observed, that the viscosities η_0 and η_∞ decreased with increasing temperature for all products. The time constant λ, which indicates the inversion of the shear rate at which the fluid changes from Newtonian to power-law behavior, was in the range λ = 0.38 - 6.46 s. The flow index ranged from n = 0.162 - 0.620. The coefficient of determination was always above $R^2 > 0.951$, indicating a good to very good fit.

Bayod et al. [38] investigated the rheological properties of ketchups prepared with different tomato paste contents at 20 °C and used the Carreau model for description of the flow curves. The reported values for the zero shear viscosity η_0 were in the range of 28 - 50 · 10³ Pas, the time constant λ was also reported to be in the range of 3.1 - 5.1 · 10³ s. Both characteristics were of a different magnitude as the observed ones, which could be explained by different boundary conditions of the test. The measurements were performed in a shear rate range of $\dot{\gamma} = 1 \cdot 10^{-5}$ - 100 s^{-1}, which provided different sets of raw data for approximation. The flow behavior index in contrast was found to be in the range of n = 0.41 - 0.43 and thus confirmed the observed results.

Table 3.9: Resulting averaged Carreau parameters at different temperatures and their corresponding goodness of fit

No.	Group	*T* [°C]	η_0 [Pas]	η_∞ [Pas]	λ [s]	*n*	R^2	*RMSE*
12	**K**	5	61.3 ± 3.6	0.055 ± 0.017	1.04 ± 0.06	0.225 ± 0.011	0.997	1.695
		25	48.3 ± 3.2	0.062 ± 0.037	1.62 ± 0.16	0.175 ± 0.028	0.984	2.208
		55	28.8 ± 1.5	0.048 ± 0.012	2.38 ± 0.18	0.194 ± 0.026	0.999	0.748
14	**K**	5	130.2 ± 3.9	0.096 ± 0.026	2.08 ± 0.14	0.359 ± 0.003	0.999	3.321
		25	111.8 ± 6.8	0.083 ± 0.006	2.46 ± 0.85	0.351 ± 0.010	0.999	2.993
		55	100.0 ± 4.8	0.066 ± 0.031	3.85 ± 0.79	0.327 ± 0.008	1.000	1.638
23	**C**	5	53.6 ± 9.6	0.622 ± 0.112	3.29 ± 0.24	0.620 ± 0.037	0.962	5.272
		25	7.9 ± 2.1	0.491 ± 0.070	0.42 ± 0.63	0.593 ± 0.008	0.980	5.879
		55	7.3 ± 0.5	0.442 ± 0.037	0.38 ± 0.03	0.452 ± 0.019	0.986	6.222
24	**C**	5	19.8 ± 2.8	0.588 ± 0.126	0.48 ± 0.12	0.411 ± 0.049	0.951	11.147
		25	13.0 ± 0.8	0.426 ± 0.086	0.43 ± 0.10	0.477 ± 0.030	0.965	8.063
		55	11.2 ± 2.7	0.313 ± 0.058	1.61 ± 0.60	0.582 ± 0.016	0.980	6.573
25	**C**	5	36.9 ± 1.7	0.308 ± 0.024	0.60 ± 0.03	0.328 ± 0.018	0.990	7.563
		25	21.7 ± 1.2	0.213 ± 0.022	0.53 ± 0.07	0.401 ± 0.008	0.982	8.345
		55	13.7 ± 2.0	0.096 ± 0.057	0.60 ± 0.21	0.494 ± 0.022	0.972	9.846
26	**C**	5	53.3 ± 5.0	0.146 ± 0.006	1.20 ± 0.11	0.314 ± 0.005	0.987	6.056
		25	43.9 ± 3.3	0.126 ± 0.004	1.54 ± 0.17	0.352 ± 0.003	0.995	3.184
		55	36.8 ± 3.9	0.119 ± 0.006	1.81 ± 0.31	0.368 ± 0.014	0.999	1.599
27	**C**	5	29.6 ± 0.8	0.307 ± 0.026	6.17 ± 0.23	0.162 ± 0.025	0.974	10.228
		25	24.0 ± 1.6	0.239 ± 0.091	6.46 ± 0.43	0.222 ± 0.006	0.961	11.939
		55	12.3 ± 2.0	0.227 ± 0.105	4.27 ± 0.62	0.441 ± 0.015	0.987	12.478

3.3 Temperature dependent flow behavior

The effect of temperature on the flow behavior was assessed by the performance of temperature ramp tests at constant shear rates.

Figure 3.6 exemplary shows the apparent viscosity in dependence of temperature, whereas a decrease of the apparent viscosity can be observed with increasing temperature. As already presented in section 0 increasing shear rate causes a decrease of the apparent viscosity, since all products exhibit shear thinning flow behavior.

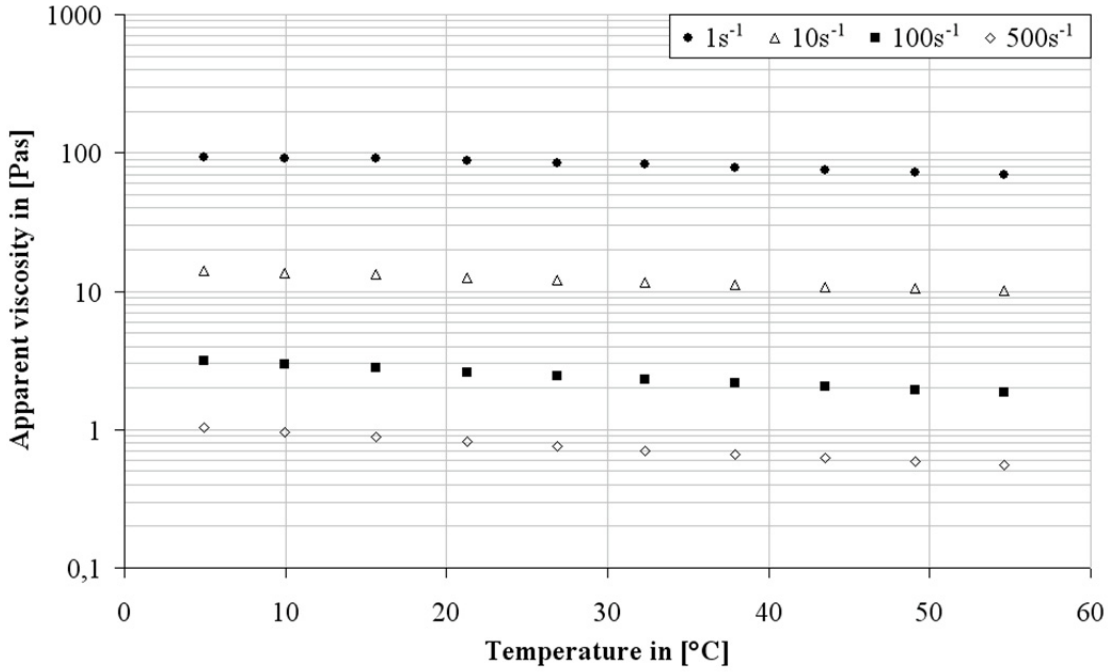

Figure 3.6: Apparent viscosity of product 9 in dependency of temperature (T = 5 – 55 °C) at constant shear rates of ($\dot{\gamma}$ = 1; 10; 100; 500 s^{-1})

The Arrhenius and Williams-Landel-Ferry model were fitted to the temperature dependent measurement data according to the procedure explained in section 2.4, the resulting predicted viscosity curves are exemplary shown in Figure 3.7.

For validation of the models, the residua of a model were tested for normal distribution, whereas a p-value exceeding 0.05 indicated normal distribution. The residua of both models followed normal distribution ($p > 0.05$). Both models described the temperature dependent flow behavior well, whereas the Arrhenius type Equation provides a fractional better fit as in Table 3.10 can be seen. The coefficient of determination for the

Arrhenius type Equation is higher ($R^2 = 0.997$) and the root mean square error (RMSE = 0.173) is lower compared to the values of the WLF model.

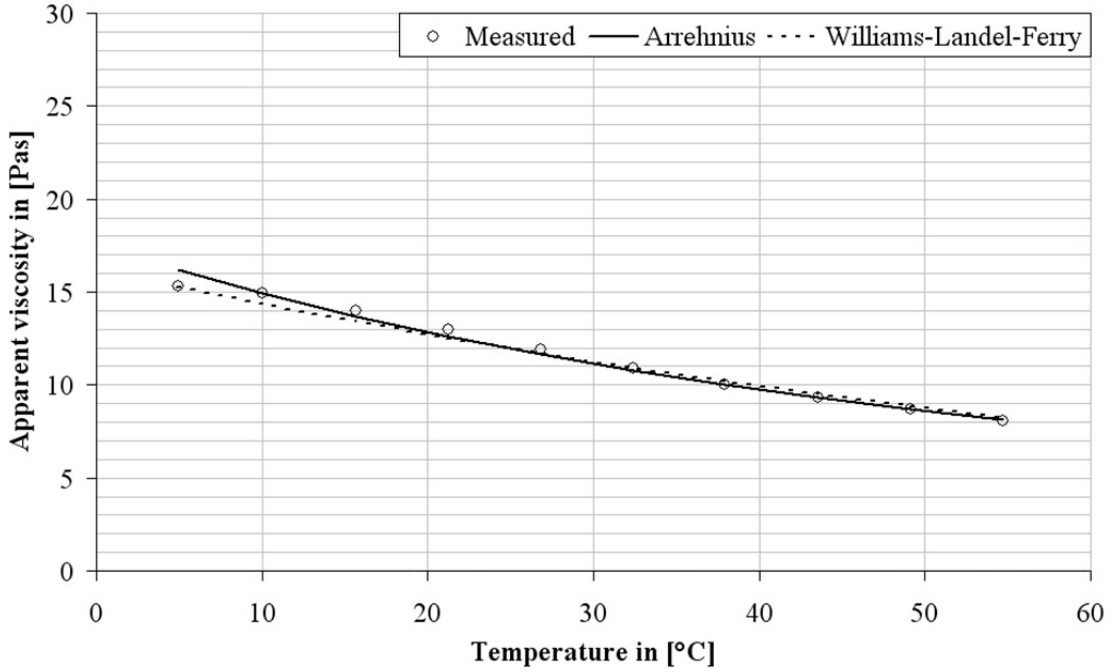

Figure 3.7: Arrhenius and WLF model applied to product 9 at $\dot{\gamma} = 10s^{-1}$

Table 3.10: Exemplary model parameters and goodness of fit of Arrhenius and Williams-Landel-Ferry model for product 9

Model	Equation	Parameters	R^2	RMSE	Residua p-value
Arrhenius	1.19	$E_a = 10.65 \frac{kJ}{mol}$ $\eta_{ref} = 10.02$ Pas $T_{ref} = 313$ K	0.997	0.173	0.091
WLF	1.211.8	$C_1 = 9.58$ $C_2 = 7.73$ $\eta_{ref} = 15.33$ Pas $T_{ref} = 278$ K	0.984	0.353	0.058

This procedure was repeated for each measurement and the overall percentage of a model, which could be validated, is shown Table 3.11.

The Arrhenius type model was accepted for almost all products, except for product no. 11. The WLF model however was accepted for 49 products. For further modeling purposes the Arrhenius type model was selected, since it was capable to describe the almost the whole product range in a sufficient way and allows a comparison of different products in dependence of the composition.

Table 3.11: Comparison of temperature dependent models and their corresponding percentage of acceptance depending on the applied model

No.	Group	Arrhenius	accepted (a) - rejected (x)	WLF	accepted (a) - rejected (x)	No.	Group	Arrhenius	accepted (a) - rejected (x)	WLF	accepted (a) - rejected (x)	No.	Group	Arrhenius	accepted (a) - rejected (x)	WLF	accepted (a) - rejected (x)
1	**K**	83	a	67	a	**20**	**K**	80	a	95	a	**38**	**L**	95	a	55	x
2	**K**	83	a	75	a	**21**	**C**	100	a	80	a	**39**	**L**	100	a	58	x
3	**K**	92	a	100	a	**22**	**C**	85	a	85	a	**40**	**L**	95	a	60	x
4	**K**	75	a	83	a	**23**	**C**	70	a	75	a	**41**	**L**	85	a	85	a
5	**K**	67	a	100	a	**24**	**C**	70	a	95	a	**42**	**L**	100	a	83	a
6	**K**	75	a	83	a	**25**	**C**	80	a	90	a	**43**	**L**	92	a	83	a
7	**K**	65	a	75	a	**26**	**C**	95	a	75	a	**44**	**L**	65	a	85	a
8	**K**	80	a	85	a	**27**	**C**	95	a	80	a	**45**	**M**	100	a	92	a
9	**K**	80	a	95	a	**28**	**C**	83	a	92	a	**46**	**M**	83	a	83	a
10	**K**	90	a	80	a	**29**	**C**	80	a	90	a	**47**	**M**	75	a	92	a
11	**K**	45	x	95	a	**30**	**C**	75	a	92	a	**48**	**M**	75	a	83	a
12	**K**	83	a	75	a	**31**	**C**	83	a	92	a	**49**	**M**	92	a	58	x
13	**K**	80	a	95	a	**32**	**C**	92	a	83	a	**50**	**M**	83	a	100	a
14	**K**	100	a	75	a	**33**	**L**	95	a	75	a	**51**	**M**	92	a	92	a
15	**K**	90	a	95	a	**34**	**L**	70	a	85	a	**52**	**M**	92	a	42	x
16	**K**	90	a	85	a	**35**	**L**	83	a	83	a	**53**	**M**	100	a	83	a
17	**K**	85	a	90	a	**36**	**L**	95	a	90	a	**54**	**M**	100	a	67	a
18	**K**	80	a	100	a	**37**	**L**	90	a	85	a	**55**	**M**	100	a	50	x
19	**K**	70	a	100	a												

Table 3.12 shows the Arrhenius (Equation 1.19) parameters and their standard deviation for shear rates of $\dot{\gamma}$ = 1, 10, 100, 500 s^{-1}. In order to evaluate the influence of the shear rate on the Arrhenius parameters an analysis of variance of the means was performed, assuming normal distribution within each group.

In general the reference viscosity at shear rates of $\dot{\gamma}$ = 1, 10, 100, 500 s^{-1} was in the range of η_{ref} = 0.19 - 129.9 Pas at a reference temperature of 25 °C (298.15 K). For every sample a significant decrease with increasing shear rate and thus shear thinning flow behavior was observed, which confirms the results of section 0. The values for the activation energy ranged from E_a = 0.18 -19.9 kJ/mol. Higher E_a values indicate a stronger dependency of viscosity on temperature [80]. The coefficient of determination ($R^2 > 0.9$) as

well as the low values for the root mean square error RMSE indicated in general a good to very good fit.

Table 3.12: Averaged Arrhenius parameters at different shear rates, a reference temperature of 298.15 K and the corresponding goodness of fit (different letters imply significant differences (α = 0.05))

No.	*Group*	$\dot{\gamma}$ [s^{-1}]	η_{ref} [Pa]		E_a [kJ/mol]		R^2	*RMSE*
1	**K**	1	53.44 ± 5.46	b	6.4 ± 0.4	b	0.982	0.728
	K	10	7.54 ± 0.88	a	8.0 ± 0.7	ab	0.998	0.043
	K	100	1.13 ± 0.09	a	8.8 ± 0.2	bc	0.997	0.009
	K	500	0.35 ± 0.04	a	9.7 ± 0.1	c	0.995	0.004
2	**K**	1	44.79 ± 5.86	b	7.8 ± 0.8	a	0.995	0.437
	K	10	7.14 ± 0.60	a	8.8 ± 0.1	ab	0.998	0.046
	K	100	1.11 ± 0.08	a	9.8 ± 0.3	bc	0.998	0.007
	K	500	0.37 ± 0.03	a	10.3 ± 0.2	c	0.998	0.003
3	**K**	1	94.04 ± 0.00	c	5.9 ± 0.1	a	0.971	1.526
	K	10	14.63 ± 2.82	a	6.7 ± 0.6	ab	0.994	0.127
	K	100	1.39 ± 0.27	b	7.1 ± 0.6	bc	0.999	0.004
	K	500	0.41 ± 0.05	b	7.8 ± 0.1	c	0.996	0.004
4	**K**	1	22.91 ± 4.13	b	6.0 ± 1.9	a	0.911	0.663
	K	10	3.49 ± 0.30	a	8.3 ± 0.3	ab	0.996	0.027
	K	100	0.60 ± 0.06	a	8.6 ± 0.0	b	0.998	0.004
	K	500	0.19 ± 0.03	a	9.3 ± 0.6	b	0.995	0.002
5	**K**	1	27.54 ± 1.93	c	6.1 ± 0.4	c	0.918	0.697
	K	10	4.74 ± 0.38	a	7.6 ± 0.5	a	0.995	0.037
	K	100	0.84 ± 0.07	b	8.8 ± 0.1	b	0.999	0.004
	K	500	0.30 ± 0.03	b	8.5 ± 0.2	b	0.998	0.002
6	**K**	1	39.68 ± 4.53	b	3.7 ± 0.5	d	0.934	0.581
	K	10	5.57 ± 0.43	a	6.1 ± 0.4	a	0.998	0.024
	K	100	0.96 ± 0.06	a	7.1 ± 0.2	b	0.998	0.005
	K	500	0.31 ± 0.01	a	10.7 ± 0.5	c	0.996	0.004
7	**K**	1	68.76 ± 5.73	c	1.9 ± 1.1	d	0.951	2.375
	K	10	10.73 ± 0.43	a	5.5 ± 0.2	a	0.994	0.073
	K	100	1.63 ± 0.14	b	7.1 ± 0.1	b	0.995	0.014
	K	500	0.53 ± 0.04	b	12.2 ± 0.6	c	0.997	0.006
8	**K**	1	106.60 ± 5.61	c	5.6 ± 1.0	a	0.992	0.909
	K	10	13.32 ± 1.06	a	6.3 ± 0.4	a	0.999	0.057
	K	100	2.10 ± 0.29	b	5.5 ± 0.7	a	0.997	0.010
	K	500	0.67 ± 0.06	b	5.7 ± 0.3	a	0.998	0.003
9	**K**	1	57.16 ± 5.79	c	4.7 ± 0.2	c	0.990	0.400
	K	10	8.71 ± 0.95	a	6.7 ± 0.5	a	0.997	0.052
	K	100	2.16 ± 0.12	b	9.4 ± 0.4	b	0.999	0.011
	K	500	0.67 ± 0.02	b	9.2 ± 0.5	b	0.999	0.004

No.	*Group*	$\dot{\gamma}$ [s^{-1}]	η_{ref} [Pa]		E_a [kJ/mol]		R^2	*RMSE*
10	**K**	1	71.29 ± 8.45	c	5.9 ± 1.4	b	0.989	0.765
	K	10	10.91 ± 0.55	a	7.5 ± 0.3	a	0.990	0.134
	K	100	1.67 ± 0.12	b	5.0 ± 0.3	b	0.950	0.031
	K	500	0.41 ± 0.03	b	4.7 ± 0.6	b	0.991	0.003
12	**K**	1	43.30 ± 3.34	b	6.4 ± 0.5	c	0.985	0.572
	K	10	6.09 ± 1.65	a	6.9 ± 0.0	a	0.999	0.021
	K	100	0.86 ± 0.15	a	7.6 ± 0.3	b	0.999	0.003
	K	500	0.25 ± 0.03	a	7.9 ± 0.2	b	0.996	0.002
13	**K**	1	65.74 ± 4.24	c	7.4 ± 0.8	a	0.994	0.676
	K	10	9.73 ± 1.56	a	8.4 ± 0.6	a	0.985	0.161
	K	100	1.22 ± 0.26	b	7.8 ± 1.1	a	0.978	0.022
	K	500	0.29 ± 0.02	b	7.8 ± 0.6	a	0.998	0.002
14	**K**	1	60.62 ± 4.45	c	6.9 ± 0.5	a	0.988	0.848
	K	10	13.23 ± 0.37	a	7.5 ± 0.2	a	0.994	0.145
	K	100	2.68 ± 0.19	b	8.0 ± 0.3	a	0.998	0.018
	K	500	0.71 ± 0.03	b	8.5 ± 0.2	a	0.998	0.004
15	**K**	1	77.88 ± 5.21	c	5.5 ± 0.5	a	0.986	0.849
	K	10	17.19 ± 2.33	a	5.6 ± 0.0	a	0.998	0.055
	K	100	2.33 ± 0.20	b	7.9 ± 0.1	b	0.998	0.013
	K	500	0.80 ± 0.08	b	9.0 ± 0.2	c	0.997	0.006
16	**K**	1	48.57 ± 4.86	c	3.5 ± 0.2	d	0.955	0.524
	K	10	7.83 ± 0.28	a	4.9 ± 0.1	a	0.998	0.024
	K	100	1.40 ± 0.03	b	6.8 ± 0.2	b	0.999	0.005
	K	500	0.46 ± 0.01	b	7.5 ± 0.1	c	0.995	0.005
17	**K**	1	64.41 ± 3.99	c	5.1 ± 0.2	d	0.973	0.873
	K	10	9.41 ± 0.09	a	6.1 ± 0.3	a	0.997	0.057
	K	100	1.36 ± 0.01	b	6.6 ± 0.1	b	0.999	0.004
	K	500	0.36 ± 0.04	b	7.6 ± 0.2	c	0.998	0.002
18	**K**	1	43.02 ± 2.07	c	7.1 ± 0.9	b	0.989	0.550
	K	10	8.85 ± 0.14	a	9.5 ± 0.1	a	0.999	0.040
	K	100	1.89 ± 0.04	b	10.4 ± 0.1	a	0.999	0.008
	K	500	0.65 ± 0.04	b	9.6 ± 0.5	a	0.995	0.007
19	**K**	1	69.90 ± 4.70	c	10.8 ± 1.8	b	0.981	1.523
	K	10	9.51 ± 0.61	a	9.1 ± 0.3	b	0.977	0.199
	K	100	1.38 ± 0.09	b	6.5 ± 0.8	a	0.977	0.022
	K	500	0.39 ± 0.05	b	6.9 ± 0.5	a	0.998	0.002
20	**K**	1	64.77 ± 4.88	c	9.6 ± 2.1	a	0.991	0.977
	K	10	8.16 ± 1.03	a	8.6 ± 0.8	a	0.995	0.078
	K	100	1.12 ± 0.08	b	8.2 ± 0.1	a	0.978	0.022
	K	500	0.29 ± 0.01	b	8.0 ± 0.2	a	0.999	0.001
21	**C**	1	32.02 ± 1.56	c	9.3 ± 0.2	b	0.997	0.289
	C	10	6.12 ± 0.28	a	10.5 ± 0.2	a	0.999	0.043
	C	100	1.56 ± 0.05	b	11.0 ± 0.2	a	0.999	0.010
	C	500	0.46 ± 0.10	b	10.6 ± 0.7	a	0.995	0.006

No.	*Group*	$\dot{\gamma}$ [s^{-1}]	η_{ref} [Pa]		E_a [kJ/mol]		R^2	*RMSE*
22	**C**	1	41.69 ± 1.68	c	8.9 ± 0.2	c	0.998	0.251
	C	10	6.62 ± 0.39	a	10.1 ± 0.2	a	0.998	0.051
	C	100	1.39 ± 0.05	b	11.3 ± 0.3	b	0.994	0.018
	C	500	0.49 ± 0.02	b	10.4 ± 0.6	a	0.994	0.005
23	**C**	1	14.70 ± 1.91	c	17.1 ± 1.6	c	0.997	0.213
	C	10	6.70 ± 0.50	a	13.7 ± 0.7	a	0.999	0.050
	C	100	1.57 ± 0.07	b	11.0 ± 0.5	b	0.997	0.015
	C	500	0.42 ± 0.06	b	12.7 ± 0.1	a	0.982	0.010
24	**C**	1	23.86 ± 2.85	c	18.0 ± 1.7	c	0.995	0.382
	C	10	7.43 ± 0.59	a	14.3 ± 0.8	a	0.984	0.197
	C	100	1.42 ± 0.09	b	10.4 ± 0.9	b	0.985	0.029
	C	500	0.49 ± 0.01	b	8.8 ± 1.1	b	0.979	0.009
25	**C**	1	25.31 ± 6.22	b	15.9 ± 1.6	a	0.998	0.277
	C	10	5.38 ± 0.52	a	14.5 ± 0.8	a	0.998	0.054
	C	100	1.70 ± 0.12	a	9.6 ± 0.6	b	0.998	0.010
	C	500	0.61 ± 0.02	a	7.5 ± 1.1	c	0.970	0.014
26	**C**	1	44.73 ± 1.70	c	9.4 ± 0.1	a	0.998	0.344
	C	10	9.64 ± 0.20	a	8.9 ± 0.2	a	1.000	0.027
	C	100	1.87 ± 0.05	b	6.7 ± 0.1	b	0.999	0.006
	C	500	0.61 ± 0.03	b	5.3 ± 0.8	c	0.980	0.008
27	**C**	1	55.26 ± 8.16	b	2.3 ± 2.7	b	0.945	0.208
	C	10	0.23 ± 1.25	a	8.3 ± 0.2	a	0.999	0.029
	C	100	1.25 ± 0.04	a	8.5 ± 0.1	a	0.999	0.006
	C	500	0.40 ± 0.01	a	7.1 ± 0.4	a	0.988	0.006
28	**C**	1	72.21 ± 5.47	c	6.9 ± 1.4	a	0.965	1.522
	C	10	9.61 ± 1.18	a	7.2 ± 0.2	a	0.986	0.130
	C	100	1.80 ± 0.00	b	7.5 ± 0.1	a	0.999	0.005
	C	500	0.63 ± 0.02	b	8.6 ± 0.7	a	0.991	0.009
29	**C**	1	36.56 ± 3.13	d	6.5 ± 0.1	d	0.979	0.557
	C	10	5.32 ± 0.30	a	7.5 ± 0.1	a	0.991	0.156
	C	100	0.87 ± 0.17	b	10.4 ± 0.1	b	0.999	0.004
	C	500	0.39 ± 0.01	c	10.8 ± 0.3	c	0.999	0.002
30	**C**	1	78.31 ± 5.62	c	8.1 ± 0.9	a	0.925	2.567
	C	10	9.79 ± 1.42	a	9.4 ± 0.9	a	0.987	0.481
	C	100	1.77 ± 0.26	b	9.8 ± 0.7	a	0.990	0.028
	C	500	0.56 ± 0.12	b	10.6 ± 1.0	a	0.998	0.004
31	**C**	1	20.45 ± 1.98	d	9.7 ± 1.4	a	0.984	0.418
	C	10	3.08 ± 0.14	a	11.4 ± 1.2	a	0.993	0.045
	C	100	0.71 ± 0.04	b	11.2 ± 0.0	a	0.979	0.021
	C	500	0.32 ± 0.02	c	9.8 ± 0.4	a	0.981	0.008
32	**C**	1	25.60 ± 3.38	b	4.0 ± 0.2	b	0.965	0.856
	C	10	4.19 ± 0.57	a	9.0 ± 1.8	ab	0.974	0.096
	C	100	1.03 ± 0.06	a	11.7 ± 0.8	a	0.989	0.021
	C	500	0.39 ± 0.09	a	12.3 ± 0.9	a	0.992	0.007

No.	*Group*	$\dot{\gamma}$ [s^{-1}]	η_{ref} [Pa]		E_a [kJ/mol]		R^2	*RMSE*
33	**L**	1	83.10 ± 5.57	b	4.9 ± 0.2	c	0.993	0.660
	L	10	9.60 ± 1.54	a	5.2 ± 0.1	a	0.999	0.035
	L	100	1.81 ± 0.02	a	7.0 ± 0.1	b	0.997	0.012
	L	500	0.72 ± 0.00	a	7.5 ± 0.2	b	0.981	0.009
34	**L**	1	89.42 ± 5.33	c	5.0 ± 0.7	a	0.996	0.402
	L	10	14.14 ± 1.28	a	6.9 ± 0.7	ab	0.997	0.068
	L	100	2.77 ± 0.16	b	8.3 ± 0.4	b	0.999	0.009
	L	500	1.02 ± 0.15	b	8.6 ± 2.1	b	0.978	0.018
35	**L**	1	129.93 ± 4.46	c	2.5 ± 0.4	c	0.988	0.652
	L	10	19.23 ± 0.33	a	4.8 ± 0.3	a	0.997	0.082
	L	100	3.92 ± 0.00	b	7.0 ± 0.1	b	0.999	0.015
	L	500	1.14 ± 0.12	b	6.5 ± 0.4	b	0.955	0.019
36	**L**	1	51.33 ± 3.10	d	8.3 ± 1.4	b	0.930	2.142
	L	10	10.93 ± 0.92	a	10.8 ± 0.0	a	0.998	0.093
	L	100	2.63 ± 0.02	b	9.3 ± 0.2	b	0.999	0.014
	L	500	0.91 ± 0.03	c	9.1 ± 0.2	b	0.998	0.006
37	**L**	1	88.93 ± 0.00	d	7.7 ± 0.4	c	0.986	1.273
	L	10	13.42 ± 0.68	a	9.5 ± 0.5	a	1.000	0.020
	L	100	2.74 ± 0.26	b	10.5 ± 0.3	b	0.996	0.030
	L	500	1.00 ± 0.08	c	9.5 ± 0.8	a	0.994	0.013
38	**L**	1	66.78 ± 1.70	d	3.4 ± 0.8	c	0.958	0.880
	L	10	12.34 ± 0.55	a	6.3 ± 0.7	a	0.991	0.127
	L	100	2.41 ± 0.11	b	8.2 ± 1.5	b	0.992	0.026
	L	500	0.81 ± 0.10	c	8.6 ± 0.2	b	0.992	0.012
39	**L**	1	21.06 ± 1.13	d	6.2 ± 0.5	c	0.939	1.548
	L	10	4.78 ± 0.07	a	9.9 ± 0.0	a	0.955	0.189
	L	100	1.58 ± 0.18	b	13.4 ± 2.3	b	0.992	0.025
	L	500	0.82 ± 0.03	c	12.5 ± 0.3	b	0.993	0.015
40	**L**	1	67.63 ± 7.04	c	6.9 ± 0.2	d	0.987	0.948
	L	10	10.91 ± 1.18	a	9.0 ± 0.1	a	0.998	0.084
	L	100	2.21 ± 0.11	b	9.9 ± 0.1	b	0.998	0.017
	L	500	0.84 ± 0.03	b	10.3 ± 0.3	c	0.994	0.011
41	**L**	1	88.86 ± 6.69	c	6.9 ± 0.4	a	0.996	0.621
	L	10	2.88 ± 0.08	a	7.3 ± 0.1	a	0.998	0.082
	L	100	0.99 ± 0.05	b	6.8 ± 0.2	a	0.993	0.031
	L	500	0.44 ± 0.03	b	8.3 ± 0.4	b	0.998	0.004
42	**L**	1	67.25 ± 4.18	d	4.0 ± 0.7	d	0.990	0.489
	L	10	10.37 ± 0.13	a	5.8 ± 0.1	a	0.998	0.050
	L	100	2.09 ± 0.05	b	7.1 ± 0.5	b	0.989	0.028
	L	500	0.80 ± 0.00	c	8.5 ± 0.0	c	0.995	0.009
43	**L**	1	94.93 ± 0.00	d	2.4 ± 0.2	d	0.994	0.339
	L	10	15.06 ± 1.04	a	5.5 ± 0.3	a	0.997	0.070
	L	100	2.84 ± 0.07	b	7.0 ± 0.4	b	0.988	0.037
	L	500	1.05 ± 0.03	c	8.4 ± 0.1	c	0.999	0.006

No.	*Group*	$\dot{\gamma}$ [s^{-1}]	η_{ref} [Pa]		E_a [kJ/mol]		R^2	*RMSE*
44	**L**	1	108.70 ± 8.82	c	3.5 ± 0.4	c	0.933	2.080
	L	10	14.54 ± 0.91	a	7.9 ± 0.4	a	0.963	0.439
	L	100	3.16 ± 0.11	b	7.3 ± 2.6	a	0.994	0.046
	L	500	0.80 ± 0.09	b	11.7 ± 0.2	b	0.948	0.019
45	**M**	1	101.17 ± 6.87	c	3.1 ± 0.1	a	0.933	3.631
	M	10	14.14 ± 0.21	a	5.0 ± 1.2	ab	0.993	0.474
	M	100	2.50 ± 0.03	b	6.7 ± 1.2	ab	0.968	0.062
	M	500	0.69 ± 0.10	b	7.2 ± 0.9	b	0.957	0.019
46	**M**	1	68.71 ± 3.99	b	10.5 ± 2.3	b	0.926	9.625
	M	10	12.47 ± 0.94	a	13.7 ± 0.8	b	0.962	0.748
	M	100	2.56 ± 0.30	a	15.1 ± 0.6	a	0.908	0.162
	M	500	0.76 ± 0.04	a	19.9 ± 1.0	c	0.986	0.018
47	**M**	1	75.72 ± 0.00	c	3.6 ± 0.4	c	0.914	1.761
	M	10	10.86 ± 1.46	a	6.0 ± 0.0	ab	0.966	0.202
	M	100	2.08 ± 0.07	b	5.8 ± 0.0	a	0.980	0.033
	M	500	0.73 ± 0.02	b	6.5 ± 0.2	b	0.994	0.007
48	**M**	1	39.63 ± 0.00	d	9.6 ± 2.0	a	0.914	1.697
	M	10	6.66 ± 0.19	a	9.1 ± 1.1	a	0.969	0.177
	M	100	1.42 ± 0.04	b	6.6 ± 0.8	a	0.965	0.083
	M	500	0.55 ± 0.01	c	7.0 ± 0.5	a	0.974	0.035
49	**M**	1	34.78 ± 2.35	c	6.2 ± 0.5	a	0.984	0.452
	M	10	5.32 ± 0.08	a	7.0 ± 1.1	ab	0.972	0.115
	M	100	1.10 ± 0.01	b	7.0 ± 0.3	ab	0.934	0.038
	M	500	0.43 ± 0.01	b	8.0 ± 0.2	b	0.962	0.013
50	**M**	1	28.50 ± 6.81	b	3.4 ± 0.0	d	0.969	1.273
	M	10	6.15 ± 0.16	a	12.4 ± 0.0	c	0.903	0.376
	M	100	2.30 ± 0.06	a	13.3 ± 0.5	a	0.950	0.143
	M	500	0.75 ± 0.00	a	19.3 ± 0.1	b	0.997	0.008
51	**M**	1	92.84 ± 1.45	c	0.2 ± 0.2	d	0.975	1.202
	M	10	0.21 ± 2.46	a	3.1 ± 0.0	a	0.981	0.237
	M	100	2.46 ± 0.03	b	4.8 ± 0.2	b	0.986	0.026
	M	500	0.76 ± 0.00	b	5.9 ± 0.4	c	0.993	0.007
52	**M**	1	103.49 ± 9.02	c	3.5 ± 0.7	c	0.925	1.914
	M	10	15.85 ± 0.99	a	7.9 ± 0.7	a	0.942	0.508
	M	100	2.93 ± 0.21	b	9.1 ± 0.7	b	0.977	0.070
	M	500	0.96 ± 0.04	b	10.8 ± 1.1	b	0.967	0.030
53	**M**	1	76.17 ± 3.26	c	3.0 ± 0.9	d	0.984	1.262
	M	10	12.59 ± 0.22	a	5.7 ± 0.4	a	0.975	0.202
	M	100	2.47 ± 0.08	b	8.0 ± 0.2	b	0.993	0.028
	M	500	0.82 ± 0.04	b	9.7 ± 0.3	c	0.995	0.009
54	**M**	1	76.41 ± 4.36	c	1.1 ± 0.5	d	0.955	0.744
	M	10	11.64 ± 0.31	a	3.5 ± 0.1	a	0.951	0.182
	M	100	2.21 ± 0.07	b	5.5 ± 0.2	b	0.968	0.043
	M	500	0.75 ± 0.03	b	7.4 ± 0.5	c	0.995	0.007
55	**M**	1	67.73 ± 3.30	c	0.8 ± 0.7	d	0.958	0.902
	M	10	9.97 ± 0.15	a	3.7 ± 0.0	a	0.948	0.175
	M	100	1.90 ± 0.03	b	5.0 ± 0.5	b	0.921	0.061
	M	500	0.64 ± 0.01	b	7.1 ± 0.1	c	0.988	0.009

Ketchups and Condiment sauces

The products of the ketchup and condiment sauce group no. 1-32 are merged in this section, because there are no mayor differences between these two groups, besides the higher amount of spices in condiment products.

The apparent viscosity for this products was in the range of η_{ref} = 0.19 - 106.6 Pas and showed a significant decrease in dependence of shear rate as expected. The activation energy for the investigated products ranged from E_a = 1.89 - 18.01 kJ/mol. These values could be confirmed by the reported observations of Koocheki et al. [59], who investigated tomato ketchups in a temperature range of 25 – 55 °C and stated values for activation energy in the range E_a = 5.4 - 21.5 kJ/mol.

Sharoba et al. [64] observed similar results for commercial ketchups and reported values of activation energy in the range of E_a = 7.12 - 10.87 kJ/mol at a shear rate of $\dot{\gamma}$= 100 s^{-1} for the temperature range 0 – 50 °C. The reference viscosity for their trails ranged from η_{ref} = 2.24 - 3.79 Pas. For tomato concentrate similar values for activation energy E_a = 9.211 kJ/mol at a shear rate of $\dot{\gamma}$ = 100 s^{-1} were reported [81].

A significant increase of the activation energy with rising shear rate was observed for the products 1, 2, 3, 4, 5, 6, 7, 9, 12, 15, 16, 17, 18, 21, 22, 27, 29 and 32. Whereas contrary behavior, implying a decrease of activation energy, was observed for the products 19, 23, 24, 25 and 26. The values of activation energy for the products 8, 10, 13, 14, 20, 28, 30 and 31 were independent from shear rate.

Fat reduced mayonnaises

The group of fat reduced mayonnaises and dressings (no. 33 - 44) can considered to be like mayonnaises oil-in-water emulsions and can be differentiated by their fat content, which is typically below 50 % and requires a thickened continuous phase to prevent phase separation.

The apparent viscosity for these products was in the range of η_{ref} = 0.44 - 129.93 Pas and showed as expected a significant decrease in dependence of shear rate as expected, since all of these products were observed to be shear thinning. The values for the activation energy ranged from E_a = 2.41 - 13.37 kJ/mol.

Parades et al. [50] investigated the temperature dependent flow behavior of different commercial salad dressings in a temperature range of T = 2 - 43.3 °C. The activation energy at a shear rate of $\dot{\gamma} = 100\ s^{-1}$ ranged between 10.47 to 20.52 kJ/mol and thus confirmed the measured results. Similar results were published by Marcotte et al. [84], who investigated the influences of temperature on selected hydrocolloid suspensions with different concentrations, which are mostly used for thickening of fat reduced products. Values of activation energy in the range of $E_a = 0.36 - 54.9$ kJ/mol with a reference viscosity $\eta_{ref} = 2.99 \cdot 10^{-10} - 1.42 \cdot 10^{-2}$ Pas were reported at a temperature range from 20 to 80 °C and a shear rate of $\dot{\gamma} = 50\ s^{-1}$. Karazhiyan et al. [52] report similar results for Lepidium sativum suspension, which is a hydrocolloid ($T = 10 – 70$ K, $\dot{\gamma} = 50\ s^{-1}$, $E_a = 7.82 - 15.59$ kJ/mol, $\eta_{ref} = 0.001 - 0.075$ Pas) and stated that E_a decreased with increasing gum concentration.

A significant increase of the activation energy with rising shear rate was observed for almost all products, only the activation energy of product 36 exhibited no significant dependency on the shear rate.

Classical mayonnaises

Classical mayonnaises no. 45 to no. 55, which represent the last group, are an oil-in-water emulsion containing 65 - 82 % of fat. The observed apparent viscosity at different shear rates of $\dot{\gamma} = 1,\ 10,\ 100,\ 500\ s^{-1}$ for this products was in the range of $\eta_{ref} = 0.21 - 103.49$ Pas and showed as expected a significant decrease in dependence of shear rate as expected, since all of these products were observed to be shear thinning. The activation energy for the investigated products ranged from $E_a = 0.18 - 19.86$ kJ/mol. The shear rate had like for the group of ketchup and fat reduced products a significant influence, implying an increase of E_a with rising shear rate, on the values of activation energy, whereas product 48 was observed to be independent from shear rate.

3.4 Combination of shear rate and temperature dependency

In the following section the different influencing factors were combined for the development of a general model, which incorporates shear rate and temperature dependent

flow characteristics. The effect of time dependency was neglected, since all measurements were performed at steady-state condition during the entire investigation [112]. An attempt to combine the calculation of shear rate and temperature dependent flow behavior of non-Newtonian samples was introduced in section 1.1.2.6, whereas the Ostwald-de-Waele and the Arrhenius model are the underlying Equations.

The flow behavior index $\bar{n}$ is assumed to be temperature independent, which leaves the consistency coefficient K_T as temperature dependent variable (see Equation 3.1) [43].

$$\eta_a = f(T, \dot{\gamma}) = K_T \cdot e^{\left(\frac{E_a}{RT}\right)} (\dot{\gamma})^{\bar{n}-1} \qquad \textbf{3.1}$$

The presented results in section 0 lead to rejection of the application of the Ostwald-de-Waele model for the description of the shear rate dependent characteristics of the investigated samples. Instead the Herschel-Bulkley model, which extends the Ostwald-de-Waele model by addition of a yield stress τ_0, was accepted.

The parameters yield stress, consistency coefficient and flow behavior index showed to be significantly dependent on temperature. However the behavior of the single parameters followed no consistent pattern, apart from a general decrease of the apparent viscosity with rising temperature and vice versa. Thus the apparent viscosity η_{ref} was calculated according to Equation 3.2 at a reference temperature (T_{ref} = 298.15 K) and subsequently shifted to the desired temperature by applying the Arrhenius type equation.

The activation energy E_a of most samples showed significant shear rate dependency, as in section 3.3 was presented. The relation of activation energy and shear rate could be described by a logarithmic function, whereas the model evaluation procedure, stated in section 2.4, was performed. The logarithmic model could be validated since the p-values were always in excess of 0.05, which indicated normal distribution of the residua. The coefficient of determination was always higher than $R^2 > 0.95$ and the root mean square error ranged from RMSE = 0.02 - 0.93, indicating a very good fit. The developed Equation was used to substitute the constant value for activation energy, which lead to Equation 3.3.

$$\eta_{T_{ref}} = \frac{\tau_{0ref}}{\dot{\gamma}} + K_{ref} \cdot (\dot{\gamma})^{[n_{ref} - 1]} \qquad \textbf{3.2}$$

$$\eta_{a,\,T,\,\dot{\gamma}} = \eta_{T_{ref}} \cdot e^{\left[\left(\frac{(E_{a1} \cdot \ln\dot{\gamma} + E_{a2})}{R}\right) \cdot \left(\frac{1}{T} - \frac{1}{T_{ref}}\right)\right]} \qquad \textbf{3.3}$$

Another approach for the combination of shear rate and temperature dependency was developed, whereas the temperature dependency of each Herschel-Bulkley parameter was characterized by a temperature dependent linear system of Equations for yield stress, consistency coefficient and flow behavior index resulting in Equation 3.4.

$$\eta_{a,\,T,\,\dot{\gamma}} = \frac{(\tau_s \cdot T + \tau_a)}{\dot{\gamma}} + (K_s \cdot T + K_a)(\dot{\gamma})^{[(n_s \cdot T + n_a) - 1]} \qquad \textbf{3.4}$$

The characteristic parameters of 47 products, which could be validated for the Herschel-Bulkley and Arrhenius type models in the sections 0 and 3.3, were used for the evaluation of the Equations 3.3 and 3.4. Figure 3.8 exemplary depicts the calculated shear rate and temperature dependent viscosity functions of product no. 17 based on the Equations 3.3 and 3.4.

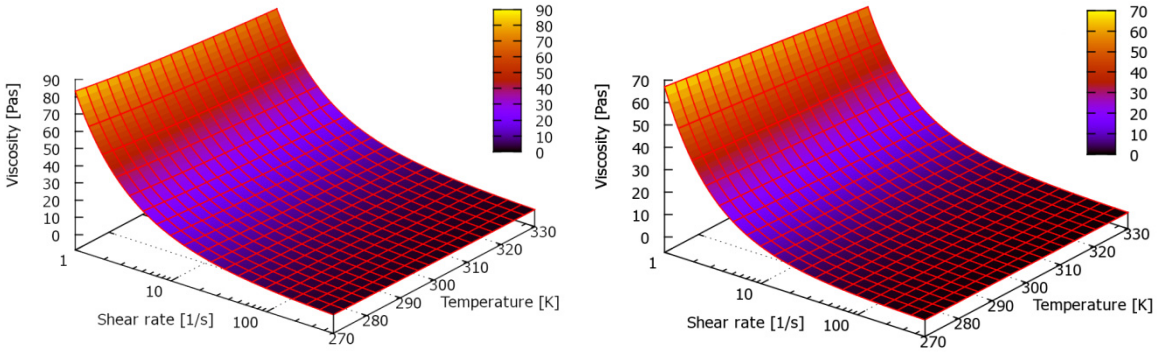

(a) Arrhenius type equation (b) Linear type equation

Figure 3.8: Two approaches for calculation of viscosity functions in dependence of temperature and shear rate of product 17

For evaluation of the models the procedure of section 2.4 was applied, whereas the residua were tested for normal distribution and the goodness of fit was described by means of the coefficient of determination and the root mean square error. Table 3.13 shows comparative the statistic measures of both models.

In general the p-value for both models was always below p = 0.05, implying no normal distribution of the residua and thus both Equations could not be validated according to the procedure of section 2.4. However the coefficient of determination for the Arrhenius type equation was in the range of R^2 = 0.828 - 0.995 with values for the root mean square error ranging from RMSE = 0.281 - 4.755. The linear type Equation 3.4 showed in comparison a lower coefficient of determination (R^2 = 0.286 - 0.995) and higher values for the root mean square error (RMSE = 1.01 - 21.62).

Table 3.13: Comparison of goodness of fit parameters and probability values of Arrhenius type (Equation 3.3) and linear type (Equation 3.4) modeling approaches for shear rate ($\dot{\gamma}$ = 1 - 500 s^{-1}) and temperature range (T = 5 - 55°C) .

No.	Group	Arrhenius type equation 3.3			Linear type equation 3.4		
		R^2	*RMSE*	p-value	R^2	*RMSE*	p-value
1	**K**	0.983	0.78	6.88E-49	0.908	4.66	9.44E-75
2	**K**	0.982	0.70	9.94E-47	0.995	4.93	1.25E-74
3	**K**	0.941	2.55	2.06E-49	0.944	3.30	2.92E-72
4	**K**	0.893	0.83	5.69E-49	0.681	21.62	1.44E-75
5	**K**	0.931	0.80	6.29E-48	0.880	14.67	1.88E-75
6	**K**	0.946	1.03	4.81E-49	0.791	3.69	1.71E-74
7	**K**	0.920	2.14	3.47E-59	0.872	3.50	1.11E-85
8	**K**	0.991	1.14	3.24E-58	0.725	11.23	4.68E-88
9	**K**	0.978	0.95	2.40E-53	0.797	3.37	2.24E-85
10	**K**	0.964	1.57	1.29E-59	0.889	5.63	2.78E-86
13	**K**	0.991	0.70	1.94E-56	0.588	8.27	1.76E-88
15	**K**	0.936	2.18	6.68E-59	0.815	4.32	5.44E-85
16	**K**	0.974	0.88	2.07E-59	0.726	3.59	2.01E-86
17	**K**	0.993	0.60	4.32E-57	0.917	2.94	2.10E-86
18	**K**	0.989	0.53	2.16E-55	0.334	4.74	2.71E-86
19	**K**	0.890	2.68	7.07E-59	0.844	6.33	3.27E-86
20	**K**	0.961	1.49	1.48E-57	0.828	5.47	3.81E-86
21	**C**	0.995	0.28	1.93E-52	0.755	2.38	3.44E-86
22	**C**	0.992	0.44	4.00E-46	0.857	2.30	5.25E-86
28	**C**	0.954	1.73	5.48E-49	0.803	4.06	8.03E-73
29	**C**	0.958	0.86	9.37E-58	0.981	5.67	1.98E-88
30	**C**	0.828	3.64	4.73E-50	0.782	4.88	1.05E-72
31	**C**	0.971	1.29	1.59E-49	0.772	2.14	7.41E-74
32	**C**	0.975	0.48	4.36E-48	0.806	1.49	2.03E-73
33	**L**	0.903	3.06	6.69E-60	0.819	6.51	2.24E-85
34	**L**	0.985	1.24	1.07E-55	0.863	4.99	9.89E-87
35	**L**	0.979	2.18	2.19E-50	0.611	12.10	8.02E-77
36	**L**	0.902	1.98	1.71E-59	0.687	4.66	1.69E-85
37	**L**	0.930	2.64	3.29E-58	0.549	10.70	1.53E-86
38	**L**	0.988	1.01	1.94E-54	0.924	3.30	7.15E-87
39	**L**	0.910	0.79	1.37E-57	0.891	1.01	2.82E-82
40	**L**	0.940	1.91	3.93E-58	0.835	4.16	5.36E-86
41	**L**	0.913	3.08	1.32E-59	0.475	9.33	1.32E-85
42	**L**	0.990	0.77	6.32E-49	0.878	4.09	1.09E-73
43	**L**	0.986	1.30	5.94E-46	0.873	5.34	1.58E-73
44	**L**	0.870	4.76	2.20E-59	0.921	6.25	2.75E-85

No.	Group	Arrhenius type equation 3.3			Linear type equation 3.4		
		R^2	*RMSE*	p-value	R^2	*RMSE*	p-value
45	**M**	0.989	1.20	9.22E-51	0.852	6.39	3.89E-77
46	**M**	0.877	3.32	4.25E-49	0.889	5.32	4.11E-73
47	**M**	0.988	0.96	5.84E-50	0.823	4.88	2.21E-74
48	**M**	0.969	1.93	1.56E-51	0.287	9.86	1.59E-74
49	**M**	0.992	0.36	1.08E-47	0.846	2.24	8.17E-76
50	**M**	0.943	1.05	3.69E-43	0.664	3.62	5.14E-65
51	**M**	0.984	1.36	9.53E-49	0.956	3.55	4.04E-74
52	**M**	0.980	1.72	7.98E-48	0.971	3.00	5.06E-69
53	**M**	0.979	1.48	1.21E-44	0.923	3.88	5.08E-66
54	**M**	0.955	1.71	1.14E-52	0.783	7.45	4.45E-76
55	**M**	0.984	1.01	3.02E-49	0.955	2.45	1.16E-73
Mean		**0.955**	**1.51**		**0.799**	**5.54**	

The Arrhenius type equation was selected for the further proceeding, because the statistical measures indicated a better fit compared to the linear type equation. Although the residua followed no normal distribution, it can be assumed that the accuracy of this model, indicated by its in general high coefficient of determination and low root mean square error, allows the utilization for estimation of the viscosity function depending on shear rate and temperature within the measured boundary conditions.

Table 3.14 shows the resulting characteristic product parameters of the reference yield stress τ_{0ref}, consistency coefficient K_{ref}, flow behavior index n_{ref} and activation energy E_{a1} and E_{a2}. Based on Equation 3.2 and these parameters the shear rate and temperature dependent flow behavior of each sample can be estimated with a coefficient of determination $R^2 > 0.83$.

Table 3.14: Final product parameters for temperature and shear rate dependent flow behavior

No.	*Group*	τ_{0ref} [Pa]	K_{ref} [Pas^n]	n_{ref} [-]	E_{a1}[kJ·s/mol]	E_{a2} [kJ/mol]
1	**K**	42.5	6.2	0.46	0.512	6.547
2	**K**	35.4	6.6	0.43	0.408	7.837
3	**K**	24.5	46.6	0.26	0.289	5.927
4	**K**	4.1	11.9	0.33	0.493	6.434
5	**K**	0.0	20.4	0.31	0.414	6.390
6	**K**	24.7	10.3	0.43	1.028	3.528
7	**K**	42.8	23.0	0.38	1.521	1.685
8	**K**	78.2	21.6	0.37	0	5.775
9	**K**	38.8	21.9	0.45	0.791	4.904
10	**K**	56.5	27.4	0.24	0	5.775
13	**K**	49.8	14.5	0.34	0.033	7.742
15	**K**	39.2	20.5	0.43	0.605	5.017

No.	*Group*	τ_{0ref} [Pa]	K_{ref} [Pas^n]	n_{ref} [-]	E_{a1}[kJ·s/mol]	E_{a2} [kJ/mol]
16	**K**	32.9	17.3	0.43	0.667	3.485
17	**K**	42.0	21.3	0.33	0.378	5.110
18	**K**	0.0	43.5	0.29	0.424	7.760
19	**K**	63.5	28.2	0.24	-0.701	10.624
20	**K**	60.2	16.6	0.32	-0.252	9.428
21	**C**	22.3	12.2	0.51	0.222	9.623
22	**C**	30.6	10.7	0.52	0.290	9.223
28	**C**	44.3	13.2	0.46	0	7.550
29	**C**	25.0	5.8	0.47	0.761	6.303
30	**C**	22.5	23.1	0.36	0	9.475
31	**C**	2.6	7.2	0.49	0	10.525
32	**C**	17.2	6.1	0.57	1.343	4.843
33	**L**	89.3	19.3	0.44	0.458	4.647
34	**L**	71.0	18.4	0.52	0.592	5.257
35	**L**	111.7	29.8	0.49	0.700	2.905
36	**L**	46.2	22.9	0.49	0.056	9.193
37	**L**	35.3	30.4	0.38	0.327	8.226
38	**L**	48.6	13.1	0.52	0.850	3.835
39	**L**	6.0	10.3	0.57	1.105	6.875
40	**L**	42.4	11.6	0.52	0.539	7.258
41	**L**	85.8	28.0	0.47	0.162	6.793
42	**L**	57.8	15.0	0.51	0.704	4.040
43	**L**	82.6	20.7	0.5	0.936	2.755
44	**L**	134.5	19.3	0.51	1.123	3.917
45	**M**	87.4	24.9	0.42	0.677	3.280
46	**M**	74.8	22.9	0.43	1.383	10.262
47	**M**	66.4	15.3	0.49	0.411	4.127
48	**M**	31.8	9.3	0.53	0	8.075
49	**M**	28.7	7.7	0.51	0.252	6.224
50	**M**	1.5	6.6	0.64	2.308	4.529
51	**M**	48.1	33.1	0.39	0.905	0.532
52	**M**	41.2	51.7	0.36	1.111	4.180
53	**M**	27.8	38.5	0.38	1.071	3.088
54	**M**	43.4	29.9	0.41	0.995	1.112
55	**M**	37.9	22.5	0.43	0.961	0.999

4 Development of a prediction model

The objective of this section is the development of a prediction model for rheological properties based on the composition of carbohydrates, fats, proteins and water. The characteristic parameters, which were determined in section 3.4, allow the estimation of the apparent viscosity of a sample at any given shear rate - temperature combination within the given boundary conditions utilizing Equations 3.2 and 3.3.

The equation represents a combination of the Herschel-Bulkley and Arrhenius-type model and is characterized by five parameters, namely reference yield stress τ_{ref}, consistency coefficient K_{ref}, flow behavior index n_{ref}, pre-factor of activation energy E_{a1} and activation energy E_{a2}. These characteristic parameters and the composition data are subjected to linear and multiple linear regression to determine correlations, which can be used for the estimation of rheological properties.

In section 4.1 the complete product range is analyzed, whereas in section 4.2 different approaches for classification are applied to the product range to evaluate their predictive suitability for rheological properties. In section 4.3 a composition independent model is developed.

4.1 Analysis of complete product range

For the identification of correlations between composition data and rheological characteristics a multiple two-variable scatter plot was constructed. Figure 4.1 depicts a scatter plot, which implies the entire product range, whereas the framed areas show the scatter plots of the composition and the rheological parameters. In case of obvious correlations a linear and multiple linear regression analysis would be performed. However no correlations were found during graphical evaluation. As a result the product range was classified to generate subgroups, which could exhibit similar rheological characteristics.

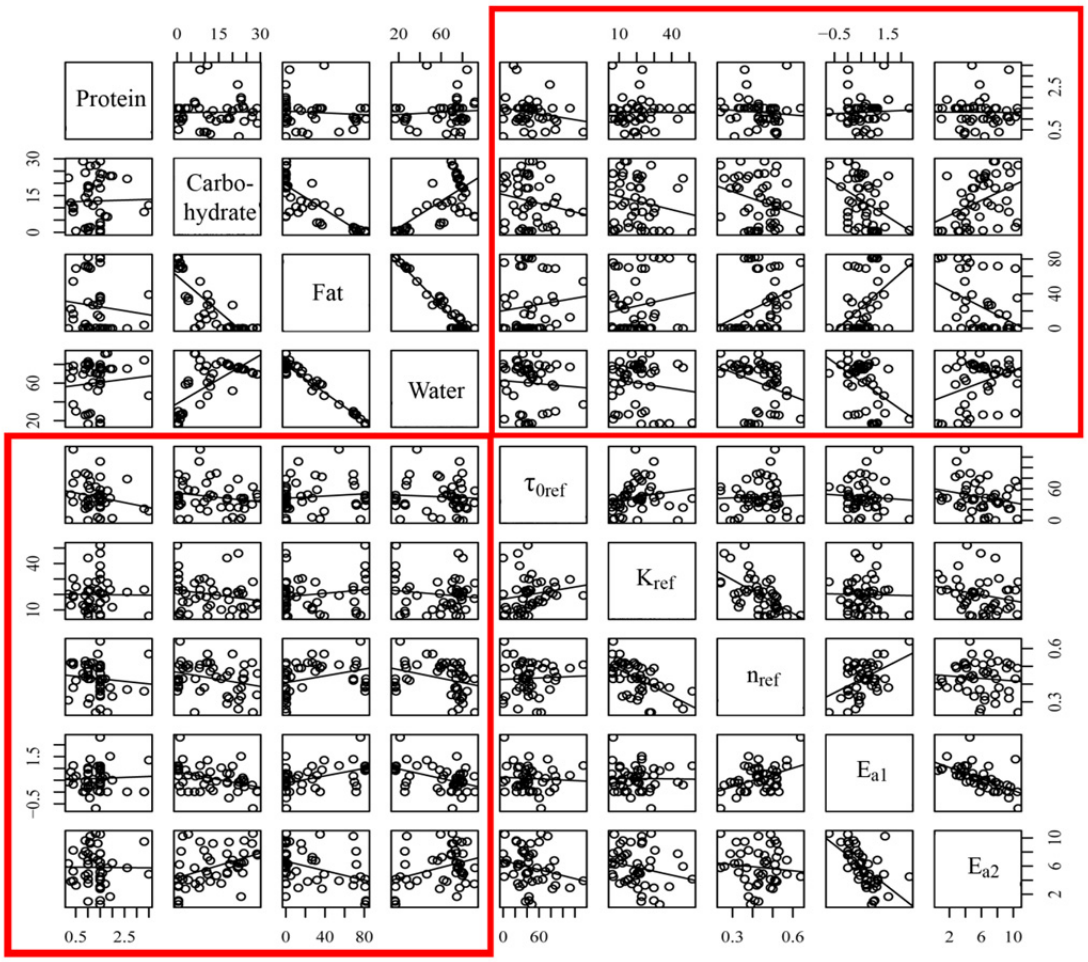

Figure 4.1: Multiple two-variable scatter plot

4.2 Classification and analysis of product range

The product range was divided into groups based on different systematic classification approaches, which were presented in section 1.1.1.3. Subsequently these approaches were applied in the sections 4.2.1 - 4.2.3 to generate subgroups. Within these subgroups it was assumed to identify specific properties, which allow the prediction of the rheological characteristics within each group based on the composition.

4.2.1 Function based classification

The product range was divided into four groups, namely condiment sauce, classic emulsion and non-classic emulsion, whereas latter was subdivided into spoon-able and pourable. The

assigned products and their corresponding minimum and maximum values for composition and rheological characteristics of each group can be seen in Table 4.1.

Table 4.1: Applied function based classification

Subgroup	**Classic emulsion**		**Non-classic spoonable emulsion**		**Non-classic pourable emulsion**		**Condiment sauce**	
Products No.	**50, 51, 52, 53, 54, 55**		**33, 34, 35, 36, 38, 40, 41, 42, 43, 44, 45, 46, 47**		**31, 32, 37, 39, 48, 49**		**1, 2, 3, 4, 5, 6, 7, 8, 9, 10, 13, 15, 16, 17, 18, 19, 20, 21, 22, 28, 29, 30**	
	min.	**max.**	**min.**	**max.**	**min.**	**max.**	**min.**	**max.**
Proteins [%]	1.0	1.5	0.3	1.5	0.4	3.5	0.2	3.3
Carbohydrates [%]	0.0	1.0	0.5	14.2	0.8	20.0	6.3	29.0
Fats [%]	76.0	82.0	4.8	70.0	16.7	72.0	0.0	4.0
Water [%]	16.0	21.5	27.0	80.1	25.8	73.1	69.4	91.8
τ_{0ref} [Pa]	1.52	48.10	42.44	134.51	2.56	35.32	0.00	78.21
K_{ref} [Pasn]	6.55	51.72	11.60	29.78	6.10	30.35	5.82	46.63
n_{ref} [-]	0.36	0.64	0.42	0.52	0.38	0.57	0.24	0.52
E_{a1} [kJs/mol]	0.90	2.31	0.06	1.38	0.00	1.34	-0.70	1.52
E_{a2} [kJ/mol]	0.53	4.53	2.75	10.26	4.84	10.53	1.69	10.62

The group of classic emulsions comprised six products, the subgroup non-classic spoonable emulsion contains 13 products and the subgroup non-classic pourable emulsion counted six products. 22 products were assigned to the subgroup condiment sauces.

The protein and carbohydrate content in general do not allow any differentiation of the different groups, since the values were superimposed. The fat content however indicates a clear separation of the groups classic emulsion and condiment sauce. The values for fat content within the non-classic spoonable and pourable group could not be distinguished. The yield stress value τ_{ref} was the only parameter, which showed only partial superimposed values for the group of non-classic spoonable and pourable emulsions. The parameters consistency coefficient K_{ref}, flow behavior index n_{ref} and activation energy E_{a1} and E_{a2} did not allow a differentiation of the subgroups.

Classic emulsion

All products within the group of classic emulsions contained no hydrocolloids and had a fat content above 76 %. For the identification of correlations between composition data and rheological characteristics a multiple two-variable scatter plot was constructed for the group of classic emulsions. Despite the fact of minor variations within the composition of this group, the rheological characteristic parameters covered a wide range of values for each parameter. The differences between the samples could be traced back to different raw materials and to different processing techniques and conditions, which could have caused different oil droplet size distributions and thus different rheological characteristics.

Figure 4.2 depicts the scatter plot, whereas the framed areas show the scatter plots of the composition and the rheological parameters. Graphically no correlations were found.

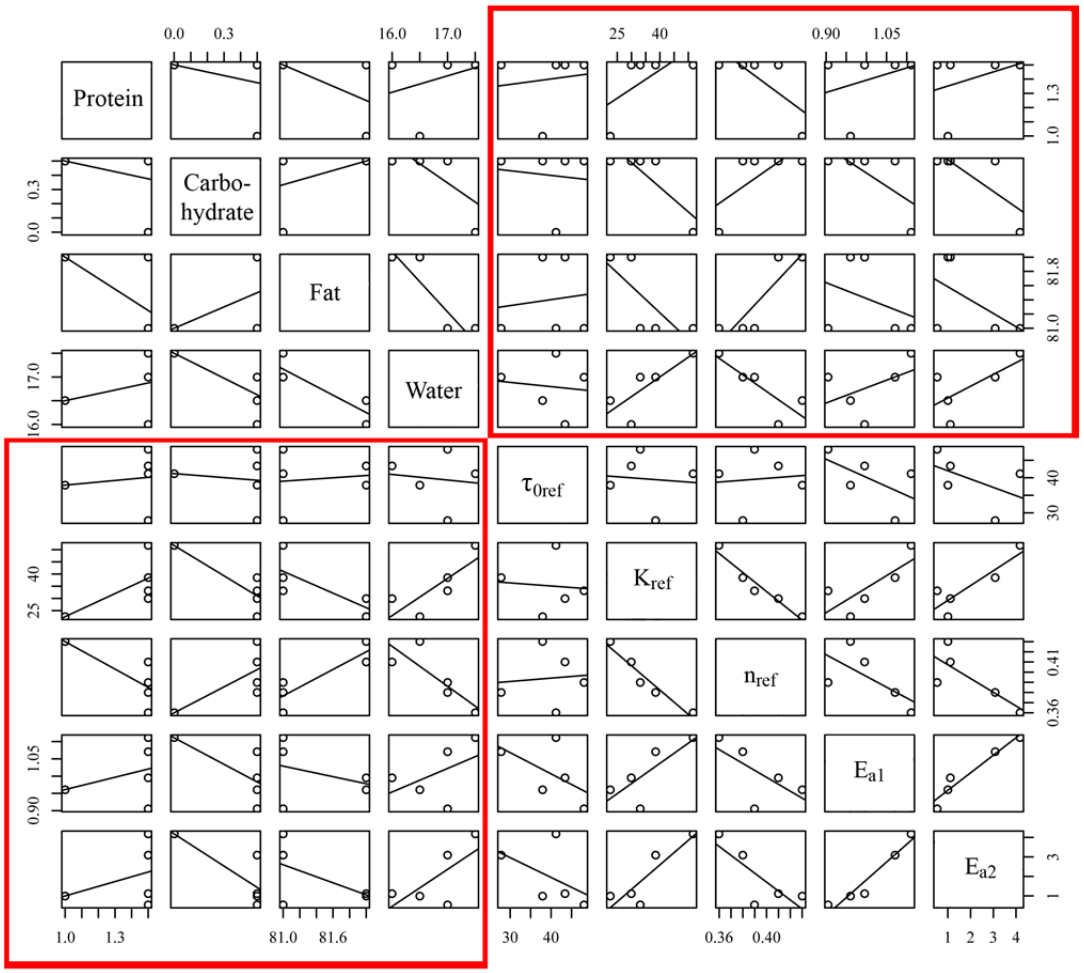

Figure 4.2: Multiple two-variable scatter plot for the subgroup classical emulsion

Non-classic spoonable emulsion

The group of non-classic spoonable emulsions could be characterized by high variation in composition and the addition of several hydrocolloids. The carbohydrate content varied from 0.5 up to 14.2 %, whereas the fat content ranged from 4.8 up to 70 %. Compared to the other groups this group exhibited a higher yield stress (τ_{ref} = 42.44 - 134.51 Pa).

A multiple two-variable scatter plot was constructed for the group of non-classic spoonable emulsions for the identification of correlations between composition data and rheological characteristics. The framed areas in Figure 4.3 depict the scatter plots of the composition and the rheological parameters. Graphically no correlations were found.

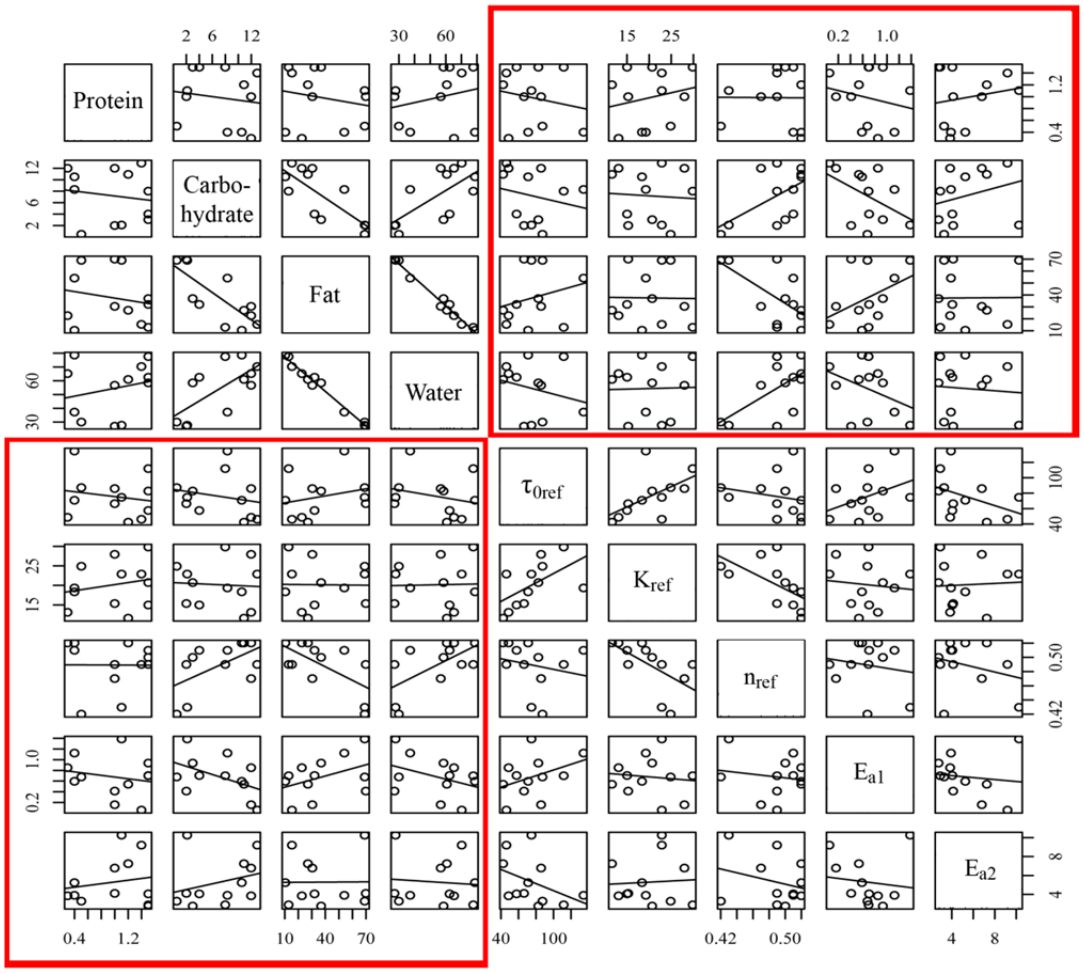

Figure 4.3: Multiple two-variable scatter plot for the subgroup non-classical spoonable emulsion

Non-classic pourable emulsion

The group of non-classic pourable emulsions is comparable to the group of non-classic spoonable emulsions from the composition point of view. However the yield stress ranged from τ_{ref} = 2.56 - 35.32 Pa and thus was lower in comparison to the non-classic spoonable emulsion. The other characteristic parameters were spread over a wide range. This difference could be explained by the fact, that the designated use of these products requires less resistance to flow to allow pouring out of a vessel.

For identification of correlations between composition data and rheological characteristics a multiple two-variable scatter plot was constructed for the group of non-classic pourable emulsions. Figure 4.4 depicts the scatter plot matrix, whereas the framed areas show the scatter plots for the composition and the rheological parameters. No correlations were graphically identified.

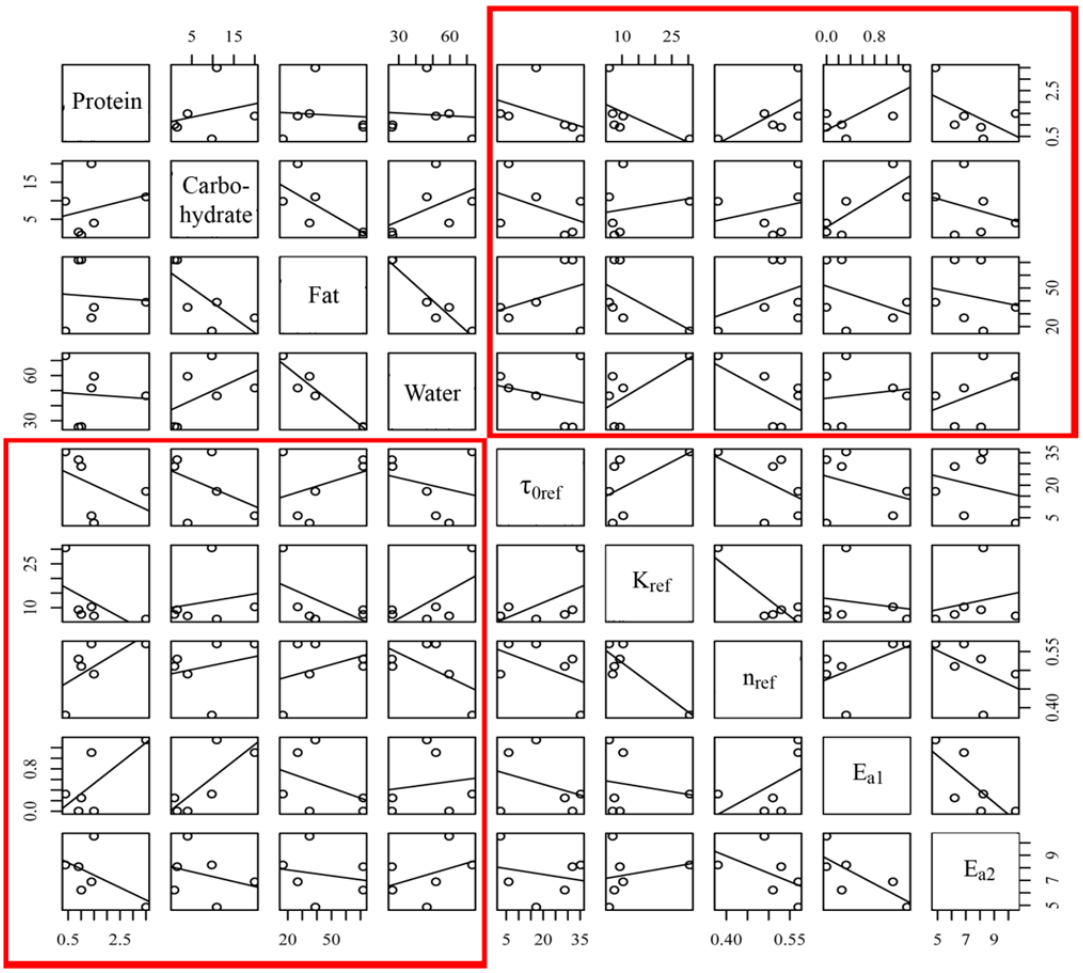

Figure 4.4: Multiple two-variable scatter plot for the subgroup non-classical pourable emulsion

Condiment sauces

The products of the group condiment sauces were characterized by a maximum amount of fat of 4 %. In contrast the carbohydrates and water content was the highest compared to the other groups. The rheological characteristics showed a broad range of variation. Correlations between composition data and rheological characteristics were identified by a multiple two-variable scatter plot, which can be seen in Figure 4.5.The framed areas depict the scatter plots of the composition and the rheological parameters and graphically indicate no correlation.

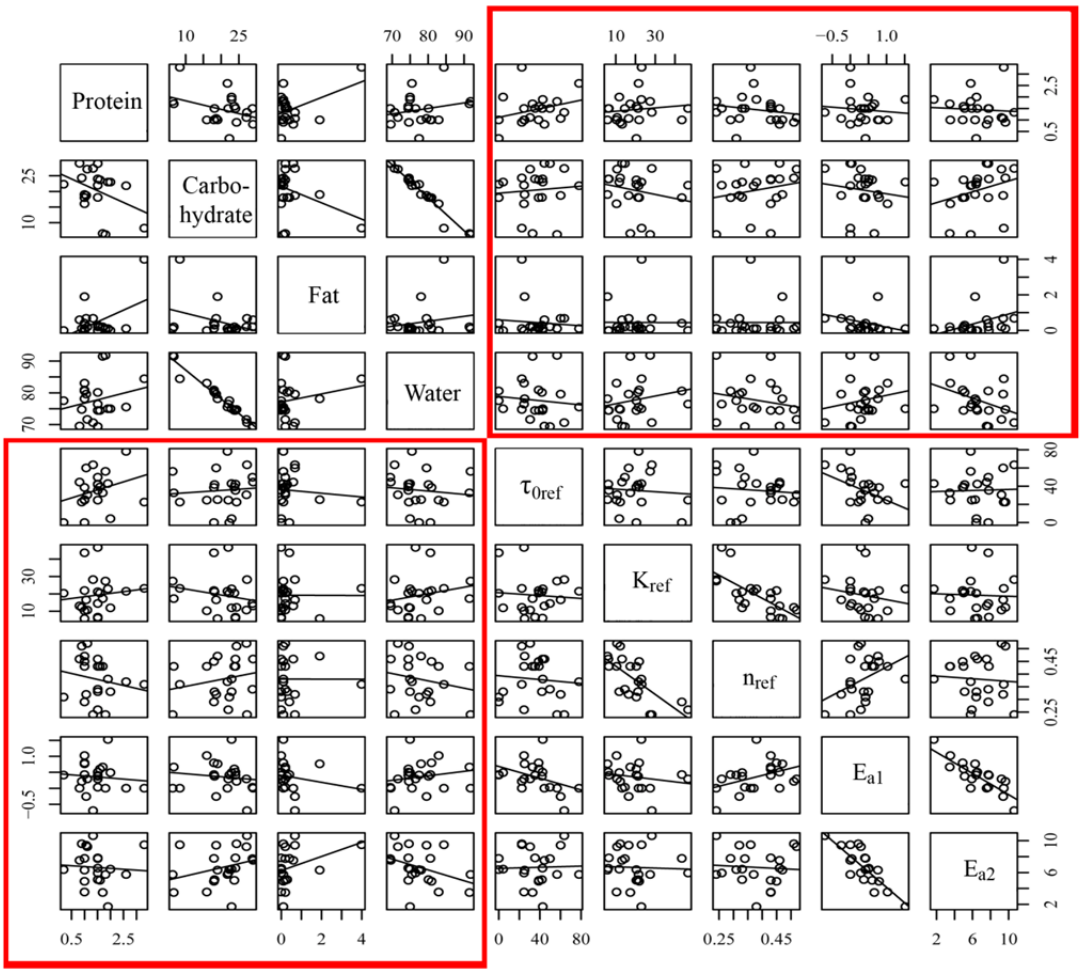

Figure 4.5: Multiple two-variable scatter plot for the subgroup condiment sauce

The function based classification in summary divided the product range into 4 different subgroups based on the macroscopic structure and the designated use of a product. The differentiation however did not allow an estimation of the rheological properties within a specific group. The variability of the characteristic parameters within each group was too high to assign specific rheological characteristics to one group.

4.2.2 Composition based classification

The composition based approach assumes that the content of oil, water and the total solids can be used as categorizing criteria. Each product was plotted according to its total solids, total water and total oil content into the ingredient combination map proposed by Sheldrake [12]. In this map 4 regions with different ranges of oil, water and total solids were defined, which can be seen in Figure 4.6.

The classified product range and their corresponding minimum and maximum values for composition and rheological characteristics can be seen in Table 4.2. In general the different groups showed superimposed values for the rheological characteristics.

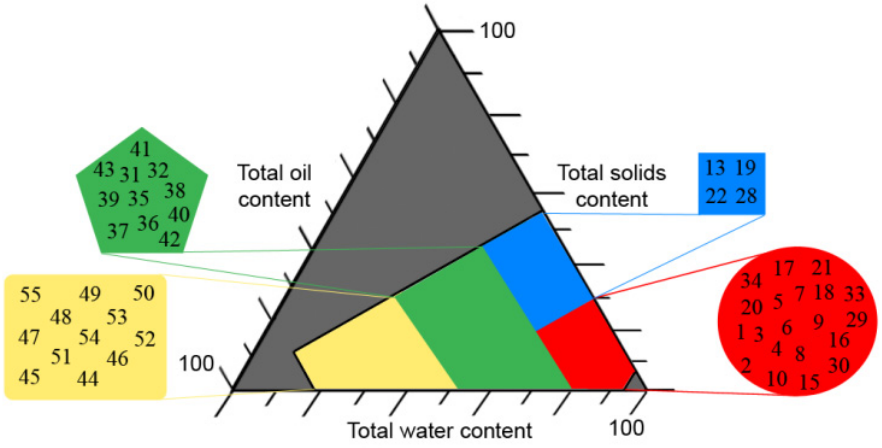

Figure 4.6: Ingredient combination scheme with 4 categories

Table 4.2: Applied composition based classification

Subgroup	red		Blue		green		yellow	
Product No.	1, 2, 3, 4, 5, 6, 7, 8, 9, 10, 15, 16, 17, 18, 20, 21, 29, 30, 33, 34		13, 19, 22, 28		31, 32, 35, 36, 37, 38, 39, 40, 41, 42, 43		44, 45, 46, 47, 48, 49, 50, 51, 52, 53, 54, 55	
	min.	max.	min.	max.	min.	max.	min.	max.
Proteins [%]	0.2	3.3	0.8	1.5	0.3	3.5	0.4	1.5
Carbohydrates [%]	6.3	24.3	27.1	29	3	20	0	8.3
Fats [%]	0	10.5	0.2	0.67	13	39	54.1	82
Water [%]	74.5	91.8	69.4	71.6	46.5	77.5	16	37.2
τ_{0ref} [Pa]	0	89.28	30.56	63.5	2.56	111.67	1.52	134.51
K_{ref} [Pasn]	5.82	46.63	10.71	28.2	6.1	30.35	6.55	51.72
n_{ref} [-]	0.24	0.52	0.24	0.52	0.38	0.57	0.36	0.64
E_{a1} [kJs/mol]	-0.25	1.52	-0.70	0.29	0	1.3433	0.00	2.31
E_{a2} [kJ/mol]	1.69	9.62	7.55	10.62	2.7548	10.525	0.53	10.26

Red

Based on the pre-determined ranges for fat, water and total solids content this group consisted of ketchups and condiment sauces, which were mostly tomato based products. 20 products were assigned to this group, which is characterized by total oil content of maximum 10 %, a total water content of minimum 75 % and a total solids content of maximum 30 %. Every rheological characteristic covered almost the entire range of measured values, which can be seen in Table 4.2.

A multiple two-variable scatter plot was generated for this group for identification of correlations between composition data and rheological characteristics. The framed areas in Figure 4.7 depict the scatter plots of the composition and the rheological parameters. Graphically no correlations were found.

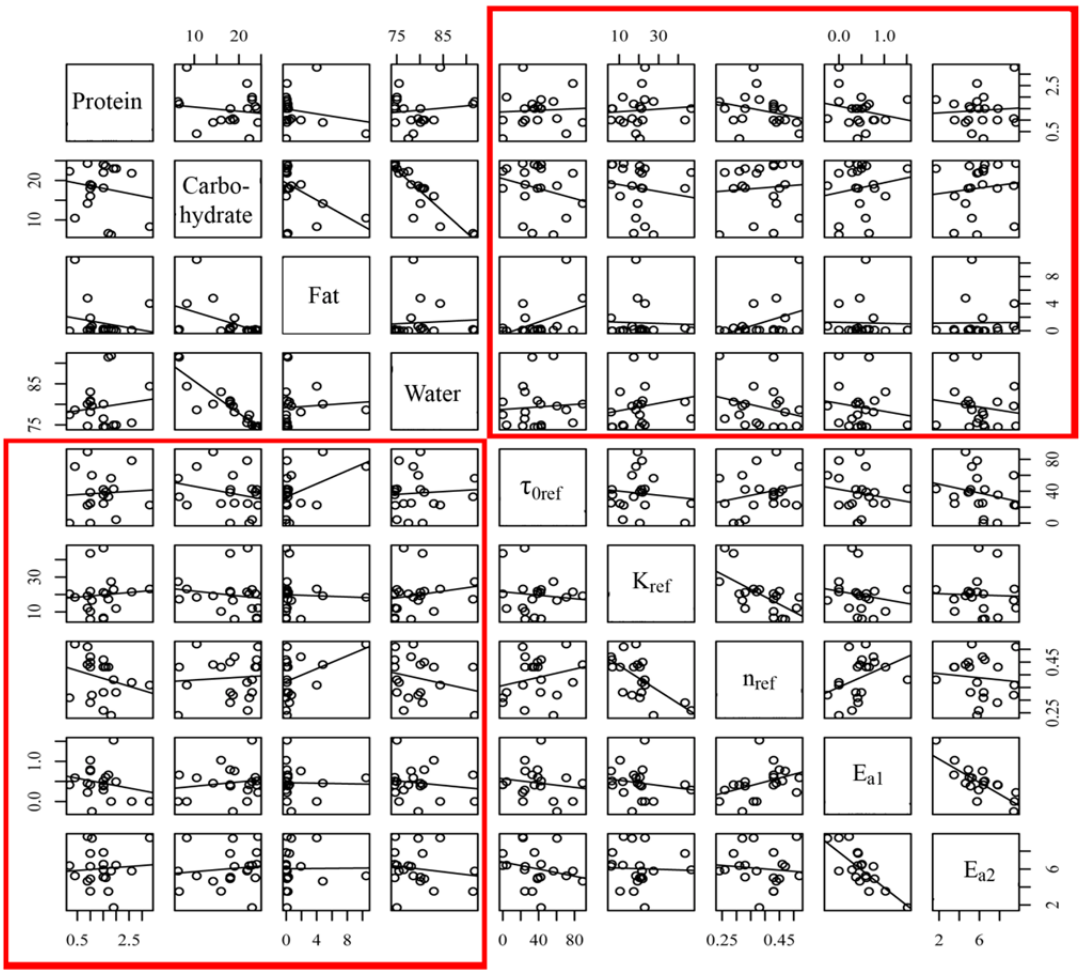

Figure 4.7: Multiple two-variable scatter plot for the red group

Blue

The blue group is typified by a maximal fat content of 10 %, whereas the total water content is in the range of 50 - 75 % and a total solid content above 30 %. Four products were numbered among this specification and can be seen in Table 4.2. Compared to the red group elevated values for the yield stress in the range of $\tau_{ref} = 30.56 - 63.5$ Pa were observed, whereas the consistency coefficient, the flow behavior index and the values for the activation energy covered a broad range.

A multiple two-variable scatter plot was created for identification of correlations between composition data and rheological characteristics. The framed areas in Figure 4.8 depict the scatter plots of the composition and the rheological and graphically indicate no correlation.

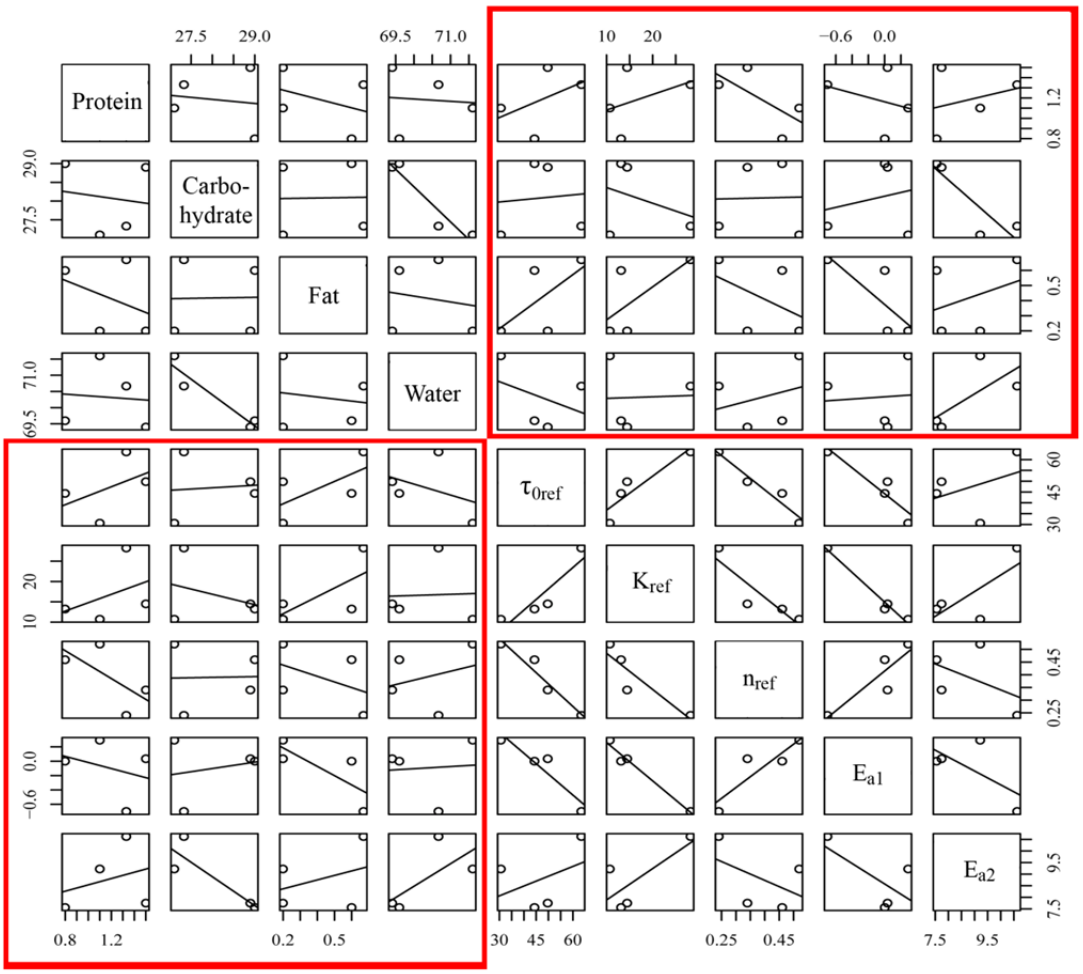

Figure 4.8: Multiple two-variable scatter plot for the blue subgroup

Green

The green region comprised eleven products and was characterized by an oil content in the range of 10 - 50 %, a total water content of 50 - 75 % and a solid content of maximum 45 %. Mostly fat reduced mayonnaises were assigned to this group. A multiple two-variable scatter plot was constructed for the green group for the identification of correlations between composition data and rheological characteristics. The framed areas in Figure 4.9 depict the scatter plots of the composition and the rheological parameters. Graphically no correlations were found.

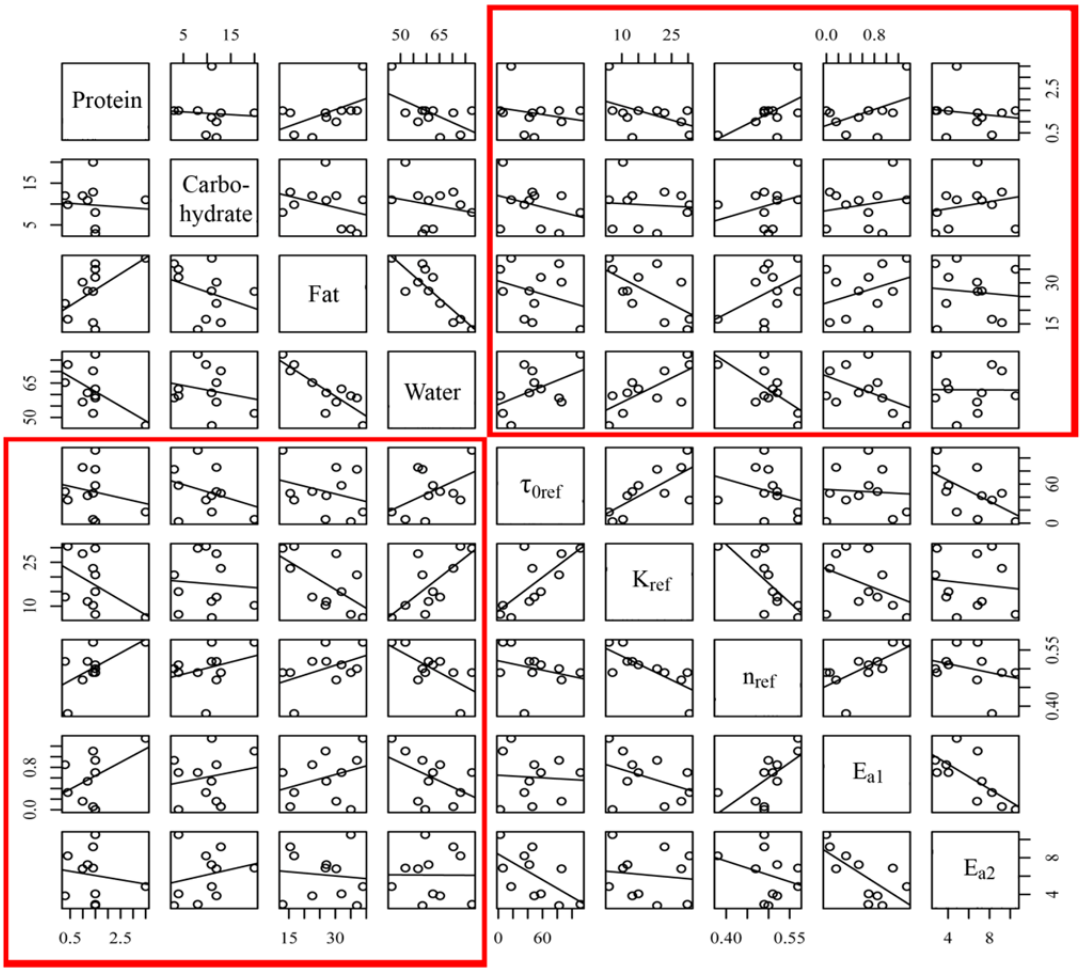

Figure 4.9: Multiple two-variable scatter plot for the green group

Yellow

The yellow region characterized by high oil content of 50 - 82 %, a water content ranging from 10 - 50 % and total solid content of maximum 30 %. The specifications of this group were fulfilled by twelve products, which were in general mayonnaises. More detailed

information on the minimum and maximum values of the rheological parameters are mentioned in Table 4.2.

A multiple two-variable scatter plot was created for identification of correlations between composition data and rheological characteristics. The framed areas in Figure 4.10 depict the scatter plots of the composition and the rheological parameters. No correlations were found during graphical evaluation.

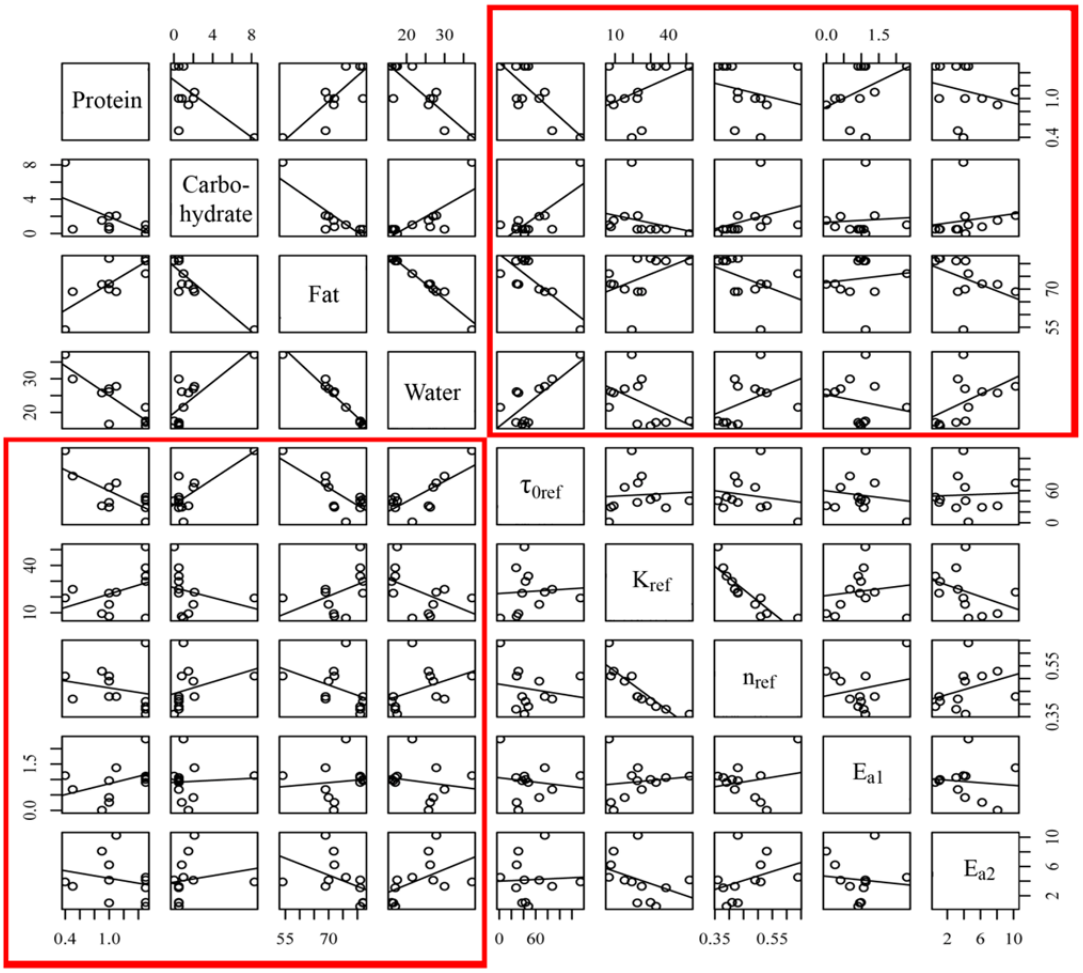

Figure 4.10: Multiple two-variable scatter plot for the yellow group

4.2.3 Rheological classification

The criteria for the differentiation according to the rheological classification is the stability of a sample, which was calculated based on the ratio of yield stress and density, which is multiplied by the gravitational acceleration.

According to Tscheuschner [24] the resulting parameter allows a classification into the groups easily flowing (x = 0.005 - 0.02); poorly flowing (x = 0.02 - 0.15) and

inherently stable (x > 0.15). Table 4.3 depicts, that only two products could be assigned to the subgroup easily flowing, whereas the rest showed values above x > 0.15.

Thus this classification model provided no improvement compared to the unclassified product range, since the products underlying rheological parameters were too similar for a differentiation according to this classification approach. For this reason no further data evaluation was performed, since the results would be comparable to the observations made for the entire product range.

Table 4.3: Applied rheology based classification

Subgroup	**Easily flowing**		**Poorly flowing**		**Inherently stable**	
Products No.	**5, 18**		**----**		**1, 2, 3, 4, 6, 7, 8, 9, 10, 13, 15, 16, 17, 19, 20, 21, 22, 28 - 55**	
	min.	**max.**	**min.**	**max.**	**min.**	**max.**
Proteins [%]	0.2	1.0	-	-	0.3	3.5
Carbohydrates [%]	18.0	22.3	-	-	0.0	29.0
Fats [%]	0.0	0.4	-	-	0.0	82.0
Water [%]	77.5	80.6	-	-	16.0	91.8
τ_{0ref} [Pa]	0.00	0.00	-	-	1.52	134.51
K_{ref} [Pasn]	20.36	43.54	-	-	5.82	51.72
n_{ref} [-]	0.29	0.31	-	-	0.24	0.64
E_{a1} [kJs/mol]	0.41	0.42	-	-	-0.70	2.31
E_{a2} [kJ/mol]	6.39	7.76	-	-	0.53	10.62

4.3 Composition independent model

In the previous sections 4.1 and 4.2 the investigated rheological characteristics and the composition data were subjected to linear and multiple linear regression analysis. However it was evaluated that the application of different classification approaches allowed no observation of correlations within the generated subgroups despite the differences in composition and in the resulting macroscopic structure.

The different basic systems emulsion and suspension could clearly be distinguished by their composition; however the resulting rheological characteristic parameters were within the same dimension and thus could not be distinguished. Concerning the shear

dependency all products showed shear thinning flow behavior, which was clearly stated by a flow behavior index in the range of n_{ref} = 0.24 - 0.64 and thus below zero. The consistency coefficient K_{ref} showed a minimum value of 5.28 Pas^n and a maximum of 51.72 Pas^n. The yield stress was observed to be in the range of τ_{0ref} = 0 - 134.51 Pa and thus almost in one order of magnitude.

For illustration Figure 4.11 and Figure 4.12 depict the range of measured data, whereas the minimal (blue line) and maximal (red line) limits of the all flow curves and the resulting viscosity curves, which clarify the similarity of all commercial products. The graphical analysis of the minimal and maximal viscosity curves showed that the variety of the apparent viscosity decreases with increasing shear rate.

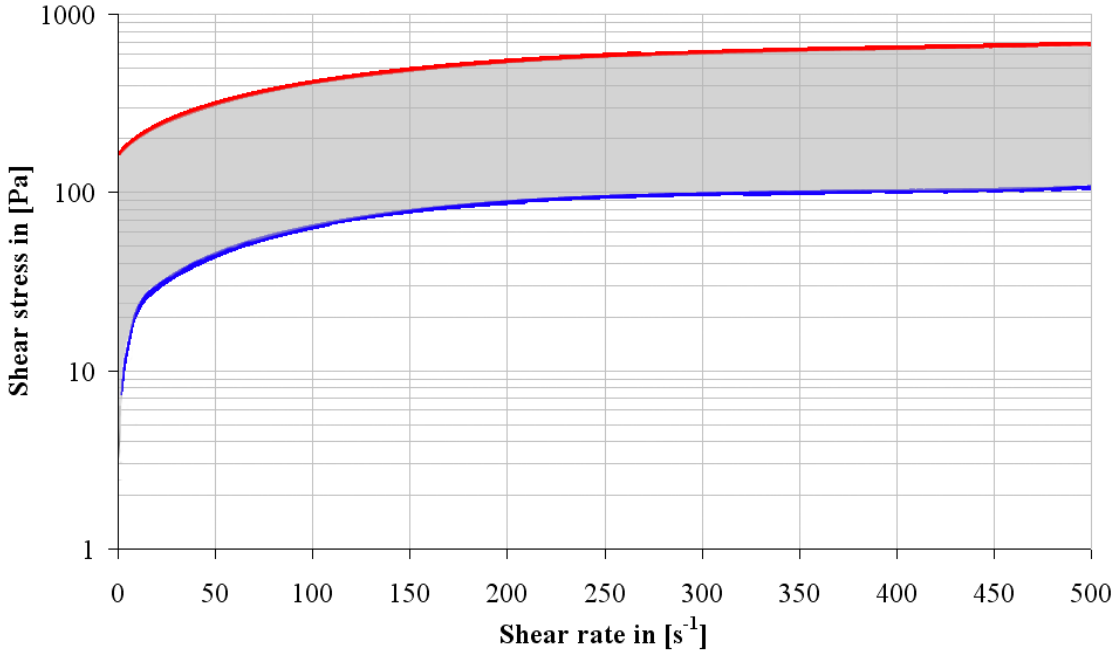

Figure 4.11: Minimal and maximal limits of the flow curve of the complete product range at reference temperature (T_{ref} = 298.15°C)

The temperature dependent flow behavior showed like the shear rate dependent flow behavior no correlation with the composition data and thus did not allow a prediction. The values for the observed activation energy were in the range of E_{a1} = -0.7 - 2.31 kJs/mol and E_{a2} = 0.53 - 10.62 kJ/mol, whereas no specific trend for emulsions or suspension could be observed. The variability of the previous indicated values were almost in the same dimension. Thus it was assumed that the investigated products originate from one main unit of commercial products regarding to their rheological properties.

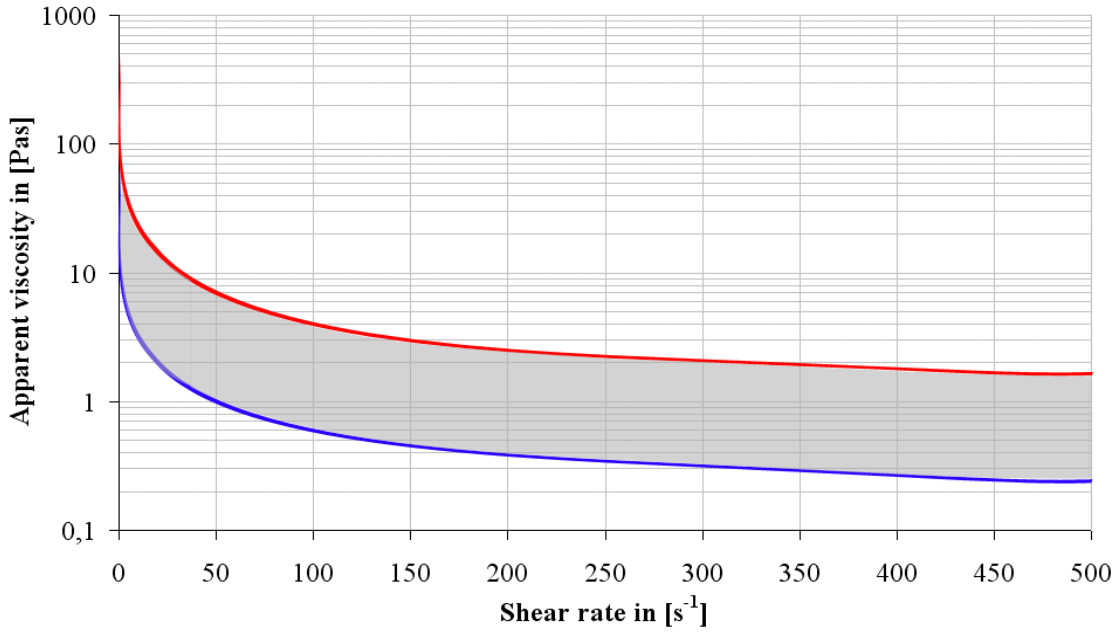

Figure 4.12: Minimal and maximal limits of the resulting viscosity curve of the complete product range at reference temperature (T_{ref} = 298.15°C)

For this reason an average model, which represents the general characteristics of commercial products was generated. The resulting parameters for the Herschel-Bulkley model at a reference temperature of T = 25 °C could be characterized by a yield stress τ_{0ref} = 25.36 Pa, consistency coefficient K_{ref} = 26.27 Pas^n and a flow behavior index of n = 0.389, which is represented by the black line in Figure 4.13.

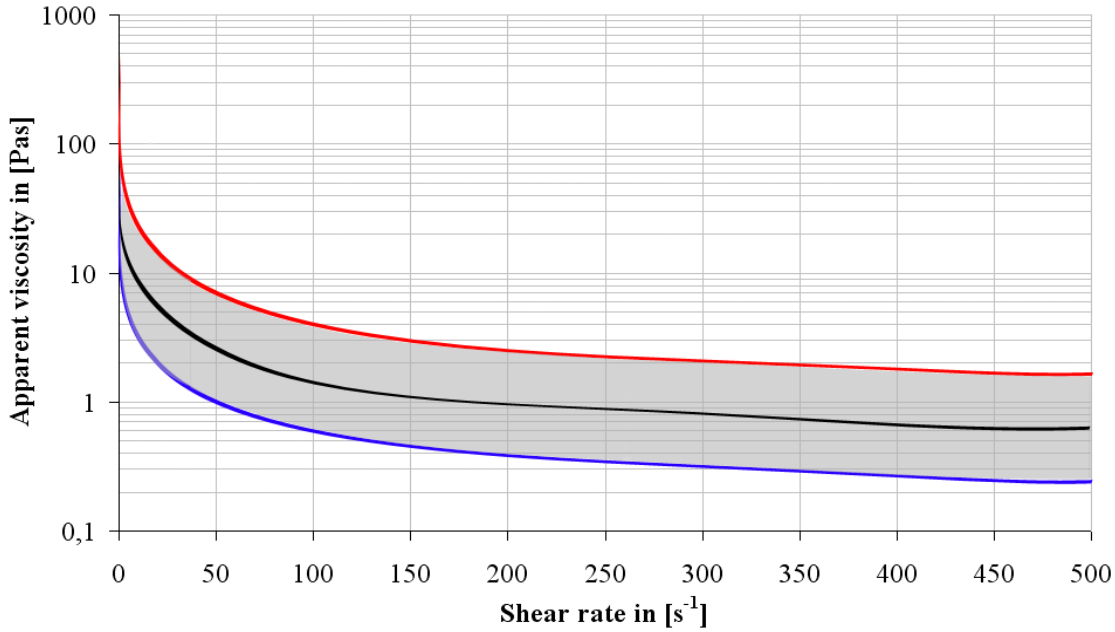

Figure 4.13: General Herschel-Bulkley equation for commercial product range at reference temperature (T = 298.15K)

The fitted parameters of the Arrhenius type model at shear rates of $\dot{\gamma}$ = 1, 10, 100, 500 s^{-1} for the entire product range can be seen in Table 4.4. The observed

apparent reference viscosity η_{ref} significantly decreased with increasing shear rate, which confirms the observations made for the shear rate dependent flow behavior. The activation energy E_a was ranging from 6.28 - 9.14 kJ/mol, but no significant shear rate dependency was observed. For this reason the arithmetic mean was calculated, thus the activation energy of the complete product range was $E_{a2} = 7.95 \pm 1.21$ kJ/mol.

Table 4.4: Fitted Arrhenius parameters for complete product range at a reference temperature of T = 298.15 K (different letters imply significant differences (α = 0.05))

$\dot{\gamma}$ [s^{-1}]	η_{ref} [Pa]		E_a [kJ/mol]		R^2	RMSE
1	61.45 ± 26.91	c	6.28 ± 3.67	a	0.068	176.3
10	9.17 ± 4.15	b	7.95 ± 2.63	a	0.139	38.88
100	1.81 ± 0.71	a	8.42 ± 2.22	a	0.173	5.23
500	0.60 ± 0.23	a	9.14 ± 2.76	a	0.189	2.04

The investigated general model parameters of the Herschel-Bulkley model and the Arrhenius type model were combined, which allows the estimation of the apparent viscosity of a commercial food emulsion or suspension at any given shear rate - temperature combination calculated by the general Equation 4.1.

$$\eta_{T,\dot{\gamma}} = \left[\frac{\tau_{0ref}}{\dot{\gamma}} + K_{ref} \cdot (\dot{\gamma})^{[n_{ref} - 1]}\right] \cdot e^{\left[\left(\frac{(E_{a1} \cdot \ln\dot{\gamma} + E_{a2})}{R}\right) \cdot \left(\frac{1}{T} - \frac{1}{T_{ref}}\right)\right]} \qquad \textbf{4.1}$$

Using the parameters reference yield stress τ_{0ref} in (Pa), consistency coefficient K_{ref} in (Pas^n), flow behavior index n_{ref} (-), pre-factor activation energy E_{a1} in ($J \cdot s \cdot mol^{-1}$), activation energy E_{a2} in ($J \cdot mol^{-1}$), universal gas constant R in ($J \cdot mol^{-1} \cdot K^{-1}$) and a reference temperature T_{ref} in (K).

The investigated reference values for the complete product range characterized by the yield stress of $\tau_{0ref} = 25.36$ Pa, consistency index of $K = 26.27$ Pas^n, flow behavior index of $n = 0.389$ and an activation energy pre-factor $E_{a1} = 0$, activation energy of $E_{a2} = 7.95$ kJ/mol at a reference temperature of T = 298.15 K leading to Equation 4.2

$$\eta_{T,\dot{\gamma}} = \left[\frac{25.36}{\dot{\gamma}} + 26.27 \cdot (\dot{\gamma})^{[0.389 - 1]}\right] \cdot e^{\left[\left(\frac{7.95}{0.00831}\right) \cdot \left(\frac{1}{T} - \frac{1}{298.15}\right)\right]} \qquad \textbf{4.2}$$

5 Discussion

5.1 Rheological characterization

All investigated products showed non-Newtonian flow behavior, whereas on the part of process engineering the parameters time, shear rate and temperature were identified as mayor influences based on literature review. The applied boundary conditions during testing were selected process orientated to avoid extrapolation of experimental data over a broad range, which may introduce significant errors. Different approximation functions, which allow the calculation of the apparent viscosity or shear stress in dependency of time, shear rate and temperature were applied. The most powerful models, which could describe the majority of products, were selected to allow a comparability of products ranging from emulsions to suspensions.

At first the influence of time on the rheological properties was investigated to identify the general time dependent flow behavior after rest and the duration until total unstructured state of a sample was reached. Most products showed as expected a rapid decrease within the first seconds of constant shearing, whereas a few exhibited an increase. However only a few products exhibited statically significant thixotropic or rheopectic flow behavior.

In literature various authors report of significant time dependent flow behavior of comparable food emulsions and suspensions. This difference could be caused by the applied measurement technique called hysteresis loop, which comprises an ascending and subsequently descending shear ramp. The area between the resulting curves indicates the degree of thixotropy or rheopexy. In doing so, time and shear rate dependency are observed superimposed, complicating the assignment of the single influences. According to Mewis and Wagner [47] the performance of a hysteresis loop only gives a relative

measurement of thixotropy, whereas the resulting values strongly is dependent on the test conditions, which imply prior shear history, acceleration rate and maximum shear rate.

The significant time dependent samples were approximated by four rheological models, namely Weltman, second order structural kinetic, first order stress decay model with a zero stress and first order stress decay model with a non-zero stress. The first order stress decay model with a non-zero stress was found to be the most appropriate model since it could be validated for all products and in addition showed very good predictive capabilities, which were indicated by a very high coefficient of determination and low values for the root mean square error. The Weltman model and the second order structural kinetic model showed also high values for the coefficient of determination, but could not be validated leading to the rejection of these models.

Under the applied conditions an equilibrium viscosity was observed for all products after a duration of $t = 120s$. This totally unstructured state implies the elimination of previous shear history and time dependent effects [49]. Since all samples were purchased at the retail market the previous shear history was unknown, which required the elimination of previous shear history to allow direct comparison of the samples and to obtain time independent samples for subsequent shear rate or temperature dependent measurements.

The shear rate dependent data were approximated using the Bingham, Ostwald de Waele, Herschel-Bulkley, Casson and Carreau model in order to identify a suitable model for description of the flow characteristics.

The Herschel-Bulkley model could be validated for almost all emulsions and suspensions and showed the best goodness of fit compared to the other models. However a small group of products with comparably high total solids content could only be validated by application of the Carreau model. The Carreau model can be distinguished from the other applied models by consideration of the areas of very low and very high shear rates, which is for some samples characterized by Newtonian flow. The transition between Newtonian and shear thinning flow behavior is usually found to be in the range of $\dot{\gamma} = 10^{-3} - 10^{-4}\ s^{-1}$ [22,102,104]. Thus it can be assumed that the measurements were performed in the shear thinning region of most products, only a few products indicated a zero shear viscosity with a transition from Newtonian to shear thinning flow behavior at $\dot{\gamma} = 4\ s^{-1}$.

The shear rate dependent flow behavior was investigated at three different temperatures, thus these measurements allowed the evaluation of the temperature dependency of the Herschel-Bulkley parameters τ_0, K and n. Significant dependency on temperature was observed for most products, but no specific pattern of variation could be determined.

The influence of temperature on viscosity was additionally characterized by the performance of temperature ramp test at different constant shear rates. The samples were fitted by application of an Arrhenius type model and the Williams-Landel-Ferry model. Both models exhibited a very good fit for the entire product range. However nearly all products, at which the Arrhenius type Equation was applied, could be validated. The Williams-Landel-Ferry model could be validated for less products. The Arrhenius parameters reference viscosity η_{ref} and activation energy E_a showed significant shear rate dependency, whereas former approved the shear thinning flow behavior of the samples. The activation energy however increased following a logarithmic function with rising shear rate for almost all products, which was confirmed by results of linear regression analysis and validation.

The combination of shear rate and temperature dependency in a combined Equation could be useful for food process engineering, because resulting set of Equation can be used to calculate the shear stress or apparent viscosity at any shear rate temperature combination [43]. Harper and Sahrigi [100] developed a model, which combines the Ostwald-de-Waele model with an Arrhenius type model, assuming a temperature dependent consistency coefficient K and a temperature independent flow behavior index n. Thus the exponential pre-factor of the Arrhenius type Equation is substituted by the consistency coefficient.

The findings of this research work deny the application of the Ostwald-de-Waele Equation for the description of shear rate dependent flow behavior. For this reason two different approaches were made, whereas the first was based on a temperature dependent linear regression of the characteristic parameters τ_0, K and n of the Herschel-Bulkley model. The second attempt was a combination of the Herschel-Bulkley and the Arrhenius-type Equations, whereas the Herschel-Bulkley model was applied to calculate the apparent viscosity at a reference temperature of 25 °C. Subsequently the calculated reference viscosity was shifted based on an Arrhenius relationship to the desired temperature.

Both approaches could not be validated, but high coefficients of determination and low values for the root mean square error would allow an estimation of the shear rate and temperature dependent viscosity.

The combination of the Herschel-Bulkley and Arrhenius type equation in general showed higher coefficients of determination and lower values for the root mean square error compared to the other attempt, therefore the estimation of the apparent viscosity at any shear rate-temperature combination with five characteristic parameters was established. The resulting set of data was used as a basis for the prediction of the rheological properties based on the composition data.

5.2 Prediction of rheological properties

All investigated products consist primarily of a mixture of lipids, proteins, carbohydrates, water. The general attempt was to analyze the selected product range for correlations of the ingredients namely proteins, carbohydrates, fats and water; and the measured parameters yield stress τ_{0ref}, consistency coefficient K_{ref}, flow behavior index n_{ref}, pre-factor activation energy E_{a1} and activation energy E_{a2} to allow the calculation of the shear rate and temperature dependent viscosity.

The graphical evaluation of the multiple two-variable scatter plots did not allow the identification of correlations of composition data and the measured values. For this reason it was assumed that a classification in different subgroups could give more information on the specific behavior within a pre-defined group. For this reason different classification models based on different systematic approaches were applied to the entire product range.

The function based classification model references on the macroscopic structure and the designated use of a product. According to this classification model the product range was divided into four subgroups; namely classic emulsion; non-classic emulsion spoonable, non-classic emulsion pourable and condiment sauce. The subgroups classic emulsion and condiment sauce could clearly be distinguished by their fat content. However the resulting rheological parameters of these subgroups were superimposed and thus did not allow a group specific differentiation. The products, which were assigned to the groups of non-classic emulsions, could not be distinguished based on their composition. The classification into “spoonable” and “pourable” however allowed a differentiation of the

yield stress, whereas in general lower values were observed for pourable non-classic emulsions. In summary it can be assumed that this classification model was nor able to distinguish specific rheological properties neither to identify general representative rheological properties of the particular subgroups.

The composition based classification takes the water, oil and total solids contents into consideration for classification, whereas it was decided to separate the entire product range into four different subgroups, which differentiated the product range into mayonnaises, fat reduced products, ketchups with high amount of total solids and ketchups with low amount of total solids. Compared to the function based classification no improvements based on the group specific behavior could be observed, since the resulting values the rheological parameters were superimposed. The graphical evaluation of the multiple two-variable scatter plots neither allowed the identification of correlations between composition data and rheological properties.

The last applied classification approach called rheological classification requires information on the yield stress value and the density of a sample, whereas the product range is divided into three product categories. This classification model requires the determination of the yield stress and the density of the sample in advance to classify the product in an appropriate way. The density of a sample can be calculated based on the composition with a good accuracy [113], but the yield stress requires previous measurements. Thus there is the need for rheological investigation, which allows the direct determination of the specific product properties without the risk to predict inaccurate data. The applied approach allowed no differentiation of the products, since only two were assigned to the group easily flowing, which was the result of the absence of a yield stress. The rest of the products were classified as inherently stable, which in summary was no improvement to an unclassified product range.

In summary it can be concluded that the applied classification models do neither generate subgroups with specific rheological behavior nor allow the identification of correlations of composition and rheological properties within the subgroups. It can also be concluded that the applied classification models in combination with the chosen data evaluation method were not applicable for the prediction of the rheological properties of an unknown sample on the basis of the given proteins, carbohydrates, fats and water content. The variations of the composition within the single subgroups did not allow the identification of specific patterns, which was supported by the observation made for the

rheological classification, at which the investigated commercial products were assigned to one group with similar rheological behavior regardless of the underlying macroscopic structure and composition.

The performed investigation and data evaluation only referred to composition data given by the manufacturer, but did not consider the variations of raw materials e.g. source and composition of oils, cultivar of plants. The processing techniques can considerably influence the resulting rheological characteristics without a change in the composition of carbohydrates, proteins, fats and water by variation of particle shapes and particle size distributions. Slight variations in the range of 0.5 up to 2 % in carbohydrate or protein content, can have considerable influence on the rheological properties, since most hydrocolloids can be assigned to this groups of ingredients. In order to estimate the influence of the utilized hydrocolloid detailed information on the used type and concentration would be required.

In summary an accurate prediction will require more comprehensive input information and a more powerful data evaluation method, which is able to identify non-linear as well as linear dependencies within the different input variables. For this reason the implementation of an artificial neuronal network for data evaluation and classification might be useful, because this technique has the ability to identify non-linear relations and interactions between the single variables allowing the determination of product and ingredient specific patterns. Thus it might be possible to identify antagonistic or synergistic effects of each ingredient, leading to a classification and prediction model.

Based on the observations and the drawn conclusions a composition independent rheological model, which represented the averaged rheological parameters of the complete investigated commercial product range, was established. The model allows a general estimation of the shear rate and temperature dependent flow behavior, whereas the accuracy of the estimation model increases with rising shear rate. For estimations of the rheological behavior above shear rates of $\dot{\gamma} > 100\ s^{-1}$ the model showed good predictive capabilities with a relatively small absolute error.

Depending on the boundary conditions and the required accuracy additional rheological measurements might be required to obtain a higher accuracy. In summary the established Equation can be seen as a reference and reflects the general flow behavior of commercial food emulsions and suspensions.

6 Conclusions and outlook

The objectives of the present research work "Examination and Modeling of Rheological Properties of Middle to High Viscosity Foodstuff" were to characterize the flow properties of commercial available food emulsions and suspensions and to develop a prediction model for the estimation of the rheological properties based on the composition of proteins, carbohydrates, fats and water. The examination led to the following conclusions:

1. All investigated commercial available food emulsions and suspensions exhibit non-Newtonian flow behavior.

2. The rheological behavior of the investigated food emulsions and suspensions was depending on time of strain, shear rate and temperature.

3. The before mentioned influencing parameters could be within the boundary conditions reliably characterized by:
   (a) the first-order stress decay model, with a non-zero stress for the time dependency.
   (b) the Herschel-Bulkley model for shear rate dependent flow behavior.
   (c) the Arrhenius type model for the temperature dependency.

4. The developed shear rate $\dot{\gamma}$ in (s^{-1}) and temperature T in (K) dependent equation allows product specific estimation of the apparent viscosity $\eta_{\dot{\gamma},T}$ in (Pas) at any shear rate-temperature combination, with the parameters reference yield stress τ_{0ref} in (Pa), consistency coefficient K_{ref} in (Pas^n), flow behavior index n_{ref} (-), pre-factor activation energy E_{a1} in ($J \cdot s \cdot mol^{-1}$), activation energy E_{a2} in ($J \cdot mol^{-1}$), universal gas constant R in ($J \cdot mol^{-1} \cdot K^{-1}$) and a reference temperature T_{ref} in (K).

$$\eta_{T,\dot{\gamma}} = \left[\frac{\tau_{0ref}}{\dot{\gamma}} + K_{ref} \cdot (\dot{\gamma})^{[n_{ref}-1]}\right] \cdot e^{\left[\left(\frac{(E_{a1} \cdot \ln\dot{\gamma} + E_{a2})}{R}\right) \cdot \left(\frac{1}{T} - \frac{1}{T_{ref}}\right)\right]}$$

5. The prediction of rheological properties based on the composition of proteins, carbohydrates, fats and water with the linear and multiple linear regression failed. The classification of the products according to different systematic approaches led to no improvement of predictive capabilities.
6. All investigated commercial products exhibit similar rheological properties, which are independent from their composition.
7. A reference equation, representing the range of commercial products, for the estimation of the rheological properties of shear rate and temperature dependency was established with the parameters:
   (a) Yield stress $\tau_{0ref} = 25.36$
   (b) Consistency coefficient $K_{ref} = 26.27$
   (c) Flow behavior index $n_{ref} = 0.389$
   (d) Pre-factor activation energy $E_{a1} = 0$
   (e) Activation energy $E_{a2} = 7.95$
8. The accuracy of the reference Equation increases with rising shear rate.

For the proceeding work following steps can be derived from this thesis:

1. To facilitate a prediction model additional production information comprising processing conditions during production and exact composition data might be required.
2. As a consequence of the additional process information the discontinuous phase, which decisively determines the rheological properties of a fluid by its concentration, particle shape and size distribution needs to be examined to improve the understanding of the resulting rheological behavior.
3. Development of a simple test method, which provides the option to observe basic rheological characteristics e.g. beaker viscosimeter, which allow an improved categorization and thus a prediction of other rheological parameters.
4. Implementation of advanced data evaluation techniques e.g. artificial neuronal networks, due its ability to take into account non-linearities and interactions between each variable. In this regard the main objective will be the determination of product and ingredients specific patterns, allowing the relation to rheological characteristics.

7 Literature

1. Sikora, M.; Badrie, N.; Desingh, A.; Kowalski, S.: Sauces and Dressings: A Review of Properties and Applications. Critical Reviews in Food Sciences and Nutrition, v. 48, p. 50-77, 2008.

2. Halder, A.; Dhall, A.; Datta, A. K.; Black, D. G.; Davidson, P. M.; Li, J. & Zivanovic, S.: A user-friendly general-purpose predictive software package for food safety. Journal of Food Engineering, v. 104, p. 173-185, 2011.

3. Choi, Y. H.; Yoo, B.: Characterization of time-dependent flow properties of food suspensions. International Journal of Food Science and Technology, v. 39, n. 7, p. 801-805, 2004.

4. Nesvadba, P.: Engineering Properties of Foods; Chapter 4: Thermal Properties of Unfrozen Foods. 3. ed. CRC Press, 2005.

5. Nesvadba, P.: Frozen Food Science and Technology. 1. ed. Wiley-Blackwell, 2008.

6. Datta, A. K.: Status of Physics-Based Models in the Design of Food Products, Processes, and Equipment. Comprehensive Reviews in Food Science and Food Safety, v. 7, p. 121-129, 2008.

7. Datta, A. K.; Halder, A.: Status of food process modeling and where do we go from here (Synthesis of the outcome from brainstorming). Comprehensive Reviews in Food Science and Food Safety, v. 7, p. 117-120, 2008.

8. Sablani, S. S.: Status of Observational Models Used in Design and Control of Products and Processes. Comprehensive Reviews in Food Science and Food Safety, v. 7, p. 130-136, 2008.

9. Arocas, A.; Sanz, T.; Fiszman, S. M.: Improving effect of xanthan and locust bean gums on the freeze-thaw stability of white sauces made by different native starches. Food Hydrocolloids, v. 23, p. 2478-2484, 2009.

10. Weltichanes, J.; Vergara-Balderas, F.; Bermadez-Aguirre, D.: Transport phenomena in food engineering: basic concepts and advances. Journal of Food Engineering, v. 67, n. 1-2, p. 113-128, 2005.

11. Genovese, D. B.; Lozano, J. E.; Rao, M. A.: The Rheology of Colloidal and Noncolloidal Food Dispersions. Jounal of Food Science, v. 72, p. 11-20, 2007.

12. Sheldrake, P.: Texture in Food; Volume 1: Semi-solid foods; Chapter 16: Controlling texture in soups, sauces and dressings. CRC Press Boca Raton, Bosten, New York, Washington DC, 2003.

13. Mandala, I.; Savvas, T. P.; Kostaropoulos, A. E.: Xanthan and locust bean gum influence on the rheology and structure of a white model-sauce. Journal of Food Engineering, v. 64, n. 3, p. 335-342, 2004.

14. Franco, J. M.; Berjano, M.; Gallegos, C.: Linear Viscoelasticity of Salad Dressing Emulsions. Journal of Agricultural and Food Chemistry, v. 45, n. 3, p. 713-719, 1997.

15. Abu-Jdayil, B.: Modelling the time-dependent rheological behavior of semisolid foodstuffs. Journal of Food Engineering, v. 57, n. 1, p. 97-102, 2003.

16. Phillips, G. O.; Williams, P. A.: Handbook of hydrocolloids; Chapter 1: Introduction to food hydrocolloids. [S.l.]: Woodhead Publishing Limited and CRC Press, 2000.

17. Peressini, D.; Sensidonia, A.; de Cindiob, B.: Rheological Characterization of Traditional and Light Mayonnaises. Journal of Food Engineering, v. 35, n. 4, p. 409-417, 1998.

18. Liu, H.; Xu, X.; Guo, S.: Rheological, texture and sensory properties of low-fat mayonnaise with different fat mimetics. LWT - Food Science and Technology, v. 40, n. 6, p. 946-954, 2007.

19. Wendin, K.; Hall, G.: Influences of Fat, Thickener and Emulsifier Contents on Salad Dressing: Static and Dynamic Sensory and Rheological Analyses. Lebensmittel-Wissenschaft und-Technologie, v. 34, n. 4, p. 222-233, 2001.

20. Dickinson, E.: Hydrocolloids at interfaces and the influence on the properties of dispersed systems. Food Hydrocolloids, v. 17, n. 1, p. 25-39, 2003.

21. Dickinson, E.: An introduction to food colloids. 1. ed. Oxford University Press; Oxford, 1992.

22. Martinez, I.; Angustiasriscardo, M.; Franco, J.: Effect of salt content on the rheological properties of salad dressing-type emulsions stabilized by emulsifier blends. Journal of Food Engineering, v. 80, n. 4, p. 1272-1281, 2007.

23. McClements, D. J.: Food emulsions: principles, practice, and techniques. 2. ed.: CRC Press, 2004.

24. Tscheuschner, H. D.: Rheologie der Lebensmittel Chapter 4: Rheologische Eigenschaften von Lebensmittelsystemen. B. Behrs Verlag GmbH & Co. Hamburg, 1993.

25. Grace, L.: On the stability of oil-in-water emulsions to freezing. Food Hydrocolloids, v. 18, p. 899-905, 2004.

26. Robins, M. M.; Watson, A. D.; Wilde, P. J.: Emulsions - creaming and rheology. Current Opinion in Colloid & Interface Science, v. 7, p. 419-425, 2002.

27. Glicksmann, M.: Food Hydrocolloids. CRC Press Florida, 1980.

28. Depree, J. A.; Savage, G. P.: Physical and flavour stability of mayonnaise. Trends in Food Science & Technology, v. 12, p. 157-163, 2001.

29. Ford, L. D.; Borwankar, R. P.; Pechak, D.; Schwimmer, B.: Food Emuslions; Chapter 13: Dressing and Sauces: Marcel Dekker Inc., 2004.

30. Guilmineau, F.; Kulozik, U.: Influence of a thermal treatment on the functionality of hens egg yolk in mayonnaise. Journal of Food Engineering, v. 78, p. 648-654, 2007.

31. Leal-Calderon, F.; Thivilliers, F.; Schmitt, V.: Structured emulsions. Current Opinion in Colloid & Interface Science, v. 12, p. 206-212, 2007.

32. Hoefler, A. C.: Hydrocolloids; Chapter 8. American Association of Cereal Chemists, 2004.

33. Robins, M. M.: Emulsions - creaming phenomena. Current Opinion in Colloid & Interface Science, v. 5, p. 265-272, 2000.

34. Castro, M. P.; Rojas, A. M.; Campos, C. A.; Gerschenson, L. N.: Effect of preservatives, tween 20, oil content and emulsion structure on the survival of Lactobacillus fructivorans in model salad dressings. LWT - Food Science and Technology, v. 42, n. 8, p. 1428-1434, 2009.

35. Lorenzo, G.; Zaritzky, N.; Califano, A.: Modeling rheological properties of low-in-fat o/w emulsions stabilized with xanthan/guar mixtures. Food Research International, v. 41, p. 487-494, 2008.

36. Sahin, H.; Ozdemir, F.: Effect of some hydrocolloids on the rheological properties of different formulated ketchups. Food Hydrocolloids, v. 18, n. 6, p. 1015-1022, 2004.

37. Sharma, S. K.; LeMaguer, M.; Liptay, A.; Poysa, V.: Effect of composition on the rheological properties of tomato thin pulp. Food Research International, v. 29, p. 175-179, 1996.

38. Bayod, E.; Willers, E. P.; Tornberg, E.: Rheological and structural characterization of tomato paste and its influence on the quality of ketchup. LWT - Food Science and Technology, v. 41, p. 1289-1300, 2008.

39. Tiziani, S.; Vodovotz, Y.: Rheological effects of soy protein addition to tomato juice. Food Hydrocolloids, v. 19, p. 45-52, 2005.

40. Casanovas, A.; Hernández, M.; Martí-Bonmatí, E.; Dolz, M.: Cluster Classification Of Dysphagia-Oriented Products Considering Flow, Thixotropy And Oscillatory Testing. Food Hydrocolloids, 2010.

41. Fischer, P.; Windhab, E. J.: Rheology of food materials. Current Opinion in Colloid & Interface Science, p. 10.1016/j.cocis.2010.07.003, 2010.

42. Rao, M. A.: Engineering Properties of Foods; Chapter 2: Rheological Properties of Fluid Foods. 3. ed. CRC Press, 2005.

43. Steffe, J.: Rheological methods in food process engineering. 2. ed., Freeman Press, 1996.

44. Mezger, T. G.: The Rheology Handbook. Vincentz Network, 2006.

45. Giesekurs, H.: Phänomenologische Rheologie: Eine Einführung. Springer-Verlag Berlin Heidelberg New Yorg, 1994.

46. de Souza Mendes, P. R.: Modeling the thixotropic behavior of structured fluids. Journal of Non-Newtonian Fluid Mechanics, v. 164, n. 1-3, p. 66-75, 2009.

47. Mewis, J.; Wagner, N. J.: Thixotropy. Advances in Colloid and Interface Science, v. 147-148, p. 214-227, 2009.

48. Razavi, S.; Karazhiyan, H.: Flow properties and thixotropy of selected hydrocolloids: Experimental and modeling studies. Food Hydrocolloids, v. 23, n. 3, p. 908-912, 2009.

49. Koocheki, A.; Razavi, S. M. A.: Effect of Concentration and Temperature on Flow Properties of Alyssum homolocarpum Seed Gum Solutions: Assessment of Time Dependency and Thixotropy. Food Biophysics, v. 4, n. 4, p. 353-364, 2009.

50. Paredes, M. D. C.; Rao, M. A.; Bourne, M. C.: Rheological Characterization of Salad Dressings. 1. Steady Shear, Thixotropy and Effect of Temperature. Journal of Texture Studies, v. 19, n. 3, p. 247-258, 1988.

51. Altan, A.; Kus, S.; Kaya, A.: Rheological Behaviour and Time Dependent Characterisation of Gilaboru Juice (Viburnum opulus L.). Food Science and Technology International, v. 11, n. 2, p. 129-137, 2005.

52. Karazhiyan, H.; Razavi, S. M. A.; Phillips, G. O.; Fang, Y.; Al-Assaf, S.; Nishinari, K.; Farhoosh, R.: Rheological properties of Lepidium sativum seed extract as a function of concentration, temperature and time. Food Hydrocolloids, v. 23, n. 8, p. 2062-2068, 2009.

53. Al-Malah, K. I.; Azzam, M. O. J.; Abu-Jdayil, B.: Effect of glucose concentration on the rheological properties of wheat-starch dispersions. Food Hydrocolloids, v. 14, p. 491-496, 2000.

54. Tárrega, A.; Durán, L.; Costell, E.: Flow behaviour of semi-solid dairy desserts. Effect of temperature*1. International Dairy Journal, v. 14, n. 4, p. 345-353, 2004.

55. Windhab, E. Rheologie der Lebensmittel Chapter 6: Allgemeine rheologische Meßprinzipe, Geräte und Methoden. B. Behrs Verlag GmbH & Co. Hamburg, 1993.

56. Barnes, H. A.; Hutton, J. F.; Walters, K.: An introduction to rheology. Elsevier Amsterdam, 1989.

57. Windhab, E. J.; Dressler, M.; Feigl, K.; Fischer, P.; Megias-Alguacil, D.: Emulsion processing - from single-drop deformation to design of complex processes and products. Chemical Engineering Science, v. 60, p. 2101-2113, 2005.

58. Barnes, H. A.: Thixotropy - a review. Journal of Non-Newtonian Fluid Mechanics, v. 70, n. 1-2, p. 1-33, 1997.

59. Koocheki, A.; Ghandi, A.; Razavi, S. M. A.; Mortazavi, S. A.; Vasiljevic, T.: The rheological properties of ketchup as a function of different hydrocolloids and temperature. International Journal of Food Science & Technology, v. 44, n. 3, p. 596-602, 2009.

60. Xu, S. Y.; Shoemaker, C. F.; Luh, B. S.: Effect of break temperature on rheological properties and microstructure of tomato juices and pastes. Journal of Food Science, v. 51, n. 2, p. 399-402, 1986.

61. Martínez-Padilla, L. P.; Rivera-Vargas, C.: Flow behavior of Mexican sauces using a vane-in-a-large cup rheometer. Journal of Food Engineering, v. 72, p. 189-196, 2006.

62. Canovas, G. V. B.; Peleg, M.: Flow Parameters of Selected Commercial Semi-Liquid Food Products. Journal of Texture Studies, v. 14, n. 3, p. 213-234, 1983.

63. Tanglertpaibul, T.; Rao, M. A.: Rheological Properties of Tomato Concentrates as Affected by Particle Size and Methods of Concentration. Journal of Food Science, v. 52, n. 1, p. 141-145, 1987.

64. Sharoba, A. M.; Senge, B.; El-Mansy, H. A.; l. M. Bahlol, H. E.; Blochwitz, R.: Chemical, sensory and rheological properties of some commercial German and Egyptian tomato ketchups. European Food Research and Technology, v. 220, n. 2, p. 142-151, 2005.

65. Fischer, P.; Pollard, M.; Erni, P.; Marti, I.; Padar, S.: Rheological approaches to food systems. Comptes Rendus Physique, v. 10, n. 8, p. 740-750, 2009.

66. Alvarez, E.; Cancela, M.; Maceiras, R.: Comparison of Rheolgical Behaviour of Salad Sauces. International Jounal of Food Properties, v. 9, p. 907-915, 2006.

67. Franco, J. M.; Guerrero, A.; Gallegos, C.: Rheology and processing of salad dressing emulsions. Rheologica Acta, v. 34, n. 6, p. 513-524, 1995.

68. Riscardo, M. A.; Franco, J. M.; Gallegos, C.: Influence of Composition of Emulsifier Blends on the Rheological Properties of Salad Dressing-Type Emulsions. Food Science and Technology International, v. 9, p. 53-63, 2003.

69. Maruyama, K.; Sakashita, T.; Hagura, Y.; Suzuki, K.: Relationship between Rheology, Particle Size and Texture of Mayonnaise. Food Science and Technology Research, v. 13, n. 1, p. 1-6, 2007.

70. Chiralt, A.; Salazar, J. A.; Ferragut, V.: Rheological study of O/W emulsions containing dried whole egg and locust bean gum. Journal of Texture Studies, v. 25, n. 1, p. 33-43, 1994.

71. Dolz, M.; Hernández, M. J.; Delegido, J.; Alfaro, M.; Munoz, J.: Influence of xanthan gum and locust bean gum upon flow and thixotropic behaviour of food emulsions containing modified starch. Journal of Food Engineering, v. 81, n. 1, p. 179-186, 2007.

72. Juszczak, L.; Fortuna, T.; Kola, A.: Sensory and rheological properties of Polish commercial mayonnaise. Nahrung/Food, v. 47, n. 4, p. 232-235, 2003.

73. Su, H. P.; Lien, C. P.; Lee, T. A.; Ho, R. S.: Development of low-fat mayonnaise containing polysaccharide gums as functional ingredients. Journal of the Science of Food and Agriculture, v. 90, p. 806-812, 2010.

74. Izidoro, D.; Sierakowski, M. R.; Waszczynskyj, N.; Haminiuk, C. W. I.; de Paula Scheer, A.: Sensory Evaluation and Rheological Behavior of Commercial Mayonnaise. International Journal of Food Engineering, v. 3, n. 1, 2007.

75. Tiu, C.; Boger, D. V.: Complete Rheological Characterization of Time-Dependent Food Products. Journal of Texture Studies, v. 5, n. 3, p. 329-338, 1974.

76. Batista, A.; Raymundo, A.; Sousa, I.; Empis, J.: Rheological characterization of coloured oil-in-water food emulsions with lutein and phycocyanin added to the oil and aqueous phases. Food Hydrocolloids, v. 20, n. 1, p. 44-52, 2006.

77. Laca, A.; Sáenz, M. C.; Paredes, B.; Díaz, M.: Rheological properties, stability and sensory evaluation of low-cholesterol mayonnaises prepared using egg yolk granules as emulsifying agent. Jou, v. 97, p. 243-252, 2010.

78. Haminiuk, C. W. I.; Sierakowski, M. R.; Vidal, J. R. M. B.; Masson, M. L.: Influence of temperature on the rheological behavior of whole araçá pulp (Psidium cattleianum sabine). LWT - Food Science and Technology, v. 39, n. 4, p. 427-431, 2006.

79. Guerrero, S. N.; Alzamora, S. M.: Effect of pH, Temperature and Glucose Addition on Flow Behavior of Fruit Purées I. Banana Purée. Journal of Food Engineering, v. 33, p. 239-256, 1997.

80. Haminiuk, C. W. I.; Sierakowski, M. R.; Izidoro, D.; Marciel, G. M.; Scheer, A. P.; Masson, M. L.: Effect of Heat Treatment on Pectic Fractions and Apparent Viscosity of Whole Blackberry (Rubus spp.) Pulp. International Journal of Food Engineering, v. 4, p. 1-15, 2008.

81. Rao, M. A.; Bourne, H. J. C. M.: Flow properties of tomato concentrates. Journal of Texture Studies, v. 12, n. 4, p. 521-538, 1981.

82. Marcotte, M.; Taheriana, A. R.; Triguia, M.; Ramaswamy, H. S.: Evaluation of rheological properties of selected salt enriched food hydrocolloids. Journal of Food Engineering, v. 48, n. 2, p. 157-167, 2001.

83. Mancini, M.; Moresi, M.; Sappino, F.: Rheological behaviour of aqueous dispersions of algal sodium alginates. Journal of Food Engineering, v. 28, n. 3-4, p. 283-295, 1996.

84. Marcotte, M.; Taheriana, A. R.; Triguia, M.; Ramaswamy, H. S.: Rheological properties of selected hydrocolloids as a function of concentration and temperature. Food Research International, v. 34, n. 8, p. 695-703, 2001.

85. Sikora, M.; Kowalski, S.; Tomasik, P.; Sady, M.: Rheological and sensory properties of dessert sauces thickened by starch-xanthan gum combinations. Journal of Food Engineering, v. 79, p. 1144-1151, 2007.

86. Wu, Y.; Cui, W.; Eskin, N. A. M.; Goff, H.: An investigation of four commercial galactomannans on their emulsion and rheological properties. Food Research International, v. 42, n. 8, p. 1141-1146, 2009.

87. Sakiyan, O.; Sumnu, G.; Sahin, S.; Bayram, G.: Influence of fat content and emulsifier type on the rheological properties of cake batter. European Food Research and Technology, v. 219, n. 6, p. 635-638, 2004.

88. Latha, R. B.; Bhat, K. K.; Bhattacharya, S.: Rheological behaviour of steamed rice flour dispersions. Journal of Food Engineering, v. 51, n. 2, p. 125-129, 2002.

89. Chen, C. R.; Ramaswamy, H. S.: Rheology of topioca starch. Food Research International, v. 32, p. 319-325, 1999.

90. Mohameed, H.; Abujdayil, B.; Eassa, A.: Flow properties of corn starch milk sugar system prepared at 368.15K. Journal of Food Engineering, v. 77, n. 4, p. 958-964, 2006.

91. Bhattacharya, S.; Battacharya, S.: Rheology of Cooked Debranned Maize Flour Suspensions. Journal of Food Engineering, v. 27, p. 97-105, 1996.

92. Vandresen, S.; Quadri, M. G. N.; de Souza, J. A. R.; Hotza, D.: Temperature effect on the rheological behavior of carrot juices. Journal of Food Engineering, v. 92, n. 3, p. 269-274, 2009.

93. Ferry, J.: Viscoelastic Properties of Polymers; Chaper: 11. Wiley, New York, 1961.

94. Nelson, K. A.; Labuza, T. P.: Water activity and food polymer science: Implications of state on Arrhenius and WLF models in predicting shelf life. Journal of Food Engineering, v. 22, p. 271-289, 1994.

95. Sopade, P. A.; Halley, P.; Bhandari, B.; Arcy, B. D.; Doebler, C.; Caffin, N.: Application of the Williams-Landel-Ferry model to the viscosity-temperature relationship of Australian honeys. Journal of Food Engineering, v. 56, p. 67-75, 2002.

96. Juszczak, L.; Fortuna, T.: Rheology of selected Polish honeys. Journal of Food Engineering, v. 75, p. 43-49, 2006.

97. Liang, J. Z.: Pressure effect of viscosity for polymer fluids in die flow. Polymer, v. 42, p. 3709-3712, 2001.

98. Först, P.: In-situ Untersuchungen der Viskosität fluider, komprimierter Lebensmittel-Modellsysteme. Lehrstuhl für Fluidmechanik und Prozeßautomation der Technischen Universität München. 2001.

99. Bourne, M. C.: Food texture and viscosity: concept and measurement. 2. ed., Academic Press Inc., 2002.

100. Harper, J. C.; Sahrigi, A. F.: Viscometric Behavior of Tomato Concentrates. Journal of Food Science, v. 30, n. 3, p. 470-476, 1965.

101. Council Directive of 24. September 1990 on nutrition labelling for foodstuffs (90/496/EEC), 1990.

102. Riscardo, M. A.; Moros, J. E.; Franco, J. M.; Gallegos, C.: Rheological characterisation of salad-dressing-type emulsions stabilised by egg yolk/sucrose distearate blends. European Food Research and Technology, v. 220, n. 3-4, p. 380-388, 2004.

103. Dolz, M.; Hernández, M. J.; Delegido, J.: Oscillatory measurements for salad dressings stabilized with modified starch, xanthan gum, and locust bean gum. Journal of Applied Polymer Science, v. 102, n. 1, p. 897-903, 2006.

104. Gaaloul, S.; Corredig, M.; Turgeon, S. L.: Rheological study of the effect of shearing process and kappa-carrageenan concentration on the formation of whey protein microgels at pH 7. Journal of Food Engineering, v. 95, n. 2, p. 254-263, 2009.

105. Quintana, J. M.; Califano, A. N.; Zaritzky, N. E.; Partal, P.; Franco, J. M.: Linear and Nonlinear Viscoelastic Behavior of Oil-In-Water Emulsions Stabilized with Polysaccharides. Journal of Texture Studies, v. 33, n. 3, p. 215-236, 2002.

106. Fox, J.: Getting Started with the R Commander: A Basic-Statistics Graphical User Interface to R. Journal of Statistical Software, p. 1-42, 2005.

107. Sachs, L.: Angewandte Statistik: Methodensammlung mit R. Springer-Verlag Berlin, Heidelberg, New York, 2006.

108. Kesel, A. B.; Junge, M. M.; Nachtigall, W.: Einführung in die angewandte Statistik für Biowissenschaftler. Springer-Verlag, 1999.

109. Groß, J.: Grundlegende Statistik mit R. Vieweg+Teubner Verlag, 2010.

110. Mao, C. F.; Chen, J. C.: Interchain association of locust bean gum in sucrose solutions: An interpretation based on thixotropic behavior. Food Hydrocolloids, v. 20, p. 730-739, 2006.

111. Richard, J. D.; Malcolm, J. J.: Time-Dependent Rheology of Starch Thickeners and the Clinical Implications for Dysphagia Therapy. Dysphagia, v. 21, p. 264-269, 2006.

112. Koocheki, A.; Mortazavi, S. A.; Shahidi, F.; Razavi, S. M. A.; Taherian, A. R.: Rheological properties of mucilage extracted from Alyssum homolocarpum seed as a new source of thickening agent. Journal of Food Engineering, v. 91, p. 490-496, 2009.

113. Singh, R. P.; Heldman, D. R.: Introduction to Food Engineering - 4th edition. Academic Press, 2008.